ALBERTIANA

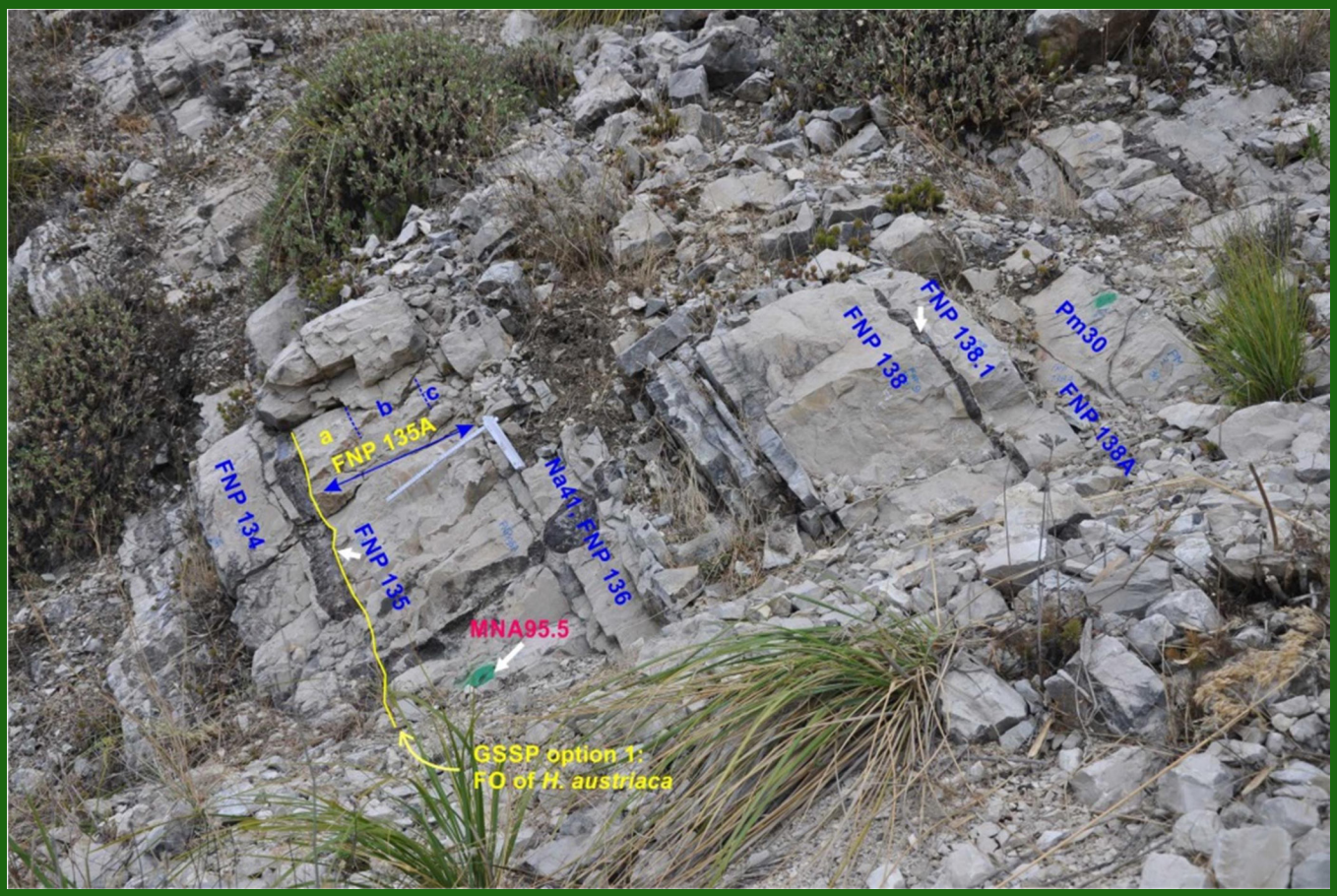

46

December 2021

ISSN 0619-4324

CONTENTS

Albertiana is the international journal of Triassic research. The primary aim of *Albertiana* is to promote the interdisciplinary collaboration and understanding among members of the I.U.G.S. Subcommission on Triassic Stratigraphy. *Albertiana* serves as the primary venue for the dissemination of orignal research on Triassic System. *Albertiana* also serves as a newsletter for the announcement of general information and as a platform for discussion of developments in the field of Triassic stratigraphy. *Albertiana* thus encourages the publication of contributions in which information is presented relevant to current interdisciplinary Triassic research and at provides a forum for short, relevant articles including. original research articles, reports on research and works in progress, reports on conferences, news items and conference announcements, *Albertiana* Forum: letters, comment and reply, and literature reviews. *Albertiana* is published bianually by SUNY Cortland's Paleontological Laboratory for the Subcommission on Triassic Stratigraphy. *Albertiana* is available as PDF at http://paleo.cortland.edu/Albertiana/

Cover Image: *Choristoceras marshi*, from Fraas (1895 Der Petrefaktensammler. - Leitfaden zum Sammeln und Bestimmen der Versteinerungen Deutschlands; K.G. Lutz' Verlag; Stuttgart).

Research Article

STABLE CARBON ISOTOPE RECORD OF CARBONATE ACROSS THE CARNIAN–NORIAN BOUNDARY AT THE PROSPECTIVE GSSP SECTION AT BLACK BEAR RIDGE, BRITISH COLUMBIA, CANADA

Jerry Z. X. Lei[1], Jon M. Husson[1], Martyn L. Golding[2], Michael J. Orchard[2], and John-Paul Zonneveld[3]

[1]*School of Earth and Ocean Sciences, University of Victoria, 3800 Finnerty Road, Bob Wright Centre A405. Victoria, British Columbia, Canada V8P 5C2. jerrylei@uvic.ca, jhusson@uvic.ca*
[2]*Geological Survey of Canada, Pacific - Vancouver, 605 Robson Street. Vancouver, British Columbia, Canada V6B 5J3. martyn.golding@canada.ca, mjorchard.micro@gmail.com*
[3]*Department of Earth and Atmospheric Sciences, University of Alberta, 1-26 Earth Sciences Building. Edmonton, Alberta, Canada T6G 2E3. zonnevel@ualberta.ca*

Abstract – The Black Bear Ridge section is exposed on the shores of Williston Lake, British Columbia, Canada, with Late Triassic carbonate strata encapsulating the Carnian–Norian boundary as constrained by several fossil indices. Analysis of $\delta^{13}C_{carb}$ from this section reveals a six-meter-thick interval of increased instability proximal to the boundary. This excursion interval features anomalously low negative values, a shift of approximately -3 ‰ from the pre- and post- excursion interval values which average -0.95 ‰. It also features high point-to-point variability between these anomalously negative values and values comparable to the average outside of the excursion. This atypical feature of the excursion interval is interpreted to be the result of rapid, local-scale carbon cycle variation related to the global faunal turnover at the Carnian–Norian boundary, suggesting prolonged ecosystem instability around the stage boundary.

INTRODUCTION

The Black Bear Ridge section is exposed along the northern shore of Williston Lake. The continuous and abundantly fossiliferous limestone succession, which formed through deep marine deposition on the northwestern margin of Pangea, spans an interval stretching from the upper Carnian into the lower Hettangian (e.g., Zonneveld et al., 2010). This section is a strong candidate for the base-Norian Global Boundary Stratotype Section and Point (GSSP) (Orchard, 2007). The Carnian–Norian boundary interval (CNB) at Black Bear Ridge has been studied using a wide variety of approaches, including ammonoid biostratigraphy (Orchard et al., 2001; Balini et al., 2012), conodont biostratigraphy (Orchard, 2007, 2014, 2019), bivalve biostratigraphy (McRoberts, 2007, 2011), sedimentary facies (Zonneveld et al., 2010), $\delta^{13}C_{org}$ analysis (Williford et al., 2007a), $^{87}Sr/^{86}Sr$ chemostratigraphy (Onoue et al., 2016), and $\delta^{18}O_{PO4}$ chemostratigraphy (Sun et al., 2020). Ammonoids from Black Bear Ridge indicate the traditional CNB falls within an approximately six-meter interval that includes the first occurrance datum (FOD) of both the conodont *Metapolygnathus parvus* and the bivalve *Halobia austriaca* (Orchard, 2014). Both these species have been proposed as the defining fossil datum for the CNB (McRoberts & Krystyn, 2011; Mazza et al., 2018).

From prior studies, any $\delta^{13}C$ excursion at the CNB at Black Bear Ridge appears to be minor, with documented excursions inconsistent between studies. Williford et al. (2007a) found a small negative 0.5 ‰ excursion in $\delta^{13}C_{org}$ just above the base of the *Metapolygnathus parvus* Subzone. Subsequently, Onoue et al. (2016) conducted analysis of $\delta^{13}C_{carb}$ alongside other geochemical proxies across the CNB and found a positive shift of 1.5 ‰ in $\delta^{13}C_{carb}$ coinciding with the same datum. Major disturbances of global ocean $\delta^{13}C$ have been established to typically be preserved in both $\delta^{13}C_{carb}$ and $\delta^{13}C_{org}$ records, the assumption being the

Published online: March 12, 2021

Lei, J.Z.X., Husson, J.M., Goldring, M.L., Orchard, M.J., & Zonnevld, J.-P. 2021. Stable carbon isotope record of carbonate across the Carnian–Norian boundary at the prospective GSSP section at Black Bear Ridge, British Columbia, Canada. *Albertiana*, vol. 46, 1–10.

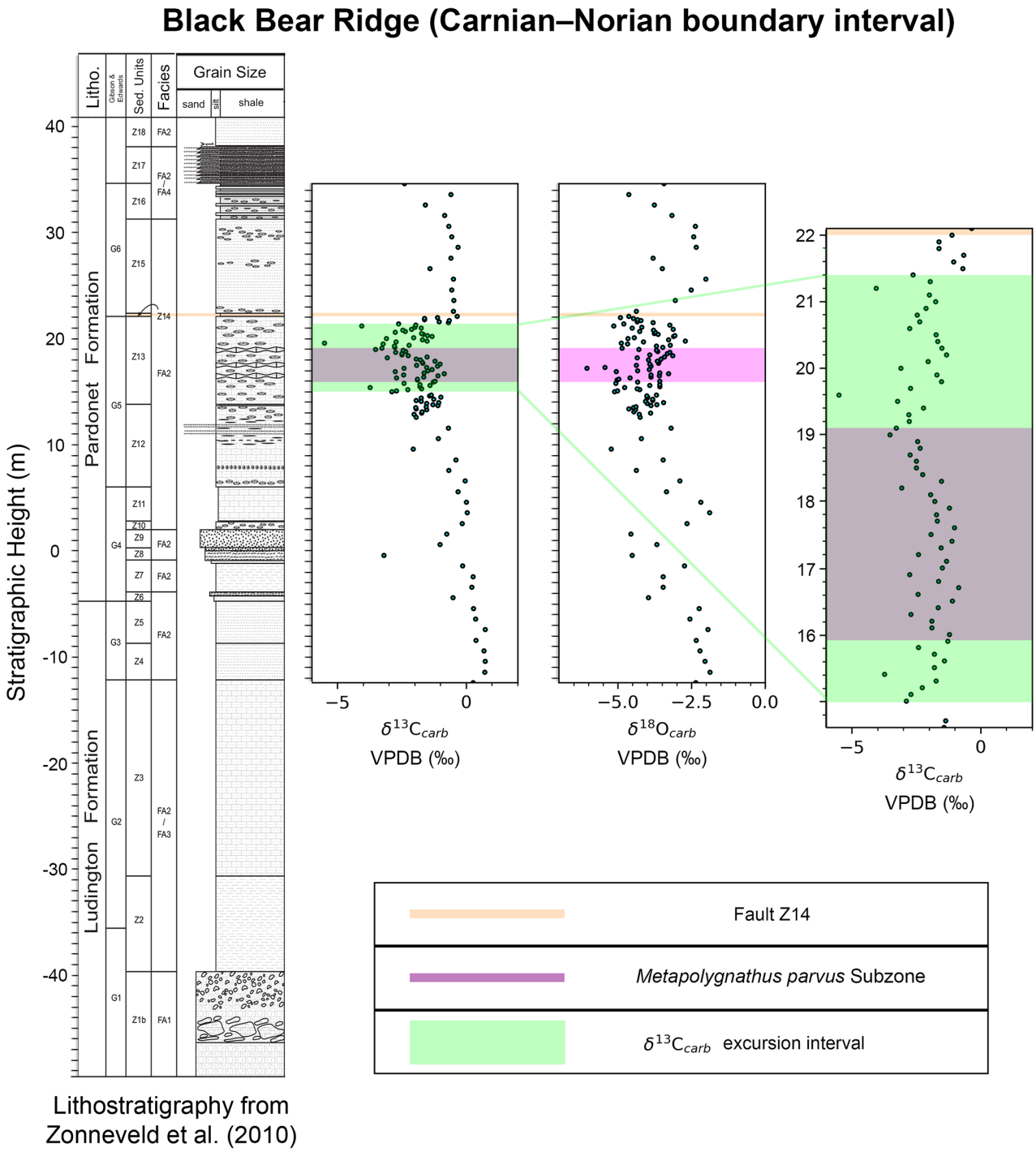

Figure 1–The CNB interval at Black Bear Ridge aligned with $\delta^{13}C_{carb}$, $\delta^{18}O_{carb}$, and zoomed-in $\delta^{13}C_{carb}$. A prominent excursion interval spanning 15.0–21.4 meters stratigraphically is highlighted in green. The *Metapolygnathus parvus* Subzone, as defined by the range of *M. parvus morphotype* alpha (Orchard, 2014), is highlighted in purple, spanning 15.9–19.1 meters stratigraphically. This representation is thicker than depicted in Orchard (2019, fig. 1), in order to more accurately reflect the thickness of the subzone as per Orchard (2019, figs. 2, 6). The 'Z14' fault is highlighted in orange.

organic material largely formed from the same dissolved inorganic carbon (DIC) pool (e.g., Kump & Arthur, 1999; Meyer el al., 2013). Strong correlations between the $\delta^{13}C_{carb}$ and $\delta^{13}C_{org}$ records are commonly utilized as evidence for primary signal preservation, since diagenesis would not alter the two records in parallel (e.g., Kump & Arthur, 1999; Meyer el al., 2013). This present study contributes a more complete high-resolution $\delta^{13}C_{carb}$ record for the CNB at Black Bear Ridge.

Beyond Black Bear Ridge, the $\delta^{13}C$ record for this stage boundary has been studied at a multitude of Tethyan sections, but with no greater consistency of signal. Muttoni et al. (2004) conducted $\delta^{13}C_{carb}$ analysis across the CNB boundary at Pizzo

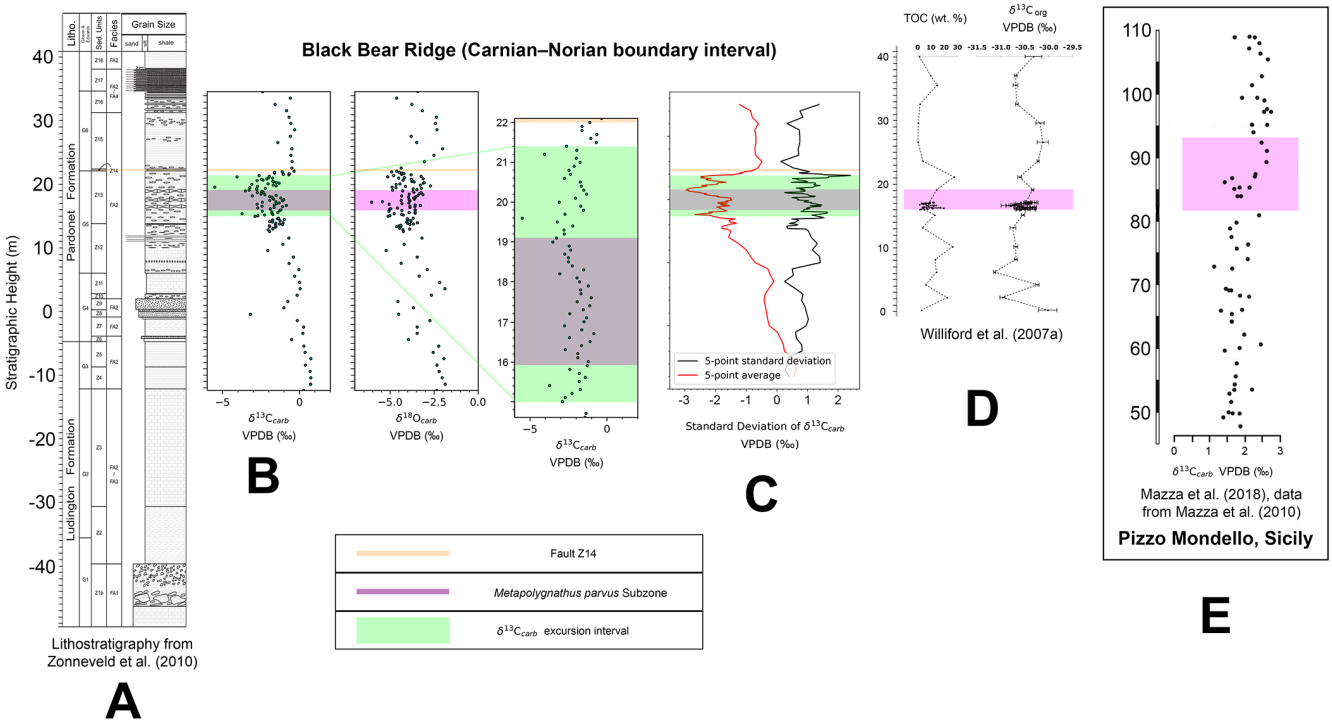

Figure 2 – Present study results aligned with select prior studies along the base of the *Metapolygnathus parvus* Subzone. All studies are displayed with the same scale for stratigraphic height except for the zoomed-in $\delta^{13}C_{carb}$ portion of the present study data. Also aligned is present study standard deviation and average $\delta^{13}C_{carb}$ calculated with a rolling set of five sequential data points.

Mondello, Italy, which is an alternate candidate for the base-Norian GSSP. A positive shift of 0.8 ‰ was identified just below the FOD of *Metapolygnathus parvus* (Muttoni et al., 2004, 2014). Mazza et al. (2010) also conducted $\delta^{13}C_{carb}$ analysis across the CNB at Pizzo Mondello and identified a positive shift of 0.6 ‰ at the same level, their T2 faunal turnover. Korte et al. (2005) conducted $\delta^{13}C_{carb}$ analysis across the CNB at Silická Brezová, Western Carpathians, but did not identify any excursions or shifts. Muttoni et al. (2014) conducted $\delta^{13}C_{carb}$ analysis across the CNB at Guri Zi, Albania, as well as at Aghia Marina, Greece. A minor positive shift of 0.3 ‰ was identified to coincide with the stage boundary in the former, whereas no shifts were identified in the latter. Jin et al. (2018, 2019) conducted $\delta^{13}C_{carb}$ and $\delta^{13}C_{org}$ analyses across the CNB at Hanwang, southern China, and identified a negative excursion of 4 ‰ and a positive shift of 2 ‰ respectively across the FOD of *M. parvus*. The negative excursion in $\delta^{13}C_{carb}$ is attributed to diagenesis, as only considering values from brachiopod shells displaying high preservation potential for primary $\delta^{13}C_{carb}$ signal reduces the excursion to a negative shift of 1 ‰ (Jin et al., 2018). Sun et al. (2019) conducted $\delta^{13}C_{carb}$ analysis at the Wadi Mayhah section in Oman and did not identify any excursions in the late Carnian through Norian portion of the section.

METHODS

Samples for $\delta^{13}C_{carb}$ were taken every meter throughout the Black Bear Ridge section, avoiding veins, soft-sediment deformation structures, bioclasts, and recrystallized zones when possible. Sampling density was increased to 10 cm for approximately 10 m through the CNB interval. Samples were cut into 1.2-cm-thick slabs, perpendicular to bedding when visible. The slabs were microdrilled using a carbide burr to extract approximately 60 mg of powder, preferentially from fine-grained calcite matrix and avoiding veins, bioclasts, and weathered surfaces. The powders were heated at 90°C for 12 hours to remove any moisture, then acidified with H_3PO_4 in airtight, helium flushed glass vials. $\delta^{13}C_{carb}$ and $\delta^{18}O_{carb}$ measurements were conducted at the University of Victoria on a Sercon 20-22 gas-source continuous-flow isotope ratio mass spectrometer with GasBox II front end. Measurements were corrected with internal standard VTS, and international standards IAEA-CO-8, and IAEA-603. Outliers were reanalyzed, measuring powder drilled from a different portion of the sample to ensure the results are not a product of measurement error nor intra-sample variability. Long-term standard reproducibility of the machine is calculated to be within 0.05–0.1 ‰ (1σ) for $\delta^{13}C_{carb}$, and within 0.15–0.2 ‰ (1σ) for $\delta^{18}O_{carb}$. Both $\delta^{13}C_{carb}$ and $\delta^{18}O_{carb}$ results are presented in delta notation relative to Vienna Pee Dee Belemnite (VPDB). Refer to Appendices 1 and 2 for tabulated measurements of all samples and standards.

RESULTS

$\delta^{13}C_{carb}$ values around the CNB at Black Bear Ridge largely fall between 1 and -2 ‰. A notable exception is an excursion interval

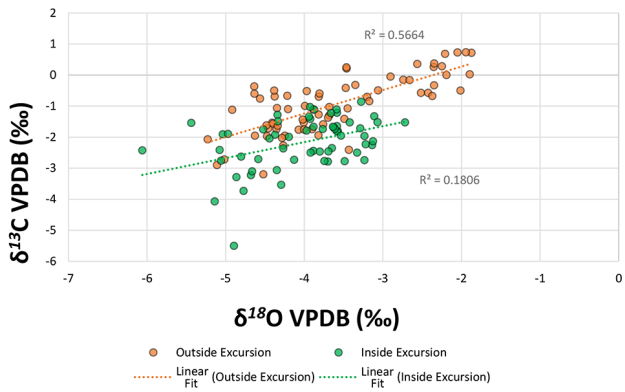

Figure 3–Correlation plot of $\delta^{13}C_{carb}$ vs. $\delta^{18}O_{carb}$ from the CNB at Black Bear Ridge, separating out data points within the excursion interval in green from data points outside the excursion interval in orange.

spanning 15.0–21.4 meters stratigraphically, where more negative values are observed and reach as low as -5.5 ‰, or -4.1 ‰ when excluding a $\delta^{13}C_{carb}$ single point outlier at 19.6 meters (Figure 1). Outside of this excursion interval, the average value for $\delta^{13}C_{carb}$ is -0.95 ‰. Single point outliers outside the excursion interval still reach low values, but no significant systematic shifts are observed, establishing a baseline range for typical $\delta^{13}C_{carb}$ values in the absence of major ecosystem disturbance. Inside of the excursion interval, the average value for $\delta^{13}C_{carb}$ is -2.2 ‰. However, 53% of $\delta^{13}C_{carb}$ values within the excursion interval still fall within the baseline range of 1 to -2 ‰, with the rest reaching lower values and resulting in high point-to-point variability. The excursion interval begins 0.9 meters below the base of the *Metapolygnathus parvus* Subzone and extends 2.3 meters above it (Figure 2A).

The excursion interval is defined by both the occurrence of $\delta^{13}C_{carb}$ values more negative than the background range observed further away from the CNB, as well as increased standard deviation. Standard deviation of $\delta^{13}C_{carb}$ is calculated with a rolling set of five sequential data points (the $\delta^{13}C_{carb}$ value at a given height, plus two above it, and two below it). A rolling 5-point average for $\delta^{13}C_{carb}$ is similarly calculated. These analyses show a series of standard deviation local maxima occur in the excursion interval, coinciding with a series of average $\delta^{13}C_{carb}$ local minima (Figure 2C). Increased standard deviation is also observed below the excursion interval at approximately 7–13 meters, however this does not coincide with average $\delta^{13}C_{carb}$ values as low as inside the excursion interval (Figure 2C). $\delta^{13}C_{carb}$ single point outliers at -0.4 and 19.6 meters are excluded in these analyses.

DISCUSSION

The $\delta^{13}C_{carb}$ values at the CNB of Black Bear Ridge are moderately well correlated with their corresponding $\delta^{18}O_{carb}$ values, indicating some degree of diagenetic influence on the $\delta^{13}C_{carb}$ record has likely occurred (Figure 3; Marshall, 1992). However, this correlation is much lower within the excursion interval at a R^2 value of 0.18, compared to the R^2 value of 0.57 outside. When excluding the $\delta^{13}C_{carb}$ single point outlier at 19.6 meters, the R^2 value within the excursion interval decreases further to 0.16. This suggests that while minor variations in $\delta^{13}C_{carb}$ values have likely been caused by diagenetic processes, the instability of the excursion interval shift could potentially be a primary, non-diagenetic signal.

Aligning the present study's results with the lithostratigraphy of Zonneveld et al. (2010), the excursion interval roughly correlates with sedimentary unit Z13, which lies entirely within the lithological facies FA2 of thin- / medium-bedded turbidites (Figure 2A). The lack of correlation with any lithological facies shift indicates that the $\delta^{13}C_{carb}$ signal is facies-independent, supporting primary seawater signal being preserved. Aligning the present study's results with the conodont biostratigraphy of Orchard (2019), the excursion is encompassed within the *Primatella primitia* Zone; it begins in the middle of the *Acuminatella acuminata-Parapetella prominens* Subzone, and extends through the *Metapolygnathus parvus* Subzone, into the lower portion of the *Primatella asymmetrica-Norigondolella* Subzone.

Comparing the Black Bear Ridge $\delta^{13}C_{org}$ results from Williford et al. (2007a) to the present study, the most extreme $\delta^{13}C_{carb}$ values observed in the present study excursion interval are beyond the portion that Williford et al. (2007a) sampled in 10 cm intervals (Figure 2D). Given the high point-to-point variability of the excursion interval, and how Williford et al. (2007a) increased the sampling interval to approximately 2–3 meters outside of this portion, it can be seen how Williford et al. (2007a) could have missed the excursion interval of the present study (Figure 2D).

Although several studies globally have proposed a positive shift in $\delta^{13}C$ at the CNB, issues such as small shift magnitude (Muttoni et al., 2004, 2014; Mazza et al., 2010), and poor sampling distribution (Onoue et al., 2016) makes the recognition of a positive shift questionable compared to background variation. Jin et al. (2019) provide a more convincing $\delta^{13}C_{org}$ positive shift in southern China, but this is not corroborated by $\delta^{13}C_{carb}$ results from the same section, which instead shows a negative excursion (Jin et al., 2018). The $\delta^{13}C_{carb}$ signal is dismissed as being caused by diagenesis because when utilizing only data points from select brachiopods, the negative excursion diminishes to a magnitude of approximately 1 ‰ (Jin et al., 2018). However, the positive shift in $\delta^{13}C_{org}$ of approximately 1.5 ‰ is not much larger than this brachiopod-carbonate negative excursion (Jin et al., 2018, 2019). Compounded by how $\delta^{13}C_{org}$ records tend to have higher amounts of variability than $\delta^{13}C_{carb}$ records (e.g., Kump & Arthur, 1999; Meyer el al., 2013), the $\delta^{13}C_{carb}$ negative excursion in southern China is no less convincing than the $\delta^{13}C_{org}$ positive shift (Jin et al., 2018, 2019). Compiling current results could suggest a global negative excursion in the $\delta^{13}C$ record at the CNB, but which is not preserved in western Tethyan sections (Muttoni et al., 2004, 2014; Korte et al., 2005; Williford et al., 2007a; Mazza et al., 2010; Onoue et al., 2016; Jin et al., 2018, 2019). However, the more likely alternative could be a lack of significant disturbance in the global $\delta^{13}C$ record at the CNB, with some manner of local effect creating the instability observed at Williston Lake and Hanwang (Muttoni et al., 2004, 2014; Korte et al., 2005; Williford et al., 2007a; Mazza et al., 2010; Onoue et al., 2016; Jin et al., 2018, 2019).

If the $\delta^{13}C_{carb}$ record preserves a perturbation to the global carbon cycle in the absence of local or diagenetic overprinting, the first-order expectation would be a systematic transition from excursion to post-excursion values (Kump & Arthur, 1999). An example would be the negative excursion in $\delta^{13}C$ established at the Triassic–Jurassic boundary, observed in many localities globally (e.g., Pálfy et al., 2007; Williford et al., 2007b). Many different mechanisms can potentially cause a negative excursion to be preserved in the $\delta^{13}C$ record. An example would include the collapse of marine productivity leading to less burial of organic matter, thus decreasing global ocean $\delta^{13}C$ (Kump, 1991). Alternatively, increasing global temperatures could dissociate sea floor methane clathrates, releasing large quantities of previously sequestered carbon with very negative $\delta^{13}C$ values, thus decreasing global ocean $\delta^{13}C$ (Dickens et al., 1995). The excursion interval observed at the CNB of Black Bear Ridge is of atypical pattern because of the rapid oscillation between anomalously negative values and values comparable to the -0.95 ‰ average outside of the excursion interval. A possible explanation is the local disruption of shallow marine carbonate formation in response to the global climatic change at the CNB. Geyman & Maloof (2019) describes a "diurnal carbon cycle engine" to explain modern Bahamian carbonate mud with positively shifted $\delta^{13}C$ precipitating in shallow marine environments, decoupled from global ocean values. During daytime, photosynthesis consumes dissolved CO_2, preferentially removing ^{12}C from the water and thus increasing $\delta^{13}C$ in the platform top environment. This $\delta^{13}C$ shift is countered by respiration at night. However, the decreased dissolved CO_2 during the day better facilitates carbonate precipitation, resulting in the carbonate recording heavier $\delta^{13}C$ values than global sea water (Geyman & Maloof, 2019). This effect would be expected most prominently in shallow waters that host extensive photosynthesis yet experience poor mixing (Geyman & Maloof, 2019). If the CNB is associated with a negative $\delta^{13}C_{carb}$ excursion in global seawater, intermittent positive shifts in $\delta^{13}C_{carb}$ stemming from local effects could result in the chaotically oscillating pattern (Figure 1). Alternatively, intermittent negative shifts in $\delta^{13}C_{carb}$ stemming from local effects could record a similar pattern in the absence of major disturbance in global sea water. Although Black Bear Ridge was not deposited in a restricted setting analogous to the Bahama Bank, carbonate sediment with these locally influenced shallow marine $\delta^{13}C_{carb}$ values could have been transported to deep marine settings by turbidity currents, for which there is abundant evidence at the CNB of Black Bear Ridge (Zonneveld et al., 2010). These periodic event beds would facilitate preservation of fine scale variations in the $\delta^{13}C_{carb}$ record originating from the shallow marine environment, which may differ from global ocean values (e.g., Patterson & Walter, 1994; Higgins et al., 2018). The length and chaotic nature of the excursion interval suggests prolonged environmental instability immediately prior and following the CNB. The $\delta^{18}O_{PO4}$ paleothermometry analysis of Sun et al. (2020) proposes an approximately 1.5-million-year period of rapid surface sea water temperature change, also suggesting prolonged environmental instability. The temperature rise within the CNB interval is immediately followed by a temperature fall (Sun et al., 2020). A subsequent pulse of temperature rise and fall extends the temperature perturbation interval well into the *Primatella asymmetrica-Norigondolella* Subzone (Sun et al., 2020).

Future complementary $\delta^{13}C_{org}$ analysis across the CNB at Black Bear Ridge could better determine to what extent the present study excursion interval is influenced by diagenesis. Continuous, well-preserved carbonate strata encompassing the CNB are exposed at a number of other sections in northeastern British Columbia. Future analysis at those sections similar to the present study could better define the geographic extent of this $\delta^{13}C$ excursion interval.

CONCLUSIONS

The CNB at Black Bear Ridge is associated with an interval of instability in the $\delta^{13}C_{carb}$ record around the *Metapolygnathus parvus* Subzone of the *Primatella primitia* Zone. This interval begins 0.9 meters below the base of the *M. parvus* Subzone within the *Acuminatella acuminata-Parapetella prominens* Subzone, and extends for 2.3 meters above it, into the *Primatella asymmetrica-Norigondolella* Subzone. This excursion interval displays high point-to-point variability, rapidly oscillating between anomalously low $\delta^{13}C_{carb}$ values and values comparable to the average outside of the excursion. This atypical feature is interpreted as the result of local carbon cycling being disrupted in response to the climatic perturbations at the CNB. The length of this excursion interval implies prolonged ecosystem instability around the stage boundary. Although the CNB can evidently be marked with significant disturbance in the $\delta^{13}C$ record, this proxy does not seem to occur with sufficiently global replicability for use as a universal marker (Muttoni et al., 2004, 2014; Korte et al., 2005; Williford et al., 2007a; Mazza et al., 2010; Onoue et al., 2016; Jin et al., 2018, 2019).

ACKNOWLEDGEMENTS

The authors would like to thank Morgan Weatherbie and Connor vanWieren for their hard work both in the field and in the lab. We also thank Travis Mayer and Alex Dyck of Williston Lake Outfitters for providing logistical support in the field. We also thank Mark Hounslow, Christopher McRoberts, and an anonymous reviewer for their helpful reviews and comments. This research was supported by a Natural Sciences and Engineering Research Council of Canada (NSERC) Discovery Grant to Jon Husson, and a NSERC Undergraduate Student Research Award to Morgan Weatherbie.

REFERENCES

Balini, M., Krystyn, L., Levera, M., & Tripodo, A. 2012. Late Carnian–Early Norian ammonoids from the GSSP candidate section Pizzo Mondello (Sicani Mountains, Sicily). Rivista Italiana di Paleontologia e Stratigrafia, 118: 47–84.

Dickens, G.R., Neil, J.R. O., Rea, D.K., & Owen, R.M. 1995. Dissociation of oceanic methane hydrate as a cause of the carbon isotope excursion at the end of the Paleocene.

Paleoceanography, 10(6): 965–971.

Geyman, E.C., & Maloof, A.C. 2019. A diurnal carbon engine explains 13C-enriched carbonates without increasing the global production of oxygen. Proceedings of the National Academy of Sciences of the United States of America, 116(49): 24433–24439.

Higgins, J.A., Blättler, C.L., Lundstrom, E.A., Santiago-Ramos, D.P., Akhtar, A.A., Crüger Ahm, A.S., Bialik, O., Holmden, C., Bradbury, H., Murray, S.T., & Swart, P.K. 2018. Mineralogy, early marine diagenesis, and the chemistry of shallow-water carbonate sediments. Geochimica et Cosmochimica Acta, 220: 512–534.

Jin, X., Shi, Z., Rigo, M., Franceschi, M., & Preto, N. 2018. Journal of Asian Earth Sciences Carbonate platform crisis in the Carnian (Late Triassic) of Hanwang (Sichuan Basin, South China): Insights from conodonts and stable isotope data. Journal of Asian Earth Sciences, 164: 104–124.

Jin, X., McRoberts, C.A., Shi, Z., Mietto, P., Rigo, M., Roghi, G., Manfrin, S., Franceschi, M., & Preto, N. 2019. The aftermath of the CPE and the Carnian–Norian transition in northwestern Sichuan basin, South China. Journal of the Geological Society, 176(1): 179–196.

Korte, C., Kozur, H.W., & Veizer, J. 2005. $\delta^{13}C$ and $\delta^{18}O$ values of Triassic brachiopods and carbonate rocks as proxies for coeval seawater and palaeotemperature. Palaeogeography, Palaeoclimatology, Palaeoecology, 226(3–4): 287–306.

Kump, L.R. 1991. Interpreting Carbon-Isotope Excursions: Strangelove Oceans. Geology, 19: 299–302.

Kump, L.R., & Arthur, M.A. 1999. Interpreting carbon-isotope excursions: Carbonates and organic matter. Chemical Geology, 161(1): 181–198.

Marshall, J.D. 1992. Climatic and oceanographic isotopic signals from the carbonate rock record and their preservation. Geological Magazine, 129(2): 143–160.

Mazza, M., Furin, S., Spötl, C., & Rigo, M. 2010. Generic turnovers of Carnian/Norian conodonts: Climatic control or competition? Palaeogeography, Palaeoclimatology, Palaeoecology, 290(1–4): 120–137.

Mazza, M., Nicora, A., & Rigo, M. 2018. *Metapolygnathus parvus* Kozur, 1972 (Conodonta): A potential primary marker for the Norian GSSP (Upper Triassic). Bollettino Della Societa Paleontologica Italiana, 57(2): 81–101.

McRoberts, C. A. 2007. The halobiid bivalve succession across a potential Carnian/Norian GSSP at Black Bear Ridge, Williston Lake, northeast British Columbia, Canada. Albertiana, 36: 142–145.

McRoberts, C.A. 2011. Late Triassic Bivalvia (chiefly Halobiidae and Monotidae) from the Pardonet Formation, Williston Lake area, northeastern British Columbia, Canada. Journal of Paleontology, 85(4): 613–664.

McRoberts, C.A., & Krystyn, L. 2011. The FOD of *Halobia austriaca* at Black Bear Ridge (northeastern British Columbia) as the base-Norian GSSP. 21st Canadian Paleontology Conference, UBC, August 19–21, Proceedings 9: 38–9.

Meyer, K.M., Yu, M., Lehrmann, D., van de Schootbrugge, B., & Payne, J.L. 2013. Constraints on Early Triassic carbon cycle dynamics from paired organic and inorganic carbon isotope records. Earth and Planetary Science Letters, 361: 429–435.

Muttoni, G., Kent, D.V., Olsen, P.E., Di Stefano, P., Lowrie, W., Bernasconi, S.M., & Hernández, F.M. 2004. Tethyan magnetostratigraphy from Pizzo Mondello (Sicily) and correlation to the Late Triassic Newark astrochronological polarity time scale. Bulletin of the Geological Society of America, 116(9–10): 1043–1058.

Muttoni, G., Mazza, M., Mosher, D., Katz, M.E., Kent, D. V., & Balini, M. 2014. A Middle–Late Triassic (Ladinian–Rhaetian) carbon and oxygen isotope record from the Tethyan Ocean. Palaeogeography, Palaeoclimatology, Palaeoecology, 399: 246–259.

Onoue, T., Zonneveld, J.-P., Orchard, M.J., Yamashita, M., Yamashita, K., Sato, H., & Kusaka, S. 2016. Paleoenvironmental changes across the Carnian/Norian boundary in the Black Bear Ridge section, British Columbia, Canada. Palaeogeography, Palaeoclimatology, Palaeoecology, 441: 721–733.

Orchard, M.J. 2007. A Proposed Carnian–Norian Boundary GSSP at Black Bear Ridge, northeast British Columbia, and a new conodont framework for the boundary interval. Albertiana, 36: 130–141.

Orchard, M.J. 2014. Conodonts from the Carnian–Norian Boundary (Upper Triassic) of Black Bear Ridge. New Mexico Museum of Natural History and Science Bulletin, 64, 146 pp.

Orchard, M.J. 2019. The Carnian–Norian boundary GSSP candidate at Black Bear Ridge, British Columbia, Canada: update, correlation, and conodont taxonomy. Albertiana, 45: 50–68.

Orchard, M.J., Zonneveld, J-P., Johns, M.J., McRoberts, C.A., Sandy, M.R., Tozer, E.T., & Carrelli, G.G. 2001. Fossil succession and sequence stratigraphy of the Upper Triassic and Black Bear Ridge, northeast B.C., and a GSSP prospect for the Carnian–Norian boundary. Albertiana, 25: 10–22.

Pálfy, J., Demény, A., Haas, J., Carter, E.S., Görög, Á., Halász, D., Oravecz-Scheffer, A., Hetényi, M., Márton, E., Orchard, M.J., Ozsvárt, P., Veto, I., & Zajzon, N. 2007. Triassic–Jurassic boundary events inferred from integrated stratigraphy of the Csovár section, Hungary. Palaeogeography, Palaeoclimatology, Palaeoecology, 244: 11–33.

Patterson, W.P., & Walter, L.M. 1994. Depletion of ^{13}C in seawater ΣCO_2 on modern carbonate platforms: significance for the carbon isotopic record of carbonates. Geology, 22(10): 885–888.

Sun, Y.D., Richoz, S., Krystyn, L., Zhang, Z.T., & Joachimski, M.M. 2019. Perturbations in the carbon cycle during the carnian humid episode: Carbonate carbon isotope records from southwestern China and Northern Oman. Journal of the Geological Society, 176(1): 167–177.

Sun, Y.D., Orchard, M.J., Kocsis, T., & Joachimski, M.M. 2020. Carnian–Norian (Late Triassic) climate change: Evidence from conodont oxygen isotope thermometry with implications for reef development and Wrangellian tectonics. Earth and Planetary Science Letters, 534: 116082.

Williford, K.H., Orchard, M.J., Zonneveld, J.-P., McRoberts, C.A., & Beatty, T.W. 2007a. A record of stable organic carbon isotopes from the Carnian–Norian boundary section at Black

Bear Ridge, Williston Lake, British Columbia. Albertiana, 36: 146–148.

Williford, K.H., Ward, P. D., Garrison, G. H., & Buick, R. 2007b. An extended organic carbon-isotope record across the Triassic–Jurassic boundary in the Queen Charlotte Islands, British Columbia, Canada. Palaeogeography, Palaeoclimatology, Palaeoecology, 244: 290–296.

Zonneveld, J.-P., Beatty, T.W., Williford, K.H., Orchard, M.J., & McRoberts, C.A. 2010. Stratigraphy and sedimentology of the lower Black Bear Ridge section, British Columbia: Candidate for the base-Norian GSSP. Stratigraphy, 7(1): 61–82.

APPENDIX 1—Measured $\delta^{13}C_{carb}$ and $\delta^{18}O_{carb}$ values for the Carnian–Norian boundary interval at the Black Bear Ridge section.

HEIGHT	$\delta^{13}C_{carb}$	$\delta^{18}O_{carb}$
-12.4	0.26	-2.35
-11.4	0.72	-1.87
-10.4	0.73	-2.05
-9.4	0.69	-2.21
-8.4	0.37	-2.35
-7.4	0.74	-1.94
-6.4	0.36	-2.56
-5.4	0.28	-2.25
-4.4	-0.51	-3.97
-3.4	0.21	-3.46
-2.4	0.25	-3.46
-1.4	-0.15	-2.74
-0.4	-3.19	-4.52
-0.4 RERUN	-2.74	-4.85
0.6	-1.03	-3.68
1.6	-0.76	-4.56
2.6	-0.16	-2.66
3.6	0.03	-1.89
4.6	0.00	-2.19
5.6	-0.32	-3.35
6.6	-0.05	-2.90
7.6	-0.69	-4.38
8.6	-0.41	-3.47
9.6	-2.07	-5.23
10.6	-1.09	-4.21
11.6	-0.70	-3.20
12.6	-1.95	-4.25
12.9	-2.03	-4.28
13	-1.74	-3.90
13.1	-1.72	-4.46
13.3	-1.53	-4.41
13.4	-1.95	-4.63
13.5	-1.97	-4.47

HEIGHT	$\delta^{13}C_{carb}$	$\delta^{18}O_{carb}$
13.6	-1.56	-4.40
13.7	-1.11	-3.89
13.8	-1.29	-3.68
13.9	-1.54	-4.01
14	-1.07	-3.45
14.1	-1.76	-4.07
14.2	-1.94	-3.82
14.3	-1.27	-3.82
14.4	-1.75	-4.00
14.5	-1.00	-3.99
14.6	-1.43	-4.02
14.7	-1.37	-3.70
15	-2.90	-5.11
15.1	-2.72	-5.02
15.2	-2.27	-4.27
15.3	-1.74	-4.35
15.4	-3.73	-4.77
15.5	-1.80	-3.57
15.6	-1.41	-3.92
15.7	-1.81	-3.58
15.8	-2.41	-5.08
15.9	-1.28	-4.34
16	-1.21	-3.58
16.1	-1.91	-5.04
16.2	-1.89	-4.97
16.3	-2.70	-4.59
16.4	-1.66	-3.88
16.5	-1.11	-3.59
16.6	-2.44	-3.88
16.7	-0.86	-3.28
16.8	-1.64	-3.58
16.9	-2.76	-5.06
17	-1.49	-4.33

APPENDIX 1 (Continued)

HEIGHT	$\delta^{13}C_{carb}$	$\delta^{18}O_{carb}$
17.1	-1.34	-3.94
17.2	-2.42	-6.06
17.3	-1.54	-5.44
17.4	-1.11	-3.87
17.5	-1.92	-4.37
17.6	-1.03	-3.93
17.7	-1.68	-3.62
17.8	-1.73	-3.61
17.9	-1.22	-3.66
18	-1.79	-3.97
18.1	-1.95	-3.53
18.2	-3.06	-4.35
18.3	-1.52	-3.42
18.4	-2.25	-3.14
18.5	-2.50	-3.92
18.6	-2.50	-3.33
18.7	-2.74	-3.23
18.8	-2.35	-3.65
18.9	-2.46	-3.69
19	-3.53	-4.29
19.1	-3.29	-4.86
19.2	-2.77	-3.49
19.3	-2.79	-3.70
19.4	-2.23	-3.22
19.5	-3.23	-4.68
19.6	-5.50	-4.89
19.6 RERUN	-5.39	-4.58
19.7	-2.73	-4.13
19.8	-1.52	-2.72
19.9	-1.71	-3.29
20	-3.10	-4.66
20.1	-2.04	-4.44
20.2	-1.32	-3.11

HEIGHT	$\delta^{13}C_{carb}$	$\delta^{18}O_{carb}$
20.3	-1.52	-3.07
20.4	-1.67	-3.63
20.5	-1.74	-3.76
20.6	-2.76	-3.74
20.7	-2.36	-4.27
20.8	-2.46	-3.80
20.9	-2.13	-3.12
21	-1.75	-4.52
21.1	-1.99	-4.20
21.2	-4.07	-5.14
21.3	-1.96	-3.23
21.4	-2.63	-4.80
21.5	-0.69	-3.81
21.6	-1.06	-4.35
21.7	-0.67	-4.22
21.8	-1.63	-4.34
21.9	-1.62	-4.48
22	-1.12	-4.92
22.1	-0.36	-4.64
22.6	-0.50	-4.38
23.6	-0.49	-3.06
24.6	-0.57	-2.52
25.6	-0.50	-2.01
26.6	-1.41	-3.49
27.6	-0.59	-3.81
28.6	-0.33	-2.35
29.6	-0.57	-2.42
30.6	-0.67	-2.37
31.6	-0.84	-3.17
32.6	-1.58	-3.76
33.6	-0.60	-4.63
34.6	-2.41	-3.43

APPENDIX 2—Analytical standard analyses for $\delta^{13}C_{carb}$ and $\delta^{18}O_{carb}$.

STANDARD	$\delta^{13}C_{carb}$	$\delta^{18}O_{carb}$
VTS	-1.65	-8.49
VTS	-1.53	-8.60
VTS	-1.51	-8.51
VTS	-1.54	-8.66
VTS	-1.49	-8.93
VTS	-1.46	-8.61
VTS	-1.47	-8.75
VTS	-1.56	-8.79
VTS	-1.54	-8.78
VTS	-1.24	-8.10
VTS	-1.26	-8.15
VTS	-1.55	-8.58
VTS	-1.40	-8.56
VTS	-1.43	-8.47
VTS	-1.54	-8.72
VTS	-1.51	-8.76
VTS	-1.52	-8.72
VTS	-1.49	-8.70
VTS	-1.53	-8.73
VTS	-1.53	-8.76
VTS	-1.63	-8.71
VTS	-1.62	-8.66
VTS	-1.59	-8.35
VTS	-1.54	-8.59
VTS	-1.47	-8.68
VTS	-1.49	-8.93
VTS	-1.59	-8.66
VTS	-1.52	-8.59
VTS	-1.54	-8.64
VTS	-1.48	-8.57
VTS	-1.46	-8.68
VTS	-1.40	-8.77
VTS	-1.55	-8.48
VTS	-1.55	-8.76
VTS	-1.39	-8.04
VTS	-1.67	-8.35
VTS	-1.55	-8.56
VTS	-1.43	-8.74
VTS	-1.53	-8.72
VTS	-1.60	-8.60
VTS	-1.49	-8.67

STANDARD	$\delta^{13}C_{carb}$	$\delta^{18}O_{carb}$
VTS	-1.42	-8.66
VTS	-1.45	-8.74
VTS	-1.45	-8.53
VTS	-1.54	-8.56
VTS	-1.57	-8.55
VTS	-1.48	-8.66
VTS	-1.54	-8.69
IAEA-CO-8	-5.78	-22.80
IAEA-CO-8	-5.77	-22.82
IAEA-CO-8	-5.70	-22.55
IAEA-CO-8	-5.73	-22.95
IAEA-CO-8	-5.68	-22.73
IAEA-CO-8	-5.72	-22.84
IAEA-CO-8	-5.68	-23.03
IAEA-CO-8	-5.80	-22.83
IAEA-CO-8	-5.52	-22.53
IAEA-CO-8	-5.64	-22.91
IAEA-CO-8	-5.68	-22.81
IAEA-CO-8	-5.69	-22.96
IAEA-CO-8	-5.72	-22.90
IAEA-CO-8	-5.71	-23.03
IAEA-CO-8	-5.72	-23.08
IAEA-CO-8	-5.75	-23.01
IAEA-CO-8	-5.75	-22.66
IAEA-CO-8	-5.79	-22.81
IAEA-CO-8	-5.73	-22.37
IAEA-CO-8	-5.67	-22.71
IAEA-CO-8	-5.72	-22.65
IAEA-CO-8	-5.69	-23.07
IAEA-CO-8	-5.73	-22.87
IAEA-CO-8	-5.69	-22.77
IAEA-CO-8	-5.70	-22.27
IAEA-CO-8	-5.71	-22.54
IAEA-CO-8	-5.75	-22.08
IAEA-CO-8	-5.67	-22.72
IAEA-CO-8	-5.63	-22.48
IAEA-CO-8	-5.76	-22.81
IAEA-CO-8	-5.68	-22.83
IAEA-CO-8	-5.67	-22.88
IAEA-CO-8	-5.72	-22.96
IAEA-CO-8	-5.59	-22.55

APPENDIX 2 (Continued)

STANDARD	$\delta^{13}C_{carb}$	$\delta^{18}O_{carb}$
IAEA-CO-8	-5.74	-23.08
IAEA-CO-8	-5.64	-22.89
IAEA-CO-8	-5.64	-22.73

STANDARD	$\delta^{13}C_{carb}$	$\delta^{18}O_{carb}$
IAEA-CO-8	-5.74	-22.68
IAEA-CO-8	-5.67	-22.72
IAEA-CO-8	-5.72	-22.86

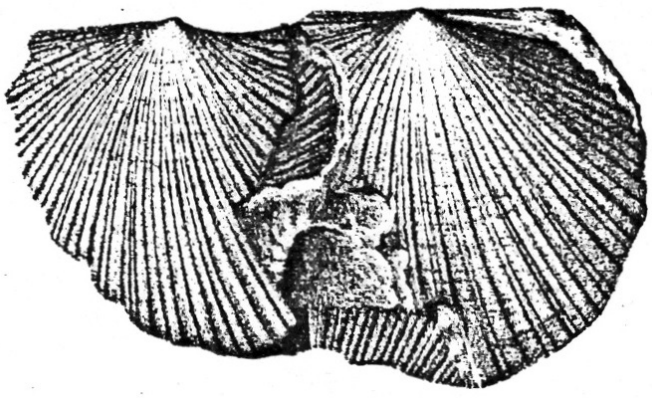

Meeting Report

16th INTERNATIONAL PERMIAN-TRIASSIC FIELD WORKSHOP IN ARDÈCHE (SOUTHEAST BORDER OF THE FRENCH MASSIF CENTRAL)

Bourquin, Sylvie

Univ. Rennes, CNRS, Géosciences Rennes, UMR 6118, F-35000, Rennes, France. sylvie.bourquin@univ-rennes1.fr

The coordination of the International Permian-Triassic Workshop was passed in 2020 from G. H. Bachmann, Halle/Germany, to S. Bourquin, and the 16th field workshop took place on September 10–13, 2021 in France. It was organized by the AGPT (Association des Géologues du Permian et du Trias, https://agpt.wordpress.com/) of which S. Bourquin is the president. This excursion was guided by J.B. Regnet, Cergy Paris Univ., C. Bailly, Paris Saclay Univ., E. Fara, Univ. Bourgogne - Franche-Comté and D. Bonijoly, BRGM (French geological survey) Orléans (Regnet et al., 2021). The aim of this excursion, initially intended for AGPT members, in July 2020, was to present recent research on the Ardèche Triassic. We were to organize another excursion in 2021 as part of the 16th workshop in order to present a synthesis of the Triassic of Ardèche. The pandemic forced us to reschedule the AGPT field trip in July 2021, which was cancelled a second time, and then in September 2021, preventing us from scheduling another field trip in 2021. Therefore, we have decided to open our field trip to the 16th International Permian-Triassic Field Workshop. In consequence, this excursion welcomed 15 participants from France, Italia, Spain and Germany, who were accommodated in a hotel in the small village of Sanilhac and two rented minibuses were used for transport.

The first morning was devoted to a presentation of the Ardèche Paleomargin, well studied in 1990s and which had led to the acquisition of seismic lines and two drilling in order to study the Triassic successions from the Anisian to the Rhaetian. At the beginning of the Mesozoic, the Ardèche area was on the western

Figure 1 – Top of fluvial sandstone deposits with vertebrate footprints of le Sartre outcrop, Formation Bariolée d'Ucel, Late Triassic. The ichnoassociation is dinosaur-dominated (*Grallator*, *Otozoum*) and rare pseudosuchian tracks (*Brachychirotherium*) also occur (Szewczyk et al., 2017; Fara et al., 2021).

Figure 2 – Workshop participants on Anisian sandstones, Grès de base Formation, of the Tétine du Vernon outcrops showing pedogenic structure.

edge of the Ligurian Ocean Basin. The subsurface data show that sedimentary thicknesses increase rapidly eastward and become more complete toward the so-called Southeast Basin. Outcrops at Uzer, 6 km SE of Sanilhac, show erosive gaps from Sinemurian to Aalenian overlain by Bathonian marls. The afternoon was focus on the observation of Middle and Late Triassic vertebrate footprints (Chirotherium at Blaze, near Sanilhac, and of dinosaurs at Le Sartre, near Aubenas, Fig. 1), whose preservation criteria in fluvial sandstone deposits (Grès du Roubreau et Formation Bariolée d'Ucel respectively) have been recently studied (Szewczyk et al., 2017, Fara et al., 2021).

The second day was devoted to fluvial deposits. First, colleagues from the Universities of Cergy and Saclay presented the ongoing studies concerning an integrated approach in sedimentology, diagenesis and rock physics. From the example of the Upper Triassic outcrops and cores, the objective is to better understand the 3D architecture of cyclic deposits of alluvial fans and dolomitic paleosols (Formation Bariolée d'Ucel) and potential applications in geothermal energy. This formation is covered, at the outcrop of Les Vans, by fine Rhaetian sandstones, topped by marls rich in Callovian fossils. In a second step, we also observed the unconformity between the Variscan basement and the first preserved fluvial deposits, the Grès de base Formation, attributed to the Anisian. These outcrops also allowed us to discuss pedogenic structures, attributed to stumps, well observed in these early Triassic deposits of Ardeche (Fig. 2). During lunch, N. Klee presented the UNESCO Monts d'Ardèche Global Geopark.

In 2022, the 17th workshop associated with the AGPT field trip will be organised in the Cantabrian Mountains, Spain, probably in early July. The excursion will focus on the Permian and the Triassic of that region based on new data and a multidisciplinary approach. We expect a more detailed announcement by the end of December.

REFERENCES:

Fara E., Moreau J.-D., Szewczyk L., Klee N., Gand G. & Vennin E. 2021. Inventory and Conservation of Triassic Vertebrate Tracks in the Montsd'Ardèche UNESCO Global Geopark, France. Geoconservation Research, 4(2), 13 p. http://dx.doi.org/10.30486/gcr.2021.1912278.1045

Regnet J.B., Bailly C., Fara E., Bonijoly D., & Bourquin S. 2017. The Triassic in Ardèche (SE border of the French Central Massif), 16th International Triassic Field Workshop and AGPT Field Trip., 10-13 septembre, 24 pp. https://agpt.wordpress.com/

Szewczyk L., Vennin E., Moreau J.-D., Gand G., Verolet M., Klee N. & Fara E. 2020. Tracking dinosaurs in coarse-grained sediments from the Upper Triassic of Ardèche (southeastern France). Palaios, 35(11): 447-460.

Research Article

HALOBIA AUSTRIACA IN NORTH AMERICA WITH A REAPPRAISAL OF ITS DISTRIBUTION ACROSS THE CARNIAN-NORIAN BOUNDARY INTERVAL AT BLACK BEAR RIDGE (NORTHEASTERN BRITISH COLUMBIA, CANADA)

Christopher A. McRoberts

Geology Department, State University of New York at Cortland, Cortland, NY 13045, USA;
Email: mcroberts@cortland.edu

Abstract – The pelagic pterioid bivalve *Halobia austriaca* occurs most commonly in earliest Norian deep-marine facies in the Tethyan and circum-Panthalassan realms, including the candidate GSSPs at the Pizzo Mondello (Sicily) and at Black Bear Ridge (British Columbia, Canada) and other localities in Haida Gwaii (western British Columbia), southern Alaska, California and Oregon and questionably in Arctic Alaska. Reported occurrences of *H. austriaca* from other North American localities are shown to be either misidentifications or based on specimens too poorly preserved for identification. Previous work on the halobiid biostratigraphy at Black Bear Ridge suggested a first occurrence of *H. austriaca* from bed 18f, at a position coinciding with a major conodont turnover between the lower and middle subdivisions of the *Metapolygnathus parvus* Subzone of the *Primatella primitia* conodont Zone, and several meters below the traditionally Norian ammonoid zone of *Stikinoceras kerri*. Reappraisal of *H. austriaca* from Black Bear Ridge now places the lower occurrence of the species from bed 22. This revised datum integrated with ammonoids and conodonts, provides for a more parsimonious correlation with the basal-Norian GSSP candidate section at Pizzo Mondello and elsewhere across Panthalassa and Tethys.

INTRODUCTION

The Carnian-Norian boundary is one of several stage boundaries of the Triassic System that remains to be defined with a Global Stratotype Section and Point (GSSP). Following years of activity within the Subcommission on Triassic Stratigraphy (STS) and its base-Norian Working Group, several base-Norian GSSPs have been variously proposed. Recent proposals include: (1) the first occurrence datum (FOD) of the conodont of *Metapolygnathus parvus* Kozur, 1972 as supported by Mazza et al. (2018), (2) the last occurrence (LOD) of the same conodont species as supported by Mazza et al. (2012) and Orchard (2019), and (3) the FOD of the pelagic bivalve *Halobia austriaca* Mojsisovics (1874) as supported by Krystyn (2010), Levera and McRoberts (2010), McRoberts & Krystyn (2011), Balini et al. (2012) and Levera (2012). These datums are recognized in the two proposed GSSP stratigraphic sections: Pizzo Mondello (Siciani Basin, Sicily) and Black Bear Ridge (Western Canada Sedimentary Basin, British Columbia, Canada). Quite recently (July, 2021), the base-Norian Working Group completed the preliminary rounds of balloting selecting the FOD of the bivalve *Halobia austriaca* from bed 135 at the Pizzo Mondello section of Sicily. If the FOD of *Halobia austriaca* at Pizzo Mondello is ultimately chosen, it would represent only the third Phanerozoic GSSP defined by a bivalve mollusc, the others being Cretaceous inoceramids *Platyceramus undulatoplicatus* defining the base of the Santonian (Lamolda et al., 2014) and *Cremnoceramus deformis erectus* which was recently approved by the Subcommission on Cretaceous Stratigraphy to define the base of the Conacian Stage and is currently being evaluated by the International Commission on Stratigraphy.

The initial advocation of *Halobia austriaca* as a defining datum for the basal Norian (Krystyn, 2010, Levera and McRoberts 2010) did not proffer any particular stratotype. In a poster presentation at the Canadian Paleontology Conference, McRoberts and Krystyn (2011) proposed the FOD of *Halobia austriaca* at the Black Bear Ridge section along the north shore of Williston Lake (British Columbia, Canada) as a potential datum for the basal Norian GSSP. This proposal was largely based on the recently completed monograph of Late Triassic Bivalvia

Published online: November 5, 2021

McRoberts, C.A. 2021. *Halobia austriaca* in North America with a reappraisal of its distribution across the Carnian-Norian boundary interval at Black Bear Ridge (northeastern British Columbia, Canada). *Albertiana*, vol. 46, 13–24.

from the Williston Lake area (McRoberts, 2011). McRoberts (2011) and McRoberts and Krystyn (2011) proposed the first occurrence *Halobia austriaca* in bed 18f of the Black Bear Ridge section as the primary marker defining the basal Norian GSSP. Since 2011, work on the halobiids from the Williston Lake area and elsewhere from North America has continued at a slow pace, yet has resulted in a re-evaluation on the taxonomic status and occurrence of *H. austriaca*. This report, therefore, provides a summary of the current status of *H. austriaca* in light of new and revised findings from Black Bear Ridge and other North American localities that have direct bearing on the position and choice of *H. austriaca* for a basal Norian GSSP.

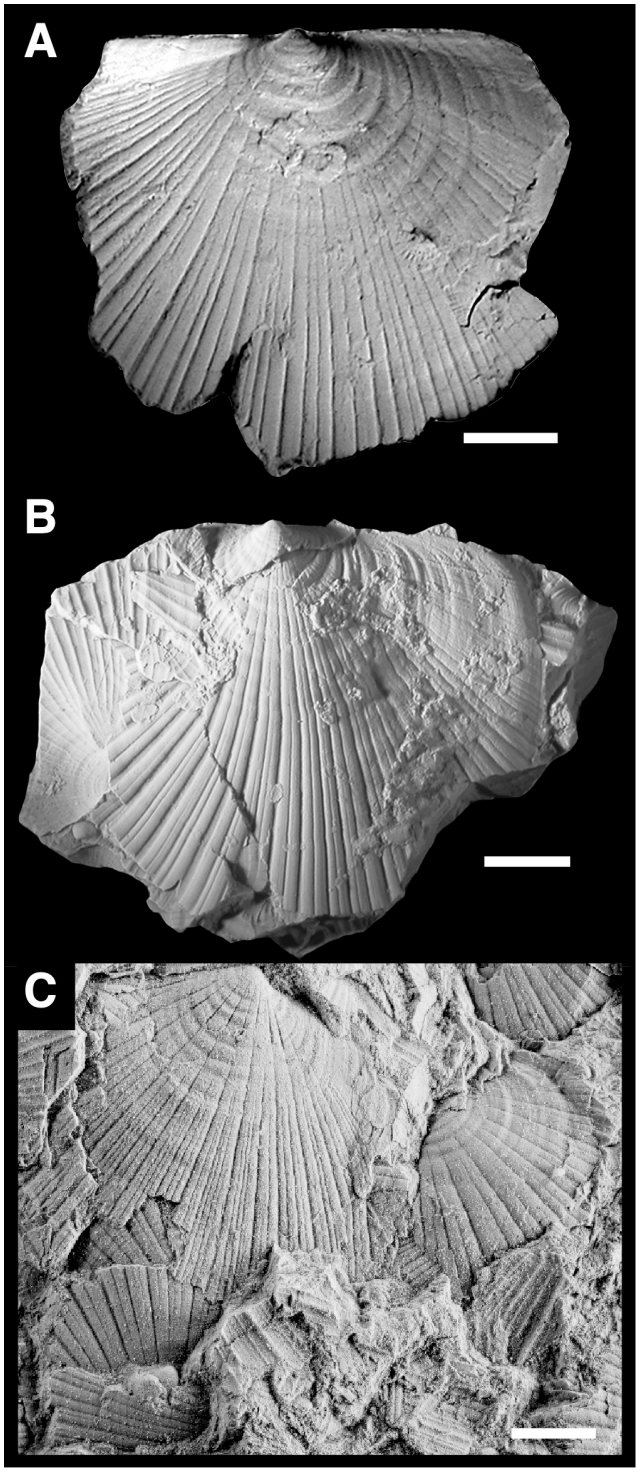

Figure 1 – **A**, *Halobia austriaca* Lectotype, a RV, from Mojsisovics (1874, pl. 4, fig. 3), Raschberg, Austria; **B**, *Halobia austriaca* Paratype, Mojsisovics, (1874, pl. 4, fig. 1), Raschberg, Austria; **C**, slab of *Halobia austriaca* from Feuerkogel Section F1-E, Austria (McRoberts unpubl. collection). Scale bars = 1 cm.

On the taxonomic status of *Halobia austriaca* and implications for regional and global correlation

Halobia austriaca is one of the most ubiquitous halobiid species, with significant occurrences reported from across the western Tethys (e.g., Austria, Italy, Bosnia-Herzegovina) and in both eastern and western Panthalassa (e.g., China, New Zealand, Timor, Japan, Canada, USA). The species was introduced by Mojsisovics (1874) who described and illustrated four specimens from what is now considered lower Norian (Lac 1) strata of the Hallstatt Limestone of Raschberg, Pötschenstein, and Röthelstein, Styria Austria. Although no type specimen was originally identified, Campbell (1994) designated one of Mosjsisovics' original specimens (GBA 1874/01/3; Mojsisovics, 1874, pl. 4, fig. 3) from Raschberg as the lectotype. Mojsisovics' (1874) types of *H. austriaca* and additional specimens from the nearby Feuerkogel locality are illustrated in Figure 1.

Since Mojsisovics introduced the species, *Halobia austriaca* has been described from more than 50 localities and seen several major taxonomic reviews and revisions. Although a complete review of all available literature of on the taxonomic position and stratigraphic and geographic distribution of *H. austriaca* is beyond the scope of this report, it is relevant to mention some of the major publications which impact on the taxonomic status of the species and its geographic and temporal distribution within biostratigraphically-controlled stratigraphic sections. Following introduction of the species by Mojsisovics (1874), several significant taxonomic works on *H. austriaca* have been published from Western Tethys including: Austria (Kittl, 1912; Gruber 1977); Bosnia-Herzegovina (Gruber, 1975); Italy, including the Apennines (De Capoa Bonardi, 1970) and Sicily (Cafiero and De Capoa Bonardi, 1982; Levera, 2010, 2012). In the eastern Tethys and western Panthalassa, *H. austriaca* is known from Timor (Krumbeck, 1924), and New Zealand (Campbell, 1994). From northeastern Russia, several early publications (e.g., Kiparisova, 1947; Vozin and Tikhomirova, 1964; Bychkov et al., 1976) noted and discussed the occurrence of *H. austriaca*. In North America, *H. austriaca* was first reported and reviewed by Smith (1927) from localities in California and Alaska and more recently by McRoberts (2011) from northeastern British Columbia.

Beginning with Mojsisovics (1874) and prior to the 1970s, *H. austriaca* was most often considered to be of late Carnian age. This was in part due to Mojsisovics' (in Mojsisovics et al., 1885) temporal inversion of the Carnian and Norian stages in the Hallstatt area of Austria, and also in part due to lack of co-occurring ammonoids in *H. austriaca*-bearing strata across the western Tethy's. More recent publications (e.g., Gruber, 1975, 1976, 1977; Cafiero and De Capoa Bonardi, 1982; Levera, 2010, 2012; McRoberts, 2010, 2011) the species is considered to

straddle a Carnian-Norian boundary or positioned it within the basal Norian (within the *Guembelites jandianus* or *Stinkinoceras kerri* ammonoid zones and equivalents).

At present, a species-level phylogenetic series including *Halobia austriaca* has not been demonstrably determined by authorities in part because morphologic traits used to define and describe halobiid species appear to exhibit mosaic and homoplastic tendencies across the history of the genus. Gruber (1977) proposed that *H. austriaca* was descendant from an as yet unknown species (itself derived from *Halobia bithynica*) sometime in the Late Carnian. Given a lack of likely immediate ancestor for *H. austriaca* in the western Tethys where *H. austriaca* may be an immigrant, it is plausible that potential ancestors could be found in the Panthalassic realm. One possible candidate ancestor is *Halobia selwyni* whose numerous similarities with *H. austriaca* are striking (see below) and is known to occur in an appropriate stratigraphic position immediately below and co-occurring with *H. austriaca* in the Black Bear Ridge section of Williston Lake. Other potential ancestors of *H. austriaca* are certainly possible and can be chosen from within the several species groups that include *H. austriaca* (e.g., Gruppe der *Halobia rarestriata* of Mojsisovics (1874); Gruppe der *Halobia austriaca* of Kittl, 1912; Reihe der *Halobia austriaca* of Gruber 1977). Even other Halobia species outside of these informal groups, including those that possess a growth-stop (deflection in ribs), such as *H. brooksi*, cannot be ruled out.

On the relationship between *Halobia austriac*a and potential synonymous species

As introduced above, the taxonomic status of *Halobia brooksi* and its potential affinity to *Halobia austriaca* is of significance in the position of potential halobiid datums in the selection of a basal Norian GSSP and inter-regional correlations. Smith (1927, pl. 99, figs. 7–9) described and illustrated three specimens from the Kuskulana River area of the Wrangell Mountains of southern Alaska which served as the basis for his new species *Halobia brooksi*. The primary criterion for differentiation between the two species as stated by Smith (1927) is the presence of a deflection in the radial ribs (here termed growth-stop) in *Halobia brooksi* whereas in *H. austriaca*, the ribs run relatively straight or are only slightly curved anterior in their course. The illustrated *H. brooksi* of Smith (1927, pl. 99, figs. 7–9) show an apparent growth-stop positioned approximately 20–25 mm from the beak. While the specimens exhibit some signs of taphonomic crushing/fracture, the growth stop in these specimens is apparently not an artifact. Apart from the possible growth-stop, the types *H. brooksi* appear superficially similar to *H. austriaca* in outline, posterior and anterior triangular fields, auricles, and radial rib profile. These similarities, however, fail to be confirmed upon closer inspection in finer details. McRoberts (2011) concluded that *H. brooksi* differs from H. austriaca in possessing a shallower anterior triangular field (23° for *H. brooksi* versus about 30° for *H. austriaca*) and perhaps more importantly in the rib bundling. The external ribbing of *H. brooksi* is strongly bundled by up to 10 fine riblets whereas *H. austriaca* generally maintains simple division into secondary and sometimes tertiary ribs of somewhat equal strength. Furthermore, Smith (1927) stated that ribbing was somewhat coarser in *H. brooksi* than in *H. austriaca*, although such a claim is not borne out in his illustrated specimens given that the holotype of *H. brooksi* (Smith, 1927, pl. 99, fig. 7) has demonstrably finer and more densely-packed ribs than several of his specimens assigned to *H. austriaca* (pl. 99, figs. 11, 12) as well as from the original *H. austriaca* of Mojsisovics (1874). Even though knowledge on the range of morphologic variation of *H. brooksi* in North America is poorly known, this species possesses a distinctive morphology and is maintained as a separate species distinct from *H. austriaca*.

Gruber (1975, 1977) synonymized several previously named species possessing a growth-stop, including *Halobia brooksi*, into an expanded concept of *H. austriaca*. By doing so (and explicitly stated in Gruber 1976) Gruber concluded that the presence of a growth-stop by itself should not be considered a character of species-level significance. Gruber (1975) synonymized *H. ocevljana* of Kittl (1912, text-fig. 36 and pl. 7, fig. 22) from the Ocevlja locality in Bosnia-Herzegovina into *H. austriaca*. This was reaffirmed in his 1977 thesis in which he also included *H. brooksi* in his synonymy of *H. austriaca*. Both synonymies were followed by Cafiero and De Capoa Bonardi (1982) and later Campbell (1994) without comment. Gruber (1975, pl. 3, figs. 1-4), illustrated four specimens assigned to *H. austriaca* from the lower Norian (Lac 1) in the Dragulac and Ocevlja sections in Bosnia-Herzegovina of which one was Kittl's original specimen of *H. ocevljana* (Kittl, 1912 pl. 7, fig. 22). These specimens appear to show a growth-stop and deflection of radial ribs in spite of signs of taphonomic fracture and deformation. As with North American *H. brooksi*, it is here maintained that synonymy of *H. ocevljana* into *H. austriaca* is not warranted.

Additional consideration of *Halobia austriaca* and its potential synonymies in northeastern Russia are also relevant. As noted by Alexey Konstantinov (communication to the base Norian task group, August 2020), *H. austriaca* has been cited to occur in northeastern Russia multiple times with occurrences in the Yana, Indigirka, and Kolyma River basins. Of particular importance is that the species has been assigned to the upper Carnian *Sirenites yakutensis* ammonoid Zone (e.g., Kiparisova, 1947; Vozin and Tikhomirova, 1964; Bychkov et al., 1976), but has not been confirmed by more recent publications (e.g., Polubotko, 1984, 1986, 1988, 2005; Polubotko et al., 1990). It is relevant that Polubotko (1986, p. 68) synonymized northeast Russian *H. austriaca* that was previously illustrated in Bychkov et al. (1976, p. 44, figs. 6-8) into her new species *Indigirohalobia kilganaensis*. In her zonal chart, Polubotko (1986, p. 65) listed both *Indigirohalobia kilganaensis* and *Zittelihalobia brooksi* (= *Halobia brooksi* herein) as occurring in the lower subzone of the *Sirenites yakutensis* ammonoid zone below the upper subzone of *Sirenites yakutensis* which was deemed equivalent to *Anatropites* bearing strata of North America. In Polubotko (2005), both *Primahalobia kilganaensis* (presumably the same taxon as *H. austriaca* of Bytchkov et al., 1976) and *Indigirohalobia* (*Popowihalobia*) *brooksi* (= *Halobia brooksi* herein) were listed as indices of the *Indigirohalobia* (*Popowihalobia*) *asperella* zone which spans a Carnian-Norian boundary interval and is the equivalent to the *Sirenites yakutensis*, *Striatosirenites kedonensis* and *Striatosirenites*

kinasovi ammonoid zones. This position (in Polubotko, 2005) appears to extend into somewhat younger ages than that suggested by earlier zonal schemes (e.g., Polubotko, 1986) which relegated *H. austriaca*-like forms to the just the *Sirenites yakutensis* zone.

NORTH AMERICAN *HALOBIA AUSTRIACA*

Given the importance of *Halobia austriaca* in global correlation and particularly its well documented occurrence in candidate GSSP sections, this section provides an assessment and re-evaluation of occurrences of *H. austriaca* as it is known or reported from western North America and in particular its occurrence in the candidate GSSP and likely auxiliary section in western Canada. Across North America, *H. austriaca* has been reported to occur in numerous tectonic settings from tectonostratigraphic terranes to strata affiliated with the Triassic North American craton (Fig. 2). Notably, many of the reported occurrences of *H. austriaca* in North America have not been re-evaluated in light of revised systematic validity since their initial descriptions, and nor have been carefully vetted with respect to stratigraphic position.

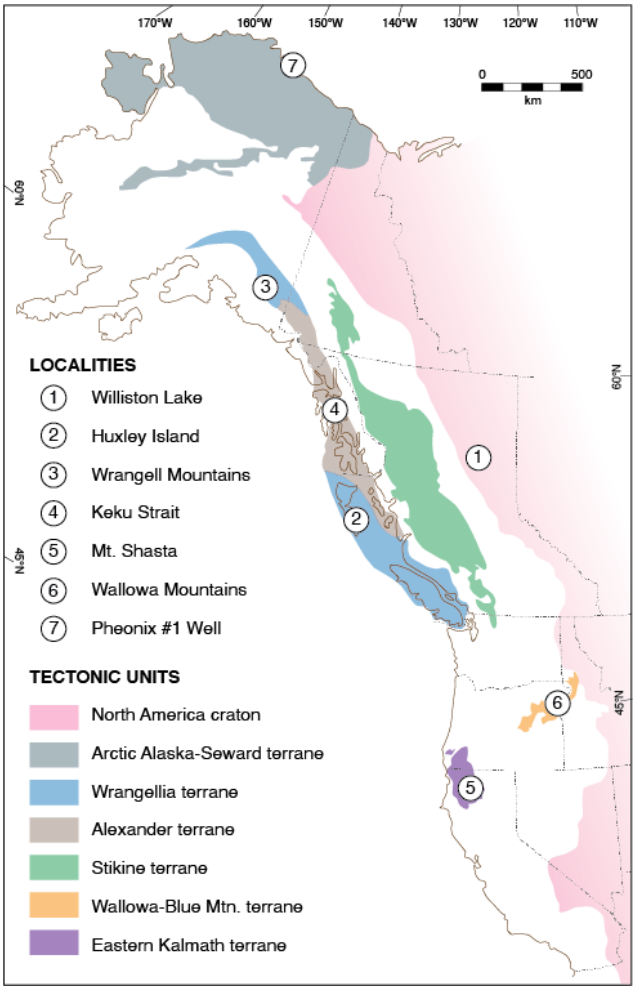

Figure 2 – Simplified map of western North America showing the distribution of several tectonostratigraphic terranes and halobiid localities discussed in text.

Re-evaluation of *Halobia austriaca* from Black Bear Ridge and other localities on Williston Lake

The Black Bear Ridge section lies on the north shore of Williston Lake (Figs. 2–5), 4 km northeast of the mouth of Nabesche River (NTS Map 94 B/3; zone 10, UTM 497670E, 6215500N). The halobiid-bearing Carnian-Norian boundary interval lies within the lower part of the Pardonet Formation and consists of thin to medium-bedded carbonaceous silty limestone, calcareous and dolomitic siltstone and shale likely deposited below fair-weather wave base in deep water setting slope well off the western margin of Pangaea (Zonneveld et al., 2010). Although stratigraphical, sedimentological and geochemical attributes of Carnian-Norian interval part of the Black Bear Ridge section and those of the nearby Pardonet Hill and Brown Hill sections can be found elsewhere (e.g., Orchard et al., 2001; Williford et al., 2007; Zonneveld et al., 2010; Onoue et al., 2016; Lei et al., 2021), a summary of section and important biostratigraphical horizons are illustrated in Figure 4.

In McRoberts (2007, 2011) and McRoberts and Krystyn (2011), the lowest occurrence (FOD) of *Halobia austriaca* was listed as occurring in bed 18f in the Black Bear Ridge section. It should be noted that in the Black Bear Ridge section (see Orchard, 2014, 2019), bed 18f occurs approximately 1.7 m above the highest occurrence of the ammonoid *Anatropites* in bed 17, and 30 cm above of the lowest occurrence of *Pterosirenites* sp., a single occurrence of *Griesbachites* and the highest occurrence of *Tropiceltites* sp. in bed 18d. Bed 18f falls within the range of several occurrences of *Gonionotites* sp. Furthermore, this datum also occurs 3.8 meters below the first occurrence of *Guembelites clavatus*, a proxy for the lower part of the *Stikinoceras kerri* Zone sensu Silberling and Tozer (1968) and Tozer (1994). Additionally, a large number of conodont species occur in bed 18f which is within 5 cm above the boundary between the lower and middle subdivisions of the *Metapolygnathus parvus* Subzone of the *Primatella primitia* conodont Zone (Orchard, 2014, 2019). Correlations of the conodont and ammonoid record (Orchard, 2014, 2019) suggest that the *Metapolygnathus parvus* Subzone is equivalent to the uppermost part of the *Klamathites macrolobatus* ammonoid zone — the youngest zone of the traditionally recognized Upper Carnian. Thus, the original determination from Black Bear Ridge (McRoberts, 2011) placed the FOD of *H. austriaca* within beds of the upper part of the *K. macrolobatus* ammonoid zone confirmed with both conodonts and ammonoids.

In the nearly 10 years since the publication of McRoberts (2011) and McRoberts and Krystyn (2011), the author has re-examined the original halobiid material from Black Bear Ridge and studied additional material of *Halobia austriaca* and other halobiid bivalves from the Black Bear Ridge locality and other localities on Williston Lake and elsewhere in North America and Europe. These studies have led me to re-evaluate the stated occurrences and provide a revised succession of the Black Bear Ridge halobiid occurrences.

The results indicate that the two lowest original data points for

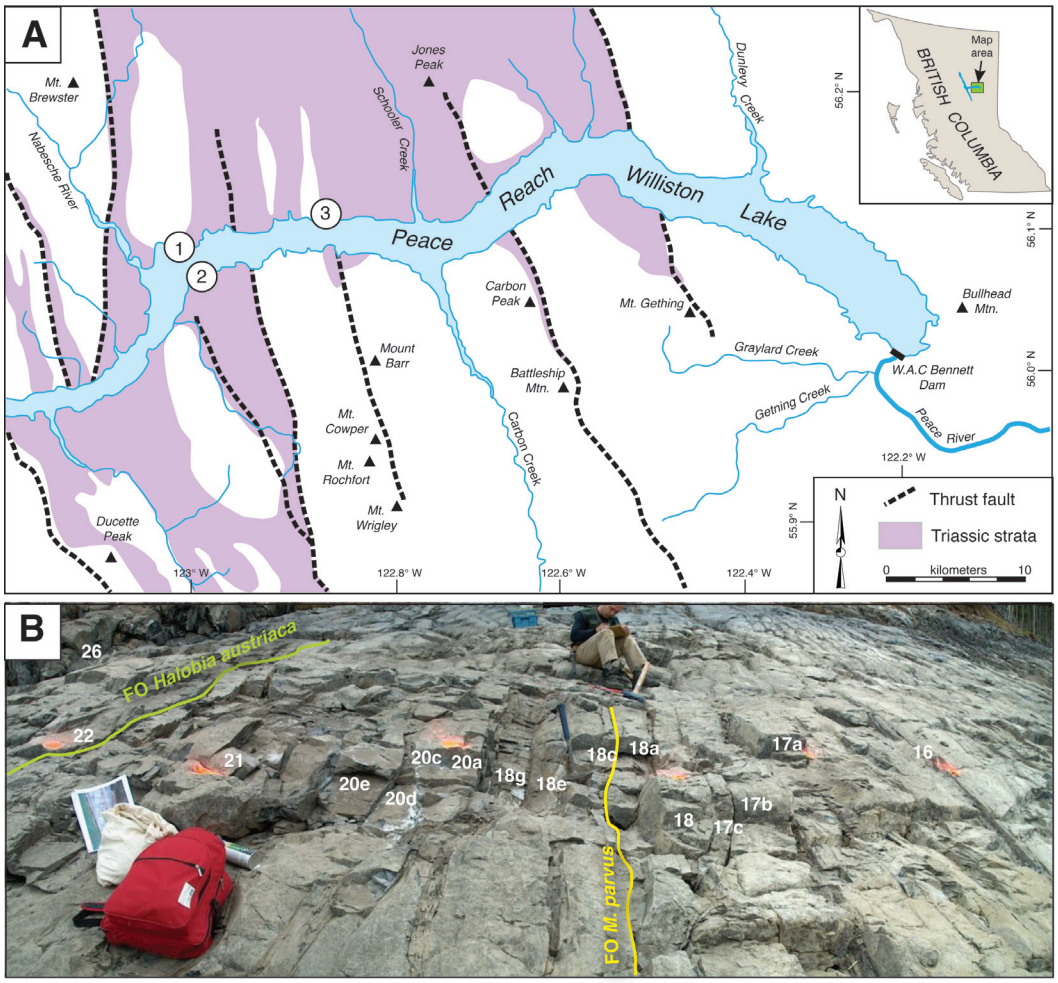

Figure 3 – **A**, Map of eastern Williston Lake area showing localities discussed in text. Numbered localities include 1, Black Bear Ridge; 2, Pardonet Hill East; 3, Borwn Hill. Modified from Zonneveld et al. (2010); **B**, Outcrop map of Black Bear Ridge Carnian-Norian boundary interval. Refer to stratigraphic log (Fig. 4) for bed numbers.

Halobia austriaca from McRoberts (2011), C-307815 (bed 18f) and CM01BBR-4 (bed 21), are based on incomplete specimens that, although shareing similarities with true *H. austriaca*, likely belong to a different *Halobia* species – most likely *H. selwyni*. An undescribed halobiid specimen collected by Mike Orchard from bed 20f (GSC loc. C-307823) within the *Metapolygnathus parvus* Subzone (see attached figure) is typical of the two aforementioned adjacent occurrences (beds 18f and 21), albeit these fragments are somewhat larger and better preserved and suggest closer affinity to *H. selwyni* but with broader and less curved ribs. It should also be noted that there are other confirmed *H. selwyni* from bed 18f (McRoberts, 2011, fig. 18.11) and several additional levels both below and above (beds 18d–24).

Based on the current understanding of halobiids at BBR, the lowest *Halobia austriaca* that can be identified with confidence occurs in bed 22 (McRoberts, 2011, fig. 18.2 and reproduced in Figure 5). It should be further noted that the *H. austriaca* occurrence in bed 22 was listed in McRoberts (2011, figs. 9, 18.2, and Appendix 5) but not included in the range chart of Orchard (2019, fig. 2). Bed 22 occurs approximately 35 cm above base of the *Primatella asymmetrica-Norigondolella* conodont Subzone above the *Metapolygnathus parvus* Subzone and 15 cm below the first occurrence of ammonite *Guembelites clavatus* in bed 22b. It is therefore likely that this level (bed 22) occurs within the lower *S. kerri* ammonoid zone. The revised stratigraphic distribution of halobiid bivalves and key ammonoid and conodont events are shown in Figure 4.

Apart from the Black Bear Ridge section, additional occurrences of *Halobia austriaca* in Williston Lake outcrops provide insight into the first occurrence of this species and possible synonymies. McRoberts (2011, fig. 18.3) illustrated a single small specimen attributed to *H. austriaca* from Brown Hill. Upon re-evaluation, this specimen, is indeed quite similar to *H. austriaca* in many of its features, but possess finer and more densely-packed ribs in its posterior sector atypical of the species and suggest placement into *H. selwyni*. Based this revision, *H. austriaca* remains to be identified from the Brown Hill section.

McRoberts (2011, figs. 18.5, 18.6) illustrated two specimens attributed to *Halobia austriaca* from beds 3 and 4 in Pardonet Hill East section. Although clearly juveniles, these specimens are only questionably assigned to *H. austriaca* and may be better placed into *H. selwyni*. According to Orchard (2014, 2019),

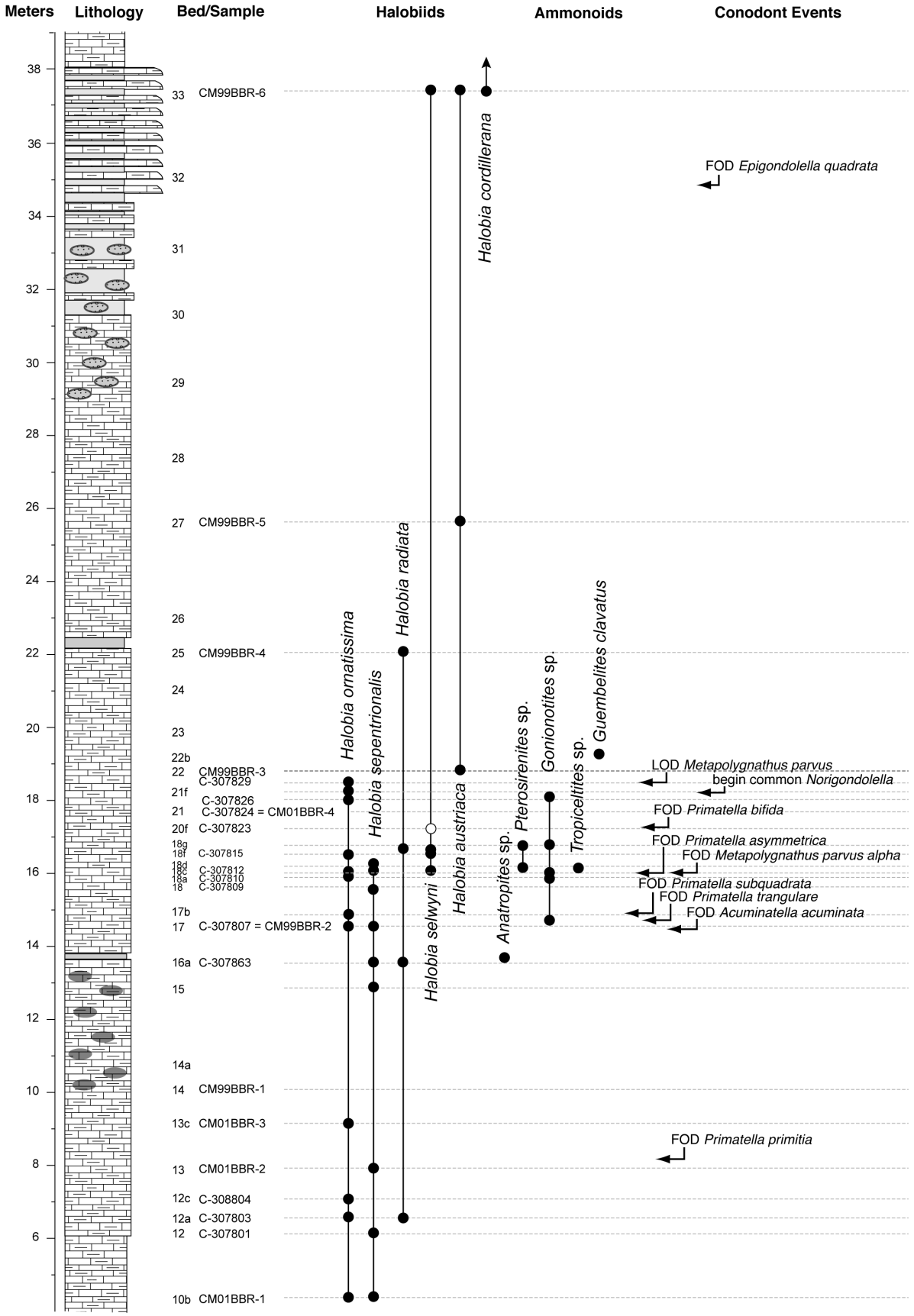

Figure 4 – Revised halobiid biostratigraphy at Black Bear Ridge. Ammonoid ranges and conodont bioevents from Orchard (2014, 2019). FOD = first occurrence datum, FAD = last occurrence datum.

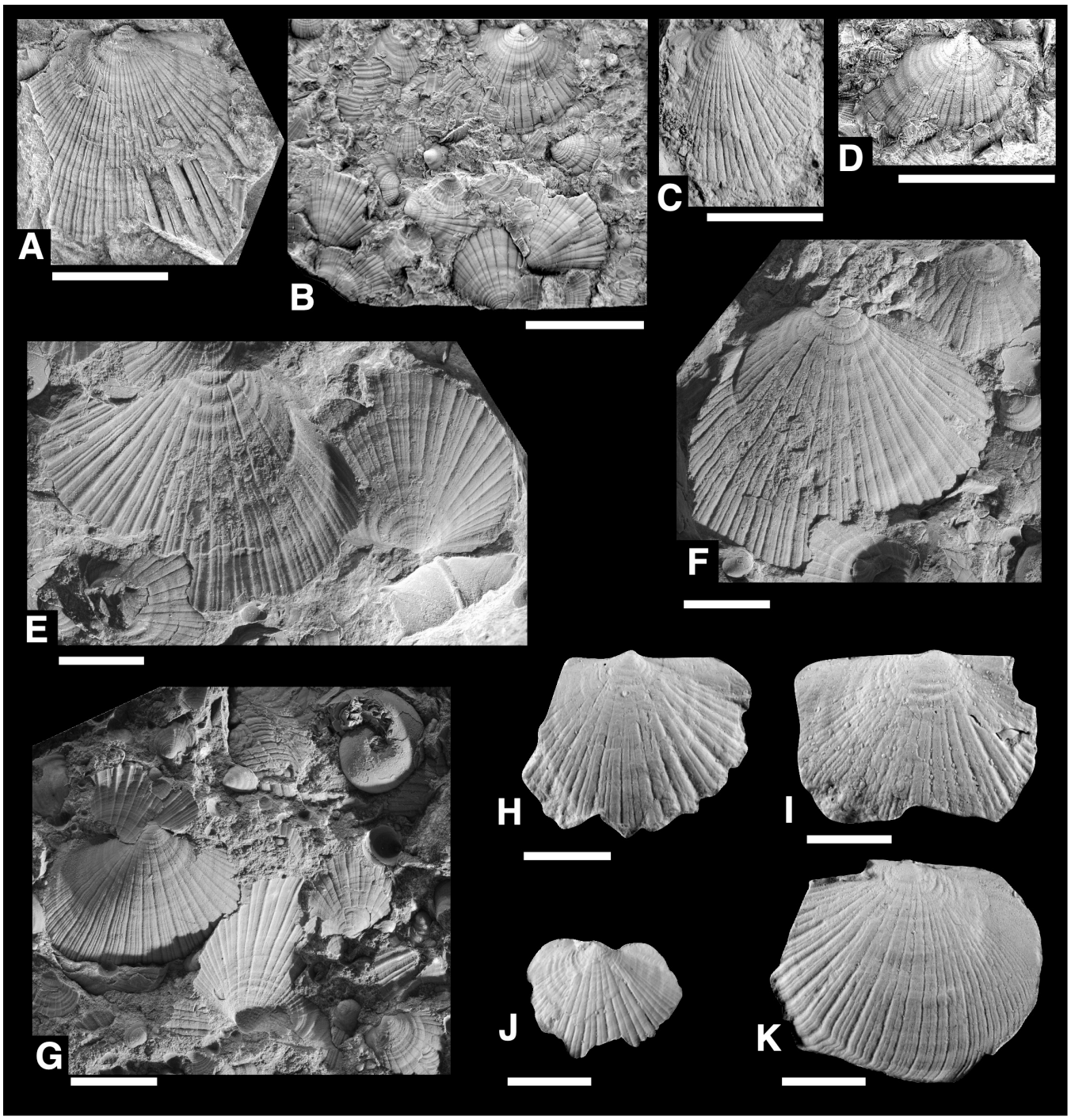

Figure 5 – **A**, *Halobia austriaca*, GSC 132229; Black Bear Ridge bed 27 (from McRoberts, 2011, fig. 18.1); **B**, *Halobia austriaca*, GSC 132230, Black Bear Ridge bed 22 (from McRoberts, 2011, fig. 18.2); **C**, *Halobia austriaca*, GSC 132232, Black Bear Ridge bed 33 (from McRoberts, 2011, fig. 18.4); **D**, *Halobia selwyni*, GSC 132231, Brown Hill, loc. CM99BRH-2 (from McRoberts, 2011, fig. 18.3); **E**, *Halobia austriaca*, GSC loc. 157119, Huxley Island, British Columbia; **F**, *Halobia austriaca*, GSC loc. 157119, Huxley Island, British Columbia; **G**, *Halobia austriaca*, GSC loc. C-157123, Huxley Island, British Columbia; **H**, *Halobia austriaca*, USNM 74190, Copper River area, Alaska (from Smith, 1927, pl. 99, fig. 12); **I**, *Halobia austriaca*, USNM 74190, Copper River area, Alaska (from Smith, 1927, pl. 99, fig. 10); **J**, *Halobia austriaca*, USNM 74189, Admiralty Island, Alaska (from Smith, 1927, pl. 99, fig. 13); **K**. *Halobia brooksi*, Holotype, USNM 74188, Copper River area, Alaska (from Smith 1927, pl. 99, fig. 7). Scale bars = 1 cm.

these two levels (beds 3 and 4), are separated by approximately 4 cm, contain the ammonoids *Gonionotites*? sp. and *Pterosirenites auritus* and are close to the boundary between the *Acuminatella acuminata-Parapetella prominens* and the lower subdivision *Metapolygnathus parvus* Subzone — approximately 1.7 m below *Guembelites* cf. *jandianus* and *Stikinoceras* cf. *kerri*. It should be noted that *Anatropites* sp. has not been recovered from the Pardonet Hill East section, but has been reported from a nearby

locality on the west side of Pardonet Hill (Tozer, 1994). There were no other occurrences of similar taxa that can confidently be attributed to *H. austriaca* recovered from the Pardonet Hill East section.

Tozer (1994, pl. 108, fig. 14a) illustrated a halobiid specimen from the west side of Pardonet Hill embedded in the umbilicus of an *Anatropites* that superficially appears to be a juvenile *Halobia austriac*a. This halobiid is, unfortunately, too small for confident identification and could potentially belong to a number of halobiid species, including *H. selwyni*. It should be noted that Tozer's locality/section at Pardonet Hill West is different than the Pardonet Hill East section logged in Orchard (2014, figs. 29, 30) and discussed above.

Thus, the re-evaluation of *Halobia austriaca* from Williston Lake suggests that the lowest occurrence identified with confidence remains in the Black Bear Ridge from bed 22 (*S. kerri* ammonoid and *Primatella asymmetrica-Norigondolella* conodont zones). A potentially lower occurrence from beds 3 and 4 in the Pardonet Hill East section (lower subdivision *Metapolygnathus parvus* Subzone) is also not confirmed and may belong to *H. selwyni*.

Halobia austriaca from Haida Gwaii, western British Columbia (Wrangellia terrane)

The Carnian-Norian boundary interval is likely represented in numerous localities across Haida Gwaii within deep-water successions of the Peril Formation rich in radiolarians, conodonts, ammonoids, and halobiid bivalves (e.g., Carter and Orchard, 2000, 2013). *Halobia austriaca*, however, is only confirmed from the section at Huxley Island (Figs. 2, 5E–5G).

Tozer (1994, pl. 104, fig. 12b) illustrated a small halobiid in the same piece as a poorly preserved *Anatropites* sp. from a locality (GSC C-157119) on Huxley Island, British Columbia, Canada. This halobiid specimen, like that from Pardonet Hill West (see above) is too small for identification and could belong to a number of different *Halobia* species. However, additional, previously unstudied specimens provided by Michael Orchard for examination from GSC C-157119 (= bed 8, Huxley B section of Orchard, 1991) and a second specimen from a likely slightly higher level GSC C-157123 (= bed 10A, Huxley B section of Orchard, 1991) appear to agree with the current understanding of *H. austriaca* (Fig. 5). The precise relationship between these levels GSC 157119 and GSC C-157123 and that of the aforementioned Tozer specimens are unclear. According to Orchard (personal communication, 2019), there is a small fault that separates C-157119 and C-157123, even though Tozer suggested that C-157123 and C-157119 were considered as probably the same bed. The possibility they are of different ages may be supported by both the ammonoid and conodont assemblages (see Orchard, 2019, fig. 5) with the *H. austriaca*-bearing GSC C-157123 occurring with the ammonoids *Styrites dawsoni*, *Gonionotites* sp. and *Thisbites* sp. Conodonts from this level (Orchard, 1991, 2019; Carter and Orchard, 2013) suggest that GSC C-157123 is just above the upper division of the *Metapolygnathus parvus* Subzone and within the lower division of the *Primatella asymmetrica-Norigondolella* conodont Subzone.

Halobia austriaca in southern Alaska (Wrangellia terrane)

Also from the Wrangellia terrane, Smith (1927, pl. 99, figs. 10-12) illustrated two specimens attributed to *Halobia austriaca* from a locality (USGS loc. 9935) along Rock Creek in the Copper River area (Chitina River District, Wrangell Mountains) of southern Alaska. Smith (1927) assigned these specimens (reproduced in Fig. 5) to his Upper Carnian *Juvavites* subzone of *Tropites subbulatus* ammonoid zone without providing evidence. While these specimens appear to be valid *H. austriaca*, their age remains in question as they are not independently collaborated by co-occurring ammonoids or other biostratigraphically informative species.

From a nearby locality (USGS loc. 8153) in the Kuskulana River area of the Wrangell Mts., Smith (1927, pl. 99, figs. 7-9) described and illustrated three specimens attributing it to his new species *Halobia brooksi*. Silberling (1963, pl. 2, figs. 14-15) also illustrated a *H. austriaca* from the same locality. The holotype of *H. brooksi* Smith (1927, pl. 99, fig. 7; USNM 74188) is listed as upper Carnian or more likely lower Norian, Roadhouse Creek (USGS loc. 8153); however, the age of the type specimens remains questionable as no ammonoids, conodonts, or other age-diagnostic fossils are known from this locality. As previously mentioned, Gruber (1977, pl. 6, fig. 2), considered *H. brooksi* as a junior subjective synonym of *H. austriaca*, and re-illustrated Smith's type (USNM 74188). It should be further noted that in his plate explanation, Gruber incorrectly listed its occurrence as Thompson's Cove on Gravina Island Alaska (which is a different locality from the Alexander terrane) and not that from where the specimen was collected.

In addition to the above-mentioned specimens, Silberling (1963, pl. 2, fig. 11) illustrated an additional specimen from the Wrangell Mountains at Canyon Creek (USGS loc. M1709) attributed to *Halobia austriaca* from the basal McCarthy Formation. This specimen is interesting as it is associated with *Anatropites* sp; and evidentially late Carnian in age. However, this single valve exhibits very thin and tightly packed radial ribs of nearly all equal strength and straightness are much more reminiscent of *H. radiata* rather than *H. austriaca*. It is possible that this illustrated specimen is similar those mentioned, but not illustrated, in a taxonomic list of fauna identified by N.J. Silberling from the Ninza Limestone from three nearby localities (USGS locs. M1792, M1793, M1794) listed in MacKevett (1970, 1971). One additional mention worth noting is the presence of *Halobia brooksi* in beds transitional between the Chitistone and overlying Ninza limestones from USGS loc. M1706 as noted by Silberling and Tozer (1968, p. 48) co-occurring with a rich bivalve and gastropod fauna that the authors suggest is of earliest Norian or latest Carnian age.

Halobia austriaca in southeastern Alaska (Alexander terrane)

Smith (1927, pl. 99, fig. 13) illustrated a single specimen attributed to *Halobia austriaca* from a locality (USGS loc. 8847) at Herring Bay, on Admiralty Island in the Keku Strait area of southeastern Alaska. Although this single specimen

(reproduced in Fig. 5J) is a small and incomplete right valve, it clearly exhibits shape/outline and ribbing characteristic of *H. austriaca*. Unfortunately, however, it was apparently not collected within a stratigraphic succession nor was it collected with other age-diagnostic fossils. Other possible occurrences of *H. austriaca* from the Keku Strait area are mentioned (e.g., Muffler, 1967; Katvala, 2004) but not illustrated. Likewise, other mentions of *Halobia austriaca* from both Bostwick Inlet and Nehenta Bay at Gravina island (e.g., Berg and Cruz, 1982) were never illustrated and are difficult to assess. Based on the above known occurrences, it can be confirmed that *H. austriaca* does indeed occur within the Alexander terrane, but for lack of ancillary biostratigraphic control, the precise age or stratigraphic position remains ambiguous.

Halobia austriaca from northern California (Eastern Kalamath terrane)

Smith (1927) illustrated *Halobia austriaca*, from the Hosselkus Limestone from the Shasta District, North Fork of Squaw Creek, 3 miles N of Kelley's Ranch (USGS loc. 15676). Smith assigned this locality to the Upper Carnian Juvavites subzone of *Tropites subbulatus* ammonoid zone, but it is distinct from a locality 2 miles NE of Madison's Ranch (USGS loc. 15678) which is the type locality of the *Tropites welleri* zone of Silberling and Tozer (1968). Smith (1927) broadly considered the ammonoid and bivalve fauna of the *Juvavites* subzone to include the entire strata, without subdivision or stratigraphic section, above the *Trachyceras*-bearing beds (= *Tropites dilleri* zone of Silberling and Tozer, 1968) and a 'coral zone' of Norian age. It is also notable that, although a species of the ammonoid *Klamathites* is known to occur in the *Juvavites* subzone of Smith at USGS loc. 15676, the *K. macrolobatus* zone has not yet been recognized from here or elsewhere in Shasta County California (see Silberling and Tozer, 1968; Tozer, 1994). According to Smith (1927), USGS loc. 15676 is reported to be many meters thick and the reported fauna of ammonoids (e.g., *Juvavites*, *Tropites*, *Gonionotites*, and *Metasibirites*) includes both upper Carnian and possible Norian taxa at different levels. Without precise stratigraphic control, the level from which *H. austriaca* was collected and its age cannot be determined.

Halobia austriaca from northeastern Oregon (Wallowa terrane)

Smith (1912, p. 95) noted the occurrence of *Halobia* cf. *austriaca* together with *H.* cf. *superba*, and *H.* cf. *salinaria* from the type locality of the Martin Bridge Formation in the southern Wallowa Mountains of northeast Oregon (Fig. 2, loc. 6). Unfortunately, little can be said of this occurrence as the specimen was never illustrated nor recorded in the known Triassic collections of J. P. Smith. From the same locality, McRoberts (1990, fig. 6.6.9) illustrated a single specimen obtained from float and provisionally assigned it to *H. austriaca*. Although this locality spans a Carnian-Norian boundary (e.g., McRoberts, 1993), it is not possible to determine the precise stratigraphic level from which the loose specimen may have come from. A second possible occurrence of *H. austriaca* was recovered from float (McRoberts, undescribed collections cited in Stanley et al., 2008) within the Martin Bridge Formation at Hells Canyon several meters below USGS loc. M2672 (the well-known and demonstrably lower Norian shallow-water silicified fauna described by Newton et al. , 1987). Without precise stratigraphic control of these two talus specimens and independent biostratigraphic evidence little can be said of their potential relationship.

Nevada (Black Rock terrane)

In an unpublished thesis, Fuller (1986, pl. 5) illustrated a specimen attributed to *Halobia* cf. *H. austriaca* from Alaska Canyon, Jackson Mountains, Humboldt Co., Nevada. The specimen in question occurs several meters below a level containing the ammonite *Discotropites* and is confidently placed in the Upper Carnian. While this specimen exhibits signs of significant tectonic shear deformation, it cannot be confused with true *H. austriaca* as it possesses much finer ribs, a distinctive growth-stop and disruptive waviness of ribs more indicative of *H. superba* or *H. ornatissima*.

North Slope Alaska (Arctic Alaska terrane)

From the Phoenix #1 drill core off-shore Arctic Alaska, McRoberts et al. (2021) illustrated three specimens attributed to *Halobia* cf. *H. austriaca* from two depth levels, situated approximately 5 m above the highest occurrence of *Halobia ornatissima* and immediately above a presumable sequence boundary. The small sample size and condition of the Phoenix #1 specimens dictate only provisional assignment to *H. austriaca.* The age of these *H.* cf. *H. austriaca* beds is not confirmed with ammonoids, conodonts or radiolarians and is only provisionally assigned as basal Norian based on broadly ranging ostracod and foraminifera species regional correlations and sequence stratigraphy.

IMPLICATIONS AND CONCLUSIONS

Based on the new specimens and a re-evaluation of existing specimens from Williston Lake and elsewhere in North America, it can be concluded that *Halobia austriaca,* while present from many localities only demonstrably occurs in few stratigraphic sections in North America with ammonoid and conodont biostratigraphic control. The lowest occurrence of *H. austriaca* from the Black Bear Ridge section, at a higher level (bed 22) than previously reported, is closely associated with the ammonoid *Guembelites clavatus* (bed 22b) as is within centimeters of the base of the recognized *Stikinoceras kerri* ammonoid zone and the *Primatella asymmetrica-Norigondolella* conodont subzone. With this report, a revised primary datum of the first occurrence of *H. austriaca* from bed 22 in the Black Bear Ridge section of Williston Lake provides a robust datum integrated with ammonoids and conodonts to correlate a basal-Norian GSSP. This revised position of *Halobia austriaca* from Black Bear Ridge also provides for a more parsimonious correlation to other sections within the western Tethys, including the candidate Pizzo Mondello GSSP and other sections in Austria, Turkey, and Slovakia. Although a

full and complete discussion on the biochronology and correlation of *H. austriaca* and potential secondary markers (ammonoids, conodonts, geochemical signatures and a geomagnetic polarity) to other regions is beyond the scope of this preliminary report and is partially available elsewhere (e.g., Krystyn and Gallet, 2002; McRoberts and Krystyn, 2011; Balini et al., 2012; Levera 2012), and will be more formally discussed in the formal proposal being prepared for the Subcommisssion on Triassic Stratigraphy on *H. austriaca* as primary datum at the Pizzo Mondello section of Sicily (Balini pers. comm., 2021).

ACKNOWLEDGEMENTS

I am grateful to M.J. Orchard and J.P. Zonneveld for logistical support and expertise while conducting fieldwork in Williston Lake in 1998, 2001, and 2010. Additional thanks to the late N.J. Silberling and the late E.T. Tozer for facilitating access to the USGS and GSC bivalve collections under their supervision. Reviews by M.J. Orchard and L. Krystyn led to an improved manuscript.

REFERENCES

Balini, M., Krystyn, L., Levera, M. & Tripodo, A. 2012. Late Carnian-Early Norian ammonoids from the GSSP candidate section Pizzo Mondello (Sicani Mountains, Sicily). Rivista Italiana di Paleontologia e Stratigrafia, 118: 47–84.

Berg, H.C., & Cruz, E.L. 1982. Map and table describing fossil collections and related samples in the Ketchikan and Prince Rupert quadrangles, southeastern Alaska. U.S. Geological Survey Open-File Report 82-1088. 27 p.

Bychkov, Y. M., Dagys, A.S., Efimova, A.F., & Polubotko, I.V. 1976. Atlas of the Triassic Fauna and Flora of Northeastern USSR. Ministry of Geology of RSFSR, "NEDRA", Moscow, 267 p. [In Russian]

Cafiero, B., & De Capoa Bonardi, P. 1980. Stratigraphy of the pelagic Triassic in the Budva-Kotor area (Crna-Gora, Montenegro, Yugoslavia). Bollettino della Società Paleontologica Italiana, 21: 179–204.

Cafiero, B., & De Capoa Bonardi, P. 1982. Biostratigrafia del Trias pelagico della Sicilia. Bollettino della Società Paleontologica Italiana, 21: 35–71.

Campbell, H. J. 1994. The Triassic bivalves *Halobia* and *Daonella* in New Zealand, New Caledonia, and Svalbard. Institute of Geological & Nuclear Sciences Monograph, 4: 1–166.

Carter, E.S. & Orchard, M.J., 2000. Intercalibrated conodont-radiolarian biostratigraphy and potential datums for the Carnian-Norian boundary within the Upper Triassic Peril Formation, Queen Charlotte Islands, British Columbia. Geological Survey of Canada, Current Research, 2000-A7: 1–11.

Carter, E.S. & Orchard, M.J., 2013. Intercalibration of conodont and radiolarian faunas from the Carnian-Norian boundary interval in Haida Gwaii, British Columbia, Canada. *In*, L.H. Tanner, J.A. Spielmann and S. Lucas (eds), The Triassic System. New Mexico Museum of Natural History and Science, Bulletin 61: 67–92.

De Capoa Bonardi, P. 1970. Le Daonelle e le Halobie della serie calcareo-silicio-marnosa della Lucania (Appennino Meridionale). Memorie della Società dei Naturalisti in Napoli, 1: 1–130.

De Capoa Bonardi, P. 1984. *Halobia* zones in the pelagic Late Triassic sequences of the central Mediterranean area. Bollettino della Società Paleontologica Italiana, 23: 91–102.

Fuller, L.R. 1986. General Geology of Triassic Rocks at Alaska Canyon in the Jackson Mountains, Humboldt County Nevada, Ms Thesis, University of Nevada, Reno, 110 p.

Gruber, B. 1975. Unternorische Halobien (Bivalvia) aus Bosnien Jugoslawien. Sitzungsberichte der Österreichische Akademie Wissenschaften, mathematisch-naturwissenschaftliche Klasse, Abt. 1, 183: 119–130.

Gruber, B. 1976. Neue Ergebnisse auf dem Gebiete der Ökologie, Stratigraphie und Phylogenie der Halobien (Bivalvia). Mitteilungen der Gesellschaft der Geologie und Bergbaustudenten in Österreich, 23: 181–198.

Gruber, B. 1977. Die Gattung *Halobia* Bronn, 1830 und *Perihalobia* Gruber, 1976 (Posidoniidae, Bivalvia) in der mediterranen Tethys und Nordamerika. PhD Dissertation, Universität Wien. 204 p.

Katvala, E.C., 2004. Conodont biostratigraphy and facies correlations in an Upper Triassic Island Arc, Keku Strait, southeast Alaska. Ms Thesis, The University of Montana, Missoula, 142 pp.

Kiparisova, L.D. 1947. Atlas of guide forms of fossil faunas of the USSR, Volume 7, Triassic System. Gosudarstvennoe Izdatel'stvo Geologicheskoj Literatury Ministerstva Geologii SSSR, Lenningrad, 253 pp. [in Russian].

Kittl, E. 1912. Materialen zu einer Monographie der Halobiidae und Monotidae der Trias. Resultate der Wissenschaftlichen Erforschung des Balatonsees, Band II, Abhandlunge IV:1–229.

Krumbeck, L. 1924. Die Brachiopoden, Lamellibranchiaten und Gastropoden der Trias von Timor, II. Paläontologie von Timor, 13: 143–417.

Krystyn, L. 2010. Long distance marine biotic correlation events around the Carnian—Norian boundary: Choice of Halobia austriaca as the defining boundary marker, p. 30–31. *In*, P. Di Stefano and M. Balini (eds.) Program and Abstracts: New Developments on Triassic Integrated Stratigraphy. Museo Geologico "G. G. Gemmerllaro", September 12–16, Palermo.

Krystyn, L., & Gallet, Y. 2002. Towards a Tethyan Carnian-Norian boundary GSSP. Albertiana, 27: 12–19.

Lamolda, M.A., Paul, C.R.C., Peryt, D. & Pons, J.M., 2014. The global boundary stratotype and section point (GSSP) for the base of the Santonian Stage,"Cantera de Margas", Olazagutia, northern Spain. Episodes, 37, 2–13.

Lei, J.Z.X., Husson, J.M., Golding, M.L., Orchard, M.J., & Zonneveld, J.-P. 2021. Stable carbon isotope record of carbonate across the Carnian–Norian boundary at the prospective GSSP section at Black Bear Ridge, British Columbia, Canada. Albertiana, 46, 1–10.

Levera, M. 2010. The pelagic bivalve *Halobia* from the Carnian-Norian Pizzo Mondello section (Sicanian Basin, Sicily) and its bearing on the definition of the GSSP of the Norian Stage. PhD. Dissertation, Università Milano, 179 p.

Levera, M. 2012. The halobiids from the Norian GSSP candidate section of Pizzo Mondello (Western Sicily, Italy): systematics and correlations. Rivista Italiana di Paleontologia e Stratigrafia, 118: 3–45.

Levera, M., & McRoberts, C.A. 2010. Halobiid bivalves as a tool for high resolution correlation between Carnian-Norian successions in Tethys and Panthalassa: A potential datum for a base-Norian GSSP, p. 34. *In*, P. Di Stefano and M. Balini (eds.) Program and Abstracts: New Developments on Triassic Integrated Stratigraphy. Museo Geologico "G. G. Gemmerllaro", September 12–16, Palermo.

MacKevett, E.M. 1970, Geologic map of the McCarthy C-5 Quadrangle, Alaska: U.S. Geological Survey, Geological Quadrangle Map GQ-899, scale 1:63,360.

MacKevett, E.M. 1971. Stratigraphy and general geology of the McCarthy C-5 Quadrangle, Alaska. U.S. Geological Survey Bulletin 1323, 35 p.

Mazza, M., Rigo, M. & Gullo, M. 2012. Taxonomy and biostratigraphic record of the Upper Triassic conodonts of the Pizzo Mondello section (western Sicily, Italy), GSSP candidate for the base of the Norian. Rivista Italiana di Paleontologia e Stratigrafia, 118: 85–130.

Mazza, M., Nicora, A. & Rigo, M. 2018. *Metapolygnathus parvus* Kozur, 1972 (Conodonta): a potential primary marker for the Norian GSSP (Upper Triassic). Bollettino della Società Paleontologica Italiana, 57 (2): 81–101.

McRoberts, C.A. 1990. Systematic paleontology, stratigraphic occurrence, and paleoecology of halobiid bivalves from the Martin Bridge Formation (Upper Triassic), Wallowa terrane, Oregon. M.S. Thesis, University of Montana. 156 p.

McRoberts, C.A. 1993. Systematics and biostratigraphy of halobiid bivalves from the Martin Bridge Formation (Upper Triassic), northeast Oregon. Journal of Paleontology, 67: 198–210.

McRoberts, C.A. 2007. The halobiid bivalve succession across a potential Carnian/Norian GSSP at Black Bear Ridge, Williston Lake, northeast British Columbia, Canada. Albertiana, 36: 142–145.

McRoberts, C.A., 2010. Biochronology of Triassic bivalves. *In*, S.G. Lucas (ed.), The Triassic Time Scale. Geological Society of London, Special Paper, 334: 201–219.

McRoberts, C.A. 2011. Late Triassic Bivalvia (Chiefly Halobiidae and Monotidae) from the Pardonet Formation, Williston Lake area, northeast British Columbia, Canada. Journal of Paleontology, 85(4): 613–664.

McRoberts, C. A., Blodgett, R.B., & Bird, K.J. 2021. Middle and Upper Triassic bivalve biostratigraphy of the Shublik Formation from the Tenneco Phoenix #1 Well, Offshore Central North Slope, Arctic Alaska. New Mexico Museum of Natural History and Science Bulletin, 82: 259–274.

McRoberts C.A., & Krystyn L. 2011. The FOD of *Halobia austriaca* at the Black Bear Ridge (north-eastern British Columbia) as the potential base-Norian GSSP. *In*, Haggart J.W. & Smith P.L. (eds), Canadian Paleontology Conference, Proceedings, 9: 38–39.

Mojsisovics, E. von. 1874. Über die triadischen Pelecypoden-Gattungen *Daonella* und *Halobia*. Abhandlungen der k. k. Geologischen Reichsanstalt, 7: 1–35.

Mojsisovics, E. von, Waagen, W.H., & Diener, C. 1895.Entwurf einer Gliederung der pelagischen Sediments des Trias-Systems. Sitzungsberichte der Wissenschaften, mathematisch-naturwissenschaftliche Klasse, 104: 1279–1302.

Muffler, L.J.P. 1967. Stratigraphy of the Keku Islets and neighboring parts of Kuiu and Kupreanof Islands, southeastern Alaska. U.S. Geological Survey, Bulletin, 1241-C: 1–52.

Newton, C.R., Whalen, M.T., Thompson, J.B., Prins, N. & Delalla, D. 1987. Systematics and paleoecology of Norian (Upper Triassic) bivalves from a tropical island arc: Wallowa Terrane, Oregon. Paleontological Society Memoir, 22, 83 pp.

Orchard, M.J. 1991. Late Triassic conodont biochronology and biostratigraphy of the Kunga Group, Queen Charlotte Islands, British Columbia. Geological Survey of Canada Paper, 90-10: 173–193.

Orchard, M.J. 2007. A proposed Carnian-Norian Boundary GSSP at Black Bear Ridge, northeast British Columbia, and a new conodont framework for the boundary interval. Albertiana, 36: 130–141.

Orchard, M.J. 2014. Conodonts from the Carnian-Norian boundary (Upper Triassic) of Black Bear Ridge, northeastern British Columbia, Canada: Bulletin New Mexico Museum of Natural History and Science, 64, 138 p.

Orchard, M.J. 2019. The Carnian-Norian boundary GSSP candidate at Black Bear Ridge, British Columbia, Canada: update, correlation, and conodont taxonomy. Albertiana, 45: 50–68.

Orchard, M.J., Zonneveld, J.P., Johns, M.J., McRoberts, C.A., Sandy, M.R., Tozer, E.T., & Carrelli, G.G. 2001. Fossil succession and sequence stratigraphy of the Upper Triassic and Black Bear Ridge, northeast B.C., and a GSSP prospect for the Carnian-Norian boundary. Albertiana, 25: 10–22.

Onoue, T., Zonneveld, J-P, Orchard, M.J., Yamashita, M., Yamashita, K., Sato, H. & Kusaka, S. 2016. Paleoenvironmental changes across the Carnian/Norian boundary in the Black Bear Ridge section, British Columbia, Canada. Palaeogeography, Palaeoclimatology, Palaeoecology, 441: 721–733.

Polubotko, I.V. 1984. Zonal and correlation significance of Late Triassic halobiids. Sovetskaya Geologiya, 6: 40–51. [In Russian]

Polubotko, I.V. 1986. Zonal complexes of Late Triassic halobiids in the northeastern USSR. *In*, A.L. Yanshin & A.S. Dagys (eds.), Biostratigrafiya mezozoya Sibiri i Dal'nego Vostoka Mesozoic Biostratigraphy of Siberia and the Far East. Trudy Instituta Geologii i Geofiziki, Novosibirisk, pp. 63–72, 179–180, 191–192. [In Russian]

Polubotko, I.V. 1988. On the morphology and systematics of the Late Triassic Halobiidae (bivalve mollusks). Annual of the All-Union Paleontological Society, 31: 90–103. [In Russian]

Polubotko, I.V. 2005, Halobiid-based biozonation of the Upper Triassic in the Northeast Russia. *In*, The Science in the Northeast Russia in the Beginning of the 21st Century.

Proc. All-Russian Sci. Conf., Dedicated to the Memory of Academician K.V. Simakov. Magadan, April 26–27, 2005), Magadan, pp. 35–39. [In Russian]

Polubotko, I.V., Alabushev, A.I., & Bychkov, Y.M. 1990. Late Triassic halobiids (Bivalve Mollusks) from the Kenkeren Range (northeast USSR). Annual of the All-Union Paleontological Society, 33: 122–139. [In Russian]

Silberling, N.J. 1963. Field guide to halobiid and monotid pelecypods of the Alaskan Triassic. U.S. Geological Survey Open File Report, 1963: 1–9.

Silberling, N.J., & Tozer, E.T. 1968. Biostratigraphic classification of the marine Triassic in North America. Geological Society of America Special Paper, 110: 1–63.

Smith, J.P. 1927. Upper Triassic marine invertebrate faunas of North America. U.S. Geological Survey Professional Paper 141, 262 p.

Stanley G.D., McRoberts, C.A., & Whalen M.T. 2008. Stratigraphy of the Triassic Martin Bridge Formation, Wallowa terrane: Stratigraphy and depositional setting The Geological Society of America Special Paper 442: 227–250.

Tozer, E.T. 1994. Canadian Triassic ammonoid faunas. Geological Survey of Canada Bulletin, 467: 1–663.

Vozin, V.F., & Tikhomirova, V.V. 1964. Field atlas of Bivalvia and Cephalopoda in the Triassic deposits of northeastern USSR. Institute of Geology, Siberian Branch, USSR Academy of Sciences, Moscow, 195 p. [In Russian]

Williford, K.H., Orchard, M.J., Zonneveld, J.P., McRoberts, C.R., & Beatty, T.W. 2007. A record of stable organic carbon isotopes from the Carnian-Norian boundary section at Black Bear Ridge, Williston Lake, British Columbia, Canada: Albertiana, 36: 146-148.

Zonneveld, J-P., Beatty, T.W., Williford, K.H., Orchard, M.J., & McRoberts, C.A. 2010. Stratigraphy and sedimentology of the lower Black Bear Ridge section, British Columbia: candidate for the base-Norian GSSP. Stratigraphy, 7: 61–82.

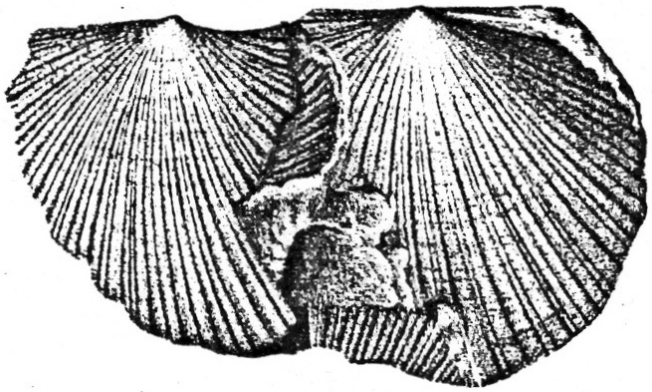

Wroking Group Report

THE CASE FOR THE GLOBAL STRATOTYPE SECTION AND POINT(GSSP) FOR THE BASE OF THE NORIAN STAGE

Mark W. Hounslow[1], and the Carnian-Norian boundary working group comprising: **Gerhard H. Bachmann[2], Marco Balini[3], Michael J. Benton[4], Elizabeth S. Carter[5], Alexey G. Konstantinov[6], Martyn L. Golding[7], Leopold Krystyn[8], Wolfram M. Kürschner[9], Spencer G. Lucas[10], Christopher A. McRoberts[11], Giovanni Muttoni[3], Alda Nicora[3], Tetsuji Onoue[12] Michael J. Orchard[7], Péter Ozsvárt[13], Niall W. Paterson[14], Sylvain Richoz[15], Manuel Rigo[16], Yadong Sun[17], Lydia S. Tackett[18], Ugar Kağan Tekin[19], Yongdong Wang[20], Yang Zhang[21], John-Paul Zonneveld[22].**

[1]LEC, Lancaster University, and Earth, Ocean and Ecological Sciences, University of Liverpool, UK; [2]Institut für Geowissenschaften, Martin-Luther-Universität Halle-Wittenberg, D-06120 Halle (Saale), Germany; [3] all'Università degli Studi di Milano,Il valore della ricerca interdisciplinare, Italy; [4]University of Bristol, Life Sciences Building, Tyndall Avenue, Bristol, BS8 1TQ, UK; [5]69745 Old Wagon Road, Sisters, OR 97759, USA; [6]Trofimuk Inst. of Petro. Geology and Geophysics, Russian Academy of Sciences, Novosibirsk, 630090 Russia; [7]Geological Survey of Canada, 1500-605 Robson Street, Vancouver, British Columbia V6B 5J3, Canada; [8]Inst. Paleontology, Geozentrum UZA2, 2B309, Althanstrasse 14, A-1090 Vienna, Austria; [9]Department of Geosciences, University of Oslo, P.O. Box 1047, Blindern, N-0316 Oslo, Norway; [10]New Mexico Museum of Natural History & Science, Albuquerque, New Mexico 87104, USA; [11]Geology Department, SUNY Cortland, P.O. Box 2000, Cortland, NY, USA; [12]Dept. of Earth & Planetary Sciences, Kyushu Univ.,744 Motooka, Nishi-ku, Fukuoka 819-0395, Japan; [13]MTA-MTM-ELTE, Research Group for Paleontology, P.O. Box 137 H-1431, Budapest, Hungary; [14]CASP, Madingley Road, Cambridge, UK; [15]Lithosphere and Biosphere Science, Lund University,Box 117, SE-221 00, Lund, Sweden; [16]Dipartimento di Geoscienze, Università degli Studi di Padova,Via Gradenigo, 6, I-35131 Padova,Italy; [17]GeoZentrum Nordbayern, Universität Erlangen-Nürnberg, Schlossgarten 5, 91054 Erlangen, Germany; [18]Department of Geosciences, North Dakota State University, Dept. 2745, Fargo, ND 58108-6050, USA; [19]Hacettepe University, Department of Geol. Engineering, 06800 Beytepe-Ankara,Turkey; [20]Nanjing Institute of Geology and Palaeontology, China; [21]Faculty of Geosciences, University of Bremen, Klagenfurter Street 2-4, 28359 Bremen, Germany; [22]Department of Earth and Atmospheric Sciences, University of Alberta, Edmonton, Canada

Abstract – The Norian Stage is the longest stage in the Phanerozoic, and some members of the boundary working group have been evaluating suitable Carnian-Norian boundary sections for roughly two decades. This has identified two possible candidate boundary sections, at Black Bear Ridge (British Columbia, Canada) and Pizzo Mondello (Sicily, Italy). After a formal voting procedure within the working group, ending on the 26th July, 2021, the Pizzo Mondello section was selected as the global stratotype section and point for the base of the Norian. We evaluated the global correlation potential of the two proposed primary markers, the conodont *Metapolygnathus parvus* and the 'flat-clam' *Halobia austriaca*. Secondary markers were also evaluated around these boundary datums for correlation potential,

Published online: December 22, 2021

Hounslow, M.W., Bachmann, G.H., Balini, M., Benton, M.J. Carter, E.S., Konstantinov, A.G., Golding, M.L., Krystyn, L., Kürschner, W., Lucas, S.G., McRoberts, C.A., Muttoni, G., Nicora, A., Onoue, T., Orchard, M.J., Ozsvárt, P., Paterson, N.W., Richoz, S., Manuel Rigo, M., Sun, Y., Tackett, L.S., Kağan Tekin, U., Wang, Y., Zhang, Y., & Zonneveld. J.-P. 2021.The case for the Global Stratotype Section and Point (GSSP) for the base of the Norian stage. Albertiana, vol. 46, 25–57.

and the veracity of the proposed sections for GSSP status. Data and arguments for the proposed sections and datums are presented here. Through a two-stage process of option elimination in voting, conforming with ICS guidelines, the working group decided by 60% majority to propose that the first occurrence datum of *Halobia austriaca* in the Pizzo Mondello section at the base of bed FNP135A should become the 'golden spike' for the base of the Norian. A secondary biotic marker for this boundary is the first occurrence of *Primatella (Carnepigondolella) gulloae*, in sample NA43, ca. 0 m below FNP135A, and the FA of *Dimorphites noricus* (sample NA42.1) ca. 3.5 m above bed FNP135 (indicating the first subzone of the Jandianus Zone). The best physical secondary marker is the magnetozone PM5n with the proposed boundary ca.40% through the thickness of PM5n. Strengths of the chosen datum are: 1) it also maintains historical priority for ammonoid zonations, which had placed the base Norian near to this level in Europe, North America and probably NE Asia; 2) *Halobia austriaca* is widely distributed in all paleolatitudes and is a long-established taxon.

INTRODUCTION

The Norian is a long established Late Triassic stage, with the pioneering work of Mojsisovics (1869) indicating a type area in the Hallstatt region of Austria. The underlying late Carnian (Tuvalian Substage) has a type area near the German-Austria border in the Tuval Mountains between Hallein and Berchtesgaden (Lucas, 2010). These divisions were historically defined by ammonoid zonations. The Norian (Late Triassic) is the longest stage in the Phanerozoic and deservedly should have a defined global stratotype and point (GSSP) for its base. This is what the Carnian-Norian boundary (CNB) working group was tasked to decide. Here we present the key arguments proposed for coming to a decision about the choice of the base Norian GSSP. The real process of coming to a final decision started in mid-2020, after decades of effort focused on the two candidates at Black Bear Ridge (BBR) in British Columbia, Canada and Pizzo Mondello (PM) in Sicily, Italy (but also at other sections). This work details the data and arguments leading the group towards a decision, which will be later formally submitted to the Subcommission on Triassic Stratigraphy (STS). For the sake of transparency, this article outlines the decision processes and key outcomes that led to the final choice.

Section 1 is a summary of the key attributes of the two candidate sections and an evaluation of the accessibility and protection of both BBR and PM. Sections 2 and 3 examine the cases for global correlation using the two primary markers (datums) previously proposed. These are the first occurrence (FO) *Metapolygnathus parvus* datum detailed in section 2 and the FO of *Halobia austriaca* detailed in section 3. These cases also consider the use of possible secondary markers to enhance the correlation potential.

Section 4 examines other correlation issues beyond the proposed primary markers. Specifically, correlation into high palaeolatitude sections (section 4.1), use of radiolarian zonations (section 4.2), isotopic changes across the boundary (section 4.3), the nature of possible condensed or hiatal intervals at BBR (section 4.4), and the strengths of historical priority if using FAD of *H. austriaca* (section 4.5). Section 5 details the outcome of the formal voting within the working group.

Inevitable there remain some divergences in interpretation of datasets and taxonomic divisions. These divergences are presented together in places in the text to express both sides of the arguments presented. Contributors to particular parts of the text are indicated at section ends to display in part this divergence of views.

1. SUMMARY OF QUALIFICATIONS OF THE BLACK BEAR RIDGE AND PIZZO MONELLO SECTIONS

1.1 Accessibility and protection of the section at Black Bear Ridge

The Black Bear Ridge section is on the north shore of the Peace Reach of Williston Lake, 3.7 kilometres northeast of the mouth of the Nabesche River. Williston Lake was created in 1967 by the damming of the Peace River. There is good exposure (Figs. 1, 2) due to periodic lake level changes that clean the shore surface. The section contains a complete section through the Late Triassic into the Hettangian.

Black Bear Ridge meets all geological requirements for a GSSP (Table 1). Black Bear Ridge includes several hundred metres of section, preserving a continuous record from the Carnian (Samueli Zone) through to the latest Norian (Bidentata Zone). Further outcrop occurs in the Rhaetian and Hettangian, but an erosional unconformity is present at the Norian-Rhaetian boundary. This unconformity is several hundred metres above the GSSP candidate horizon and post-dates it by approximately 19 million years.

The Carnian-Norian boundary interval is characterized by a single lithofacies, strong evidence of continuous sedimentation through the boundary interval, and is devoid of evidence of synsedimentary or tectonic disturbance or evidence of metamorphism/strong diagenetic alteration. The Black Bear ridge section could be considered mildly condensed, in that sedimentation rates were low and the CNB interval (here defined as the interval from several metres below the oldest datum under consideration to several metres above the highest datum being considered) is approximately 25 metres in vertical thickness.

The Carnian-Norian boundary interval at Black Bear Ridge

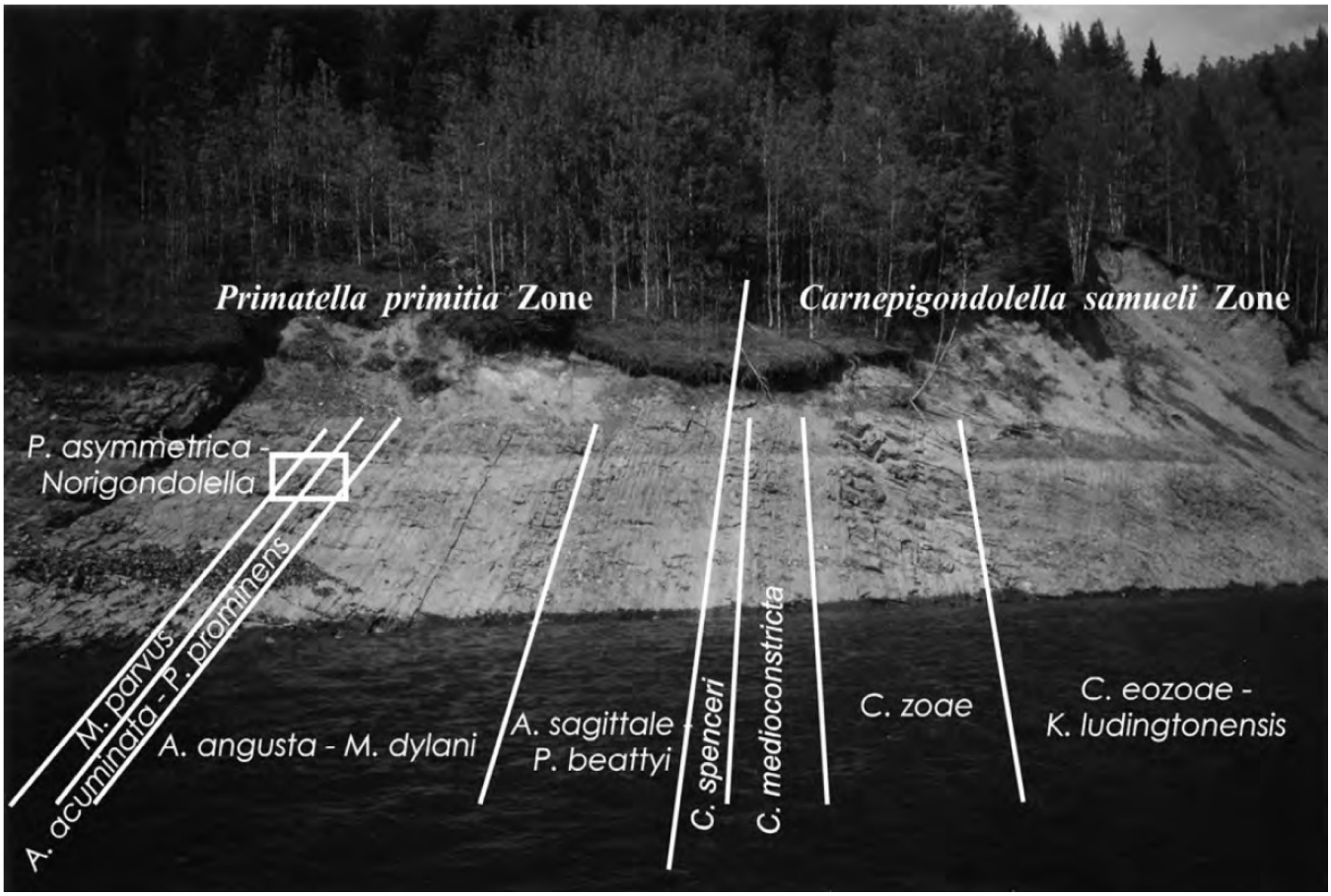

Figure 1 – Conodont zonation placed onto on the BBR section (Orchard, 2014). Fig. 2 shows the inset-square in detail.

consists of a single facies succession deposited in a quiescent deep marine basin that was well below storm wave base and that was not affected by deep marine currents. Black Bear Ridge has an exceptional fossil record with well-preserved conodonts and bivalves as well as several horizons that produce well-preserved ammonoids (Figs. 1, 2; Table 1).

It is the conodont record that renders Black Bear Ridge exceptional, with continuous conodont production throughout the entire interval. Conodont samples are diverse, abundant and very well preserved. The conodont fauna includes multiple evolutionary lineages and preserves clear morphological clines within lineages. Many collections produce hundreds of conodonts per kilogram. Similarly, the horizons with *Halobia*, including those with *H. austriaca*, are characterized by abundant specimens as well.

The conodont taxonomy and zonation developed around the CNB at BBR, and nearby locations in northeast British Columbia, has been successfully applied in lower paleolatitude

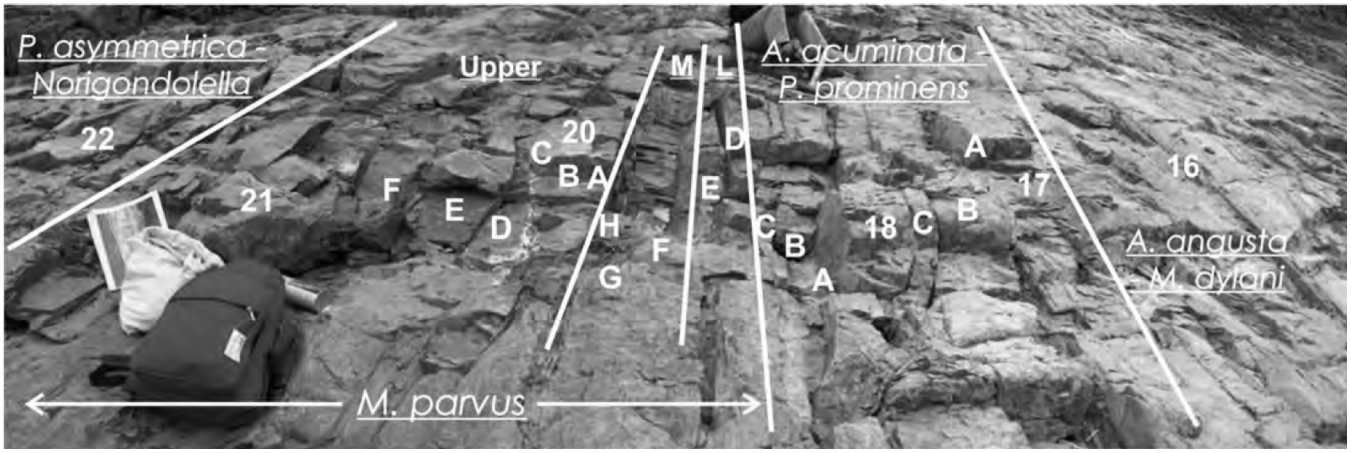

Figure 2 – Detailed conodont zonation in the critical parvus Zone interval at BBR (From Orchard, 2014). The FO of *Halobia austriaca* is in bed 22.

Table 1. Summary of the key stratigraphic attributes of the Black Bear Ridge (BBR) section.

DATA TYPE	DETAILS
Conodonts	A detailed zonation at ~15 cm precision. See Orchard (2007; 2014, 2019) and Section 2.
Halobia	See McRoberts (2007, 2010, 2021).
Ammonoids	Ammonoid recovery sporadic. Supplemented by direct (from matrix) calibration to conodont zonation from wider B.C area (fig. 5 in Orchard, 2019). Details in Orchard (2014, 2019), Balini et al. (2012) and Fig. 13.
Radiolaria	Not within the section, but calibrated to conodont zonation from Haida Gwaii sections. See Carter & Orchard (2013) and Section 4.3.
Palynology	None available
Nannofossils	None available
Foraminifera	None available
Magnetostratigraphy	None: Remagnetised in the Upper Cretaceous (Muttoni et al., 2001b)
Carbonate carbon isotope stratigraphy	An excursion, or excursions are evident, but ability to correlate these has not been fully tested (Section 4.4). Detailed sampling within the Parvus Zone (Onoue et al., 2016), and also wider within the section (Lei et al. 2021).
Organic carbon isotope stratigraphy	cm-scale record from Williford et al. (2007) through the lower and mid part of the Parvus Zone, much wider outside this interval (Fig. 10).
Sr-Isotope stratigraphy	Within the 7 m interval through the boundary interval $^{87}Sr/^{86}Sr$ declining from ca. 0.7082 to 0.7080 at base and top of Parvus Zone respectively (Onoue et al., 2016).
Oxygen-Isotope stratigraphy	Based on conodont phosphate, at ~50 cm spacing providing temperature estimates (Sun et al. 2020)
Cyclostratigraphy	None available, but a study may be possible.
Radiometric dating	None available, but possible using correlation to study of Mietto et al (2021).
Sequence stratigraphy/ sedimentology	Zonneveld et al. (2010). The CNB boundary interval is predominantly calcareous turbidites with lesser hemipelagic suspension deposits. Boundary interval with a succession showing progressive sea-level rise.
Other data	Ichthyoliths: Orchard et al. (2001)
Thermal maturity/tectonics	CAI = ~3, Black Bear Ridge occurs on the Pardonet Hill Thrust sheet (text-fig. 1), on the eastern margin of the Nabesche Syncline. Beds dip 75°. Although minor bedding plane slippage has occurred above the study interval during thrusting, fault repetition does not occur within the study interval (Riediger et al. 2004).
Nearby sections	Juvavites Cove (~3km south), Pardonet Hill East (~2 Km south-southeast), Brown Hill, West Schooler Creek, East Carbon Creek, and McLay Spur.

Nevada (Balini et al., 2015), in the Panthalassan terrane of Wrangellia (Carter & Orchard, 2013), and recently in far flung Timor (work in prep.). This demonstrates the wide distribution of BBR conodont taxa, and the latter study provides correlation with the Oceanic realm via the Haida Gwaii radiolarian succession that is fully integrated with BBR conodont zones (Section 4.3).

The nearest regional airport to Black Bear Ridge is located in Fort St. John, which is accessible via direct flights from Calgary, Edmonton and Vancouver. The site is accessed via a 90-minute drive from Fort St. John to Dunlevy boat launch east of the hamlet of Hudson Hope. From the boat launch, Black Bear Ridge is a 48 km boat ride up the Peace Reach of Williston Lake. Boat hire is simple and economic, and researchers can be dropped off on a beach 50 m from the boundary interval. Alternatively, the site can be accessed by chartering a flight from Fort St. John to the Ottertail Landing Strip, which can handle small and medium-sized planes (up to Twin-Otter). This landing strip is 3.9 km from Black Bear Ridge and is connected to a functional but disused logging road that enters the valley on the west flank of Black Bear Ridge, 300 metres from the outcrop section.

Outcrop exposure at Black Bear Ridge occur on the southern flank of a tree-covered ridge in the southern Muskwa Range. Black Bear Ridge is located on British Columbia Crown Land. This land is designated as multiuse land, on which activities such as forestry (logging), hunting, trapping and geological research are allowed. The area is also part of a hunting and guiding lease area currently held by Williston Lake Outfitters.

The entirety of Black Bear Ridge and the hills and ridges adjacent to it, consist of Jurassic and Triassic strata of the Ludington, Pardonet and Fernie formations. None of these contain economically important minerals or rocks, so mining is not a concern in this area. Black Bear Ridge is secure from development or alteration as it currently stands. Black Bear Ridge is not, at present, located within a provincial park or a national park. Obtaining further provincial protection for this locality can easily be accomplished but is not necessary. Under present rules no further development is permitted in this area. Regardless, should Black Bear Ridge be chosen as the base Norian GSSP, we will initiate the necessary steps to attain the equal protection that making this an official provincial protected area would afford.

1.2 Accessibility and Protection of the section at Pizzo Mondello

The section is part of the 430 m thick Scillato Formation (also known as "cherty limestone" or "Calcari con selce" or Halobia Limestone in Sicily). The Pizzo Mondello section (about 600 a.s.l.) is in an abandoned quarry in the lowermost part of the SW slope of Pizzo Mondello, about 3 km WNW of Bivona village (Fig. 3). Beds are well exposed and can be followed along strike for about 400 meters. The Pizzo Mondello section meets all geological requirements for a GSSP (Table 2).

The Pizzo Mondello section can be visited from January to December. The easiest access is from Palermo International Airport 'Falcone e Borsellino', well served by several car rental agencies. Bivona is 120 km from the airport, which take about two-and-a-half hours by car. The route is by the freeway E90 until Villabate, then by SS121 until Lercara Friddi, then by SS188 and SS118. The site can be reached from Bivona in 15 minutes by paved road (SP34) and dirt road, and then 5 minutes walking across peach orchards.

The Pizzo Mondello section is located in a wide area that is owned by the Municipality of Bivona.The Pizzo Mondello section is under strict protection rules, because it is included in the protected area 'Riserva Naturale Orientata Monti di Palazzo Adriano e Valle del Sosio'. This protected area is included also in the European Commission (EC) protected areas network Natura 2000, Habitat' as 'SIC Monte Rose and Monte Pernice' (code ITA020029). This area is registered by the Italian Ministry of Environment as a Special Zone of Conservation. Protection rules include strong restrictions on any anthropogenic activities but unlimited and free access for scientific studies.

A project for the development of the protected area 'SIC Monte Rose and Monte Pernice' has been granted funding by

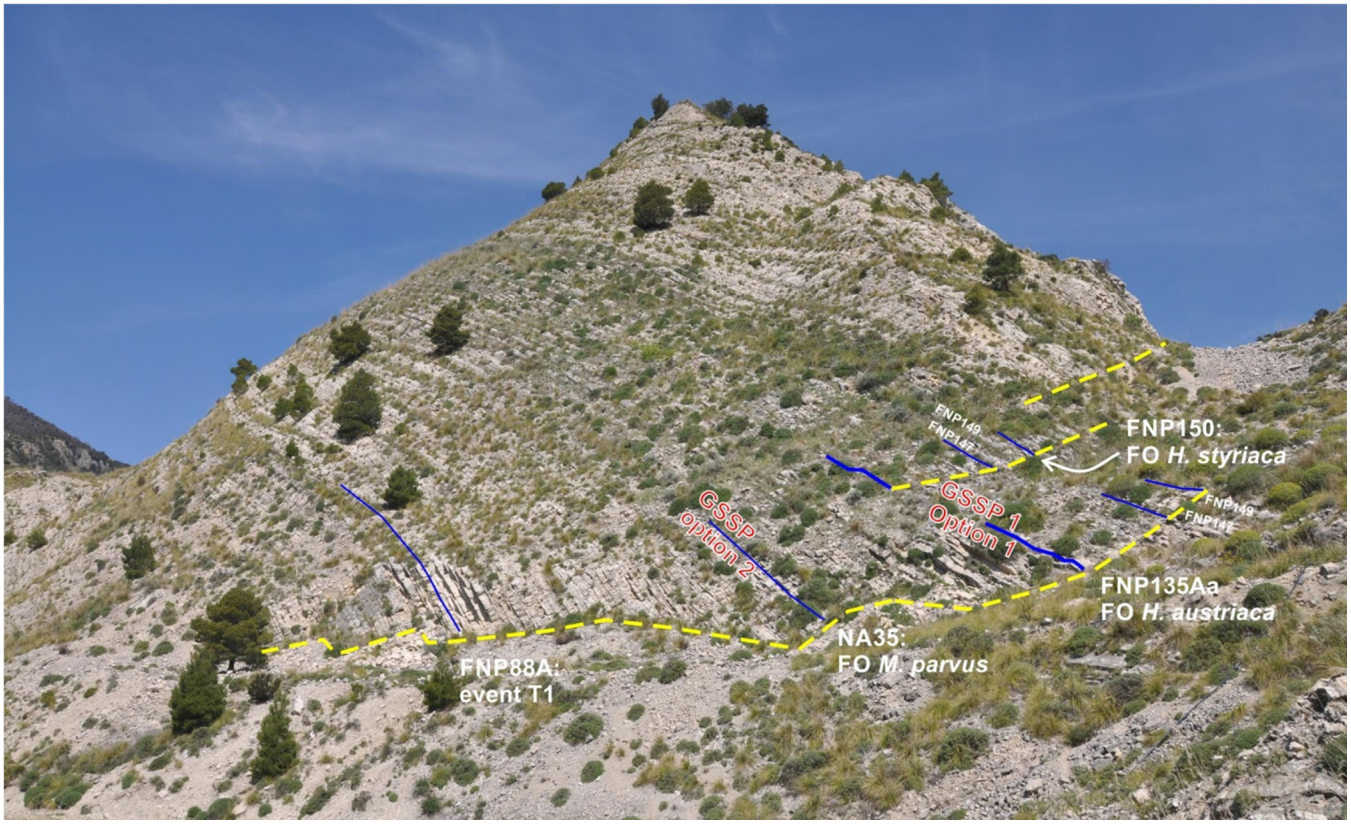

Figure 3 – Pizzo Mondello section B (see Nicora et al. 2007), with the position of some key bioevents and of the two GSSP datum options. The section has been measured and sampled along three partially overlapping segments (yellow dashed lines).

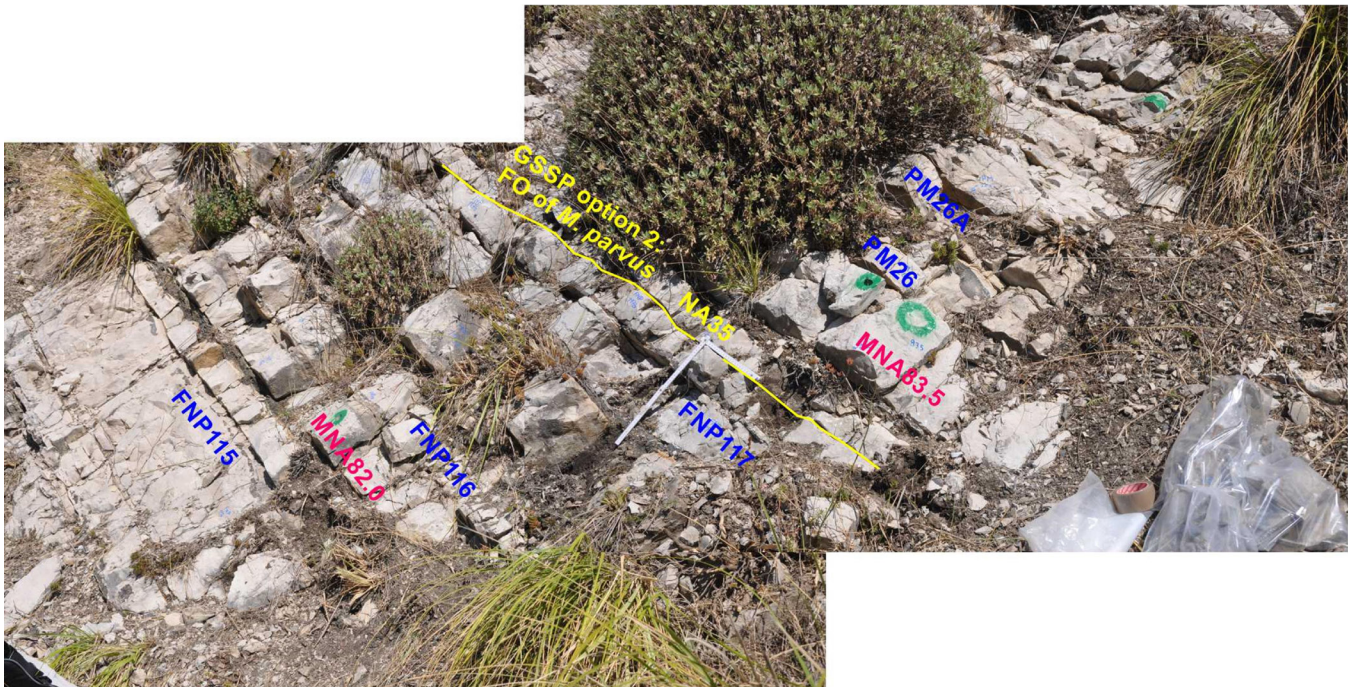

Figure 4 – The interval including the bed NA35, recording the FO of *Metapolygnathus parvus*. In purple, the paleomagnetic samples MNA82.0 (87.5 m from the base) and MNA83.5 (89 m from the base). Only the most important samples are shown in the picture.

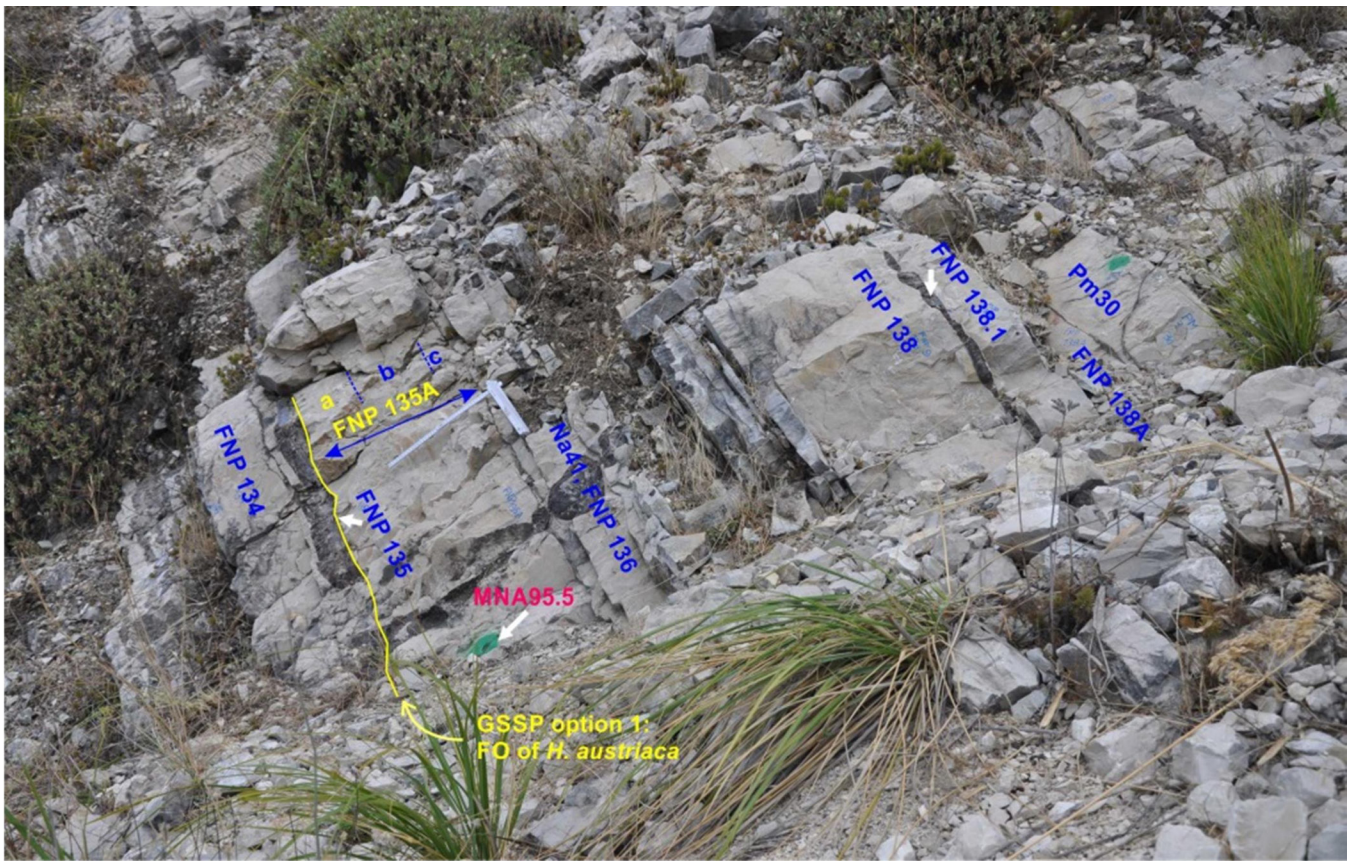

Figure 5 – Pizzo Mondello interval including the bed FNP135A, recording the FAD of *Halobia austriaca*. The bed FNP135A is 55-60 cm thick, for a more accurate location of the FO of *H. austriaca*, starting from 2012, the sampling of this bed has been done by subdividing it in three portions: a, b and c. The FAD of *H. austriaca* is recorded at the base of FNP135Aa. Paleomagnetic sample MNA95.5 (101 m from the base of the section) is in the middle of FNP135A. Only the most important samples are shown in the picture.

Table 2. Summary of the key stratigraphic data attributes of the Pizzo Mondello section.

DATA TYPE	DETAILS
Conodonts	A zonation at ~1 m precision over the CNB boundary interval (Mazza et al. 2010, 2012a, 2018). Figs. 3, 18.
Halobia	A detailed Halobiid zonation with recovery at ~0.5 m spacing (Levera, 2012). Fig. 7, 19.
Ammonoids	Around 130 ammonoids from around 100 m of section, mostly 1 per bed, sometimes more. See Balini et al. (2012) for detail and Fig. 11
Radiolaria	Common and well preserved (Nicora et al, 2007; Guaiumi, 2008, Balini et al., 2008), but not published in detail.
Palynology	None available from the section, but within the area is a study by Visscher and Krystyn (1978).
Nannofossils	Bellanca et al. (1995); Preto et al. (2013), but no detail over CNB interval
Foraminifera	Preto et al (2013), but no detail published over CNB interval
Magnetostratigraphy	Good magnetostratigraphy allowing global correlation through late Carnian to Rhaetian interval (Muttoni et al. 2001a,2004). Sample spacing ~1.2 m, but more detailed in some intervals outside CNB.
Carbonate carbon isotope stratigraphy	Whole-rock $\delta^{13}C$ sampling at ~2 m, Muttoni et al. (2014) and more detailed micro-drill sampling by Mazza et al. (2010). Shift to positive values at around the middle of the Parvus Zone (Fig. 4).
Organic carbon isotope stratigraphy	None available
Sr-Isotope stratigraphy	Sampling at ~ 2 m spacing over the CNB (Onoue et al. 2018). $^{87}Sr/^{86}Sr$ declining slightly from ca. 0.7077 through the Parvus Zone respectively (Onoue et al., 2018).
oxygen-Isotope stratigraphy	Sampling at ~ 4 m spacing over the CNB (Rigo et al. 2012b).
Cyclostratigraphy	Available for the Norian (Hüsing et al., 2011). May be possible for the boundary interval (see Fig. 17). Magnetostratigraphy allows correlation to Newark Supergroup cyclostratigraphy (Kent et al., 2017).
Radiometric dating	None available, but possible using correlation to study of Mietto et al (2021).
Sequence stratigraphy/ sedimentology	Lithologically, the succession consists mostly of evenly bedded to nodular Halobia-bearing cherty calcilutites (Guaiumi, 2008). Sequence stratigraphy: none available.
Thermal maturity/tectonics	CAI=1, maximum burial temperature < 50-80°C (Guaiumi, 2008). The section is located in the lowermost Sicanian thrust sheet (Pizzo Mondello tectonic unit) that overthursts upper Tortonian-Messinian clays, consists of three Triassic units, the Mufara Formation, the Scillato Formation and the Portella Gebbia Limestone.
Nearby sections	A number of other sections in the area at Monte Triona and Monte Cammarata. Balini et al. discussed these sections during STRATI 2019.

the EC. This project includes improvement of accessibility to the Pizzo Mondello section and preparation of explanatory panels for guided tours. The improved accessibility will allow visits to the Pizzo Mondello section by disabled visitors.

The site of the GSSP candidate is included in the list proposed as a Geosite of global importance (code NAT-1BI-0037) by the Regional Government of Sicily (Figs. 4, 5). In case of selection as the GSSP, Pizzo Mondello will also be included in the list of the GSSP Geosites by the Italian Geological Survey (Serviio Geologico d'Italia, ISPRA).

2. KEY ATTRIBUTES OF THE CONODONT *METAPOLYGNATHUS PARVUS* AS THE PRIMARY MARKER TO DEFINE THE BASE OF THE NORIAN

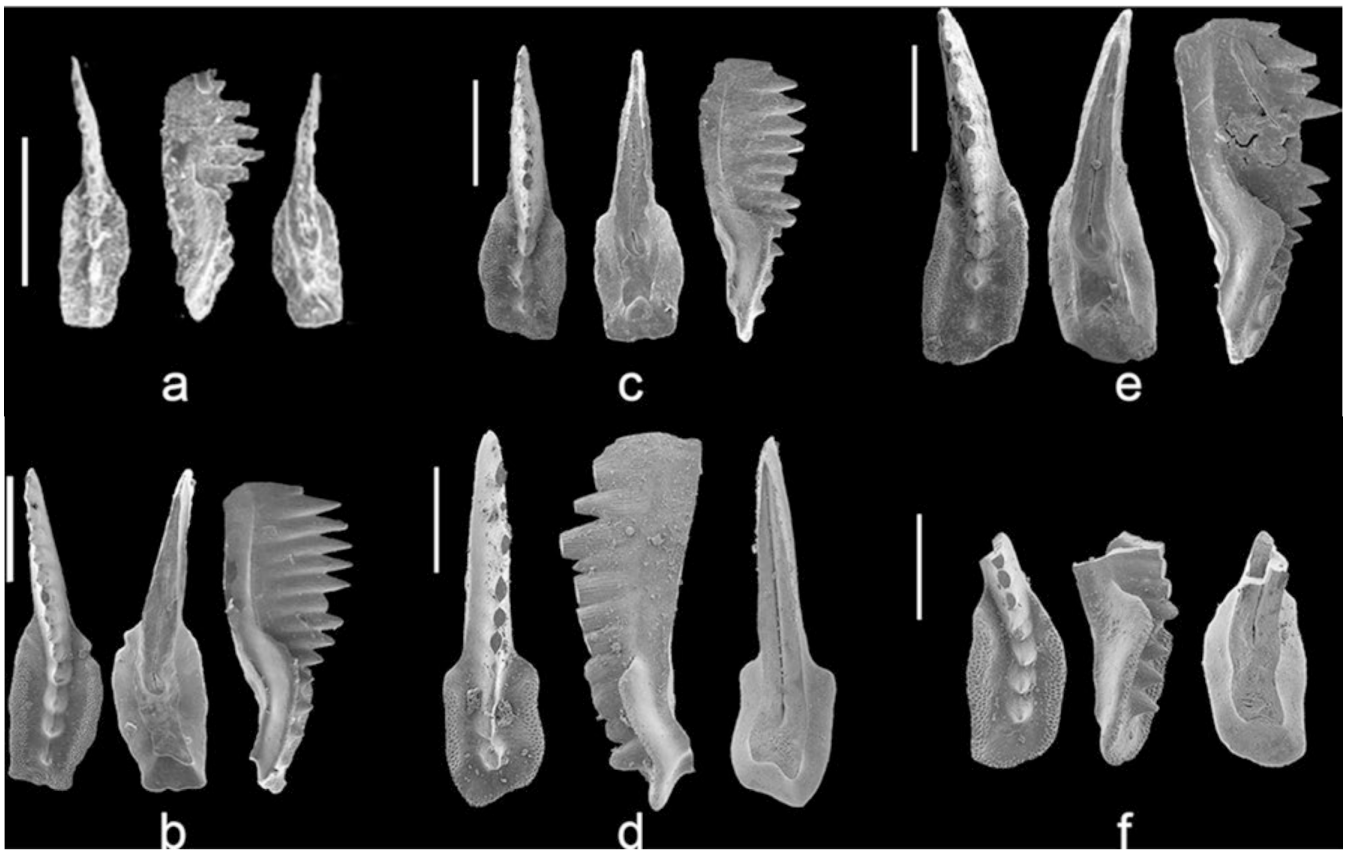

Figure 6 – This figure is fig. 6.11 in Rigo et al. (2018) where species of *Metapolygnathus parvus* Kozur are illustrated (the α morphotype sensu Orchard, 2014) from locations in: (a) The northern Tethys (from Noyan & Kozur 2007, their fig. 7.1). (b) The Neotethys (from Mazza & Martínez-Pérez 2016, Pl. 6, fig. 24). (c) Neotethys (from Mazza & Martínez-Pérez 2015, Pl. 6, fig. 23). (d) North America, from Orchard 2014, fig. 48, 14–16; (e) Neotethys (from Mazza & Martínez-Pérez 2016, Pl. 6, fig. 25). (f) North America (from Orchard 2014, fig. 48, 17–19). Scale bars are 200 µm.

It is probable that the FAD of *Metapolygnathus parvus* (Fig. 6) is the best primary marker to define the base of the Norian Stage. *Metapolygnathus parvus* is in fact, the most reliable and useful biomarker because this species is morphologically simple and easy to recognise, and its FO is globally recognisable within a clear phylogenetic lineage (Figs. 6, 7A, 7B).

Overview: Outside of the Triassic, some 23 stage bases are defined by conodont primary markers, with most of these in the Devonian-Carboniferous-Permian, indicating the widely accepted suitability of conodonts for GSSP definition. There is also an incredible level of detail published on the biostratigraphy and phylogenesis of Upper Triassic conodonts, indicating that conodont bioevents may provide the detail to make them the preferred markers for defining stage boundaries, such as the Carnian-Norian boundary (Nicora et al., 2007; Orchard, 2007, 2010, 2014, 2019; Balini et al., 2010; Rigo et al., 2018; Mazza et al., 2018). The conodont work has provided a great range of knowledge of conodont biostratigraphy across the Carnian-Norian boundary, in both GSSP candidate sections of the Norian Stage base, at Pizzo Mondello (Mutoni et al., 2001a; Nicora et al., 2007; Balini et al., 2010; Mazza et al., 2010, 2011, 2012a, b; Mazza & Martínez-Pérez, 2015) and Black Bear Ridge (Orchard et al., 2001b; McRoberts, 2007; Orchard, 2007, 2014, 2019; Balini et al., 2015). From both the Pizzo Mondello section and Black Bear Ridge section (BBR), conodonts were first described 20 years ago (Muttoni et al., 2001a; Orchard et al., 2001b).

One of the factors that has contributed to wide use of conodonts for GSSP definition is that meter to cm details of stratigraphic distribution is only limited by the density of sampling (provided conodonts are present), something that is generally not possible with macrofossils, which often have a sporadic stratigraphic distribution, particularly in the Late Triassic (Balini et al., 2012).

Evolutionary trends: In the Late Triassic, conodonts suffered four main extinction events before the end of the Rhaetian, probably related to climatic changes (Trotter et al., 2015; Sun et al., 2020): 1) in the early Julian; 2) near the Julian/Tuvalian substage boundary (mid-Carnian); 3) near the Carnian/Norian boundary; and b) near the Norian/Rhaetian boundary. After the extinction at the Julian/Tuvalian boundary, slow recovery brought conodont diversity to a new peak in the middle to late Tuvalian, e.g. the rise of the genera *Carnepigondolella*, *Kraussodontus*, *Metapolygnathus*, *Norigondolella*, *Parapatella*, *Primatella* and *Quadralella* (e.g. Mazza et al., 2010, 2018; Orchard, 2014, 2019). In eastern Panthalassa, *Acuminatella* is also widespread (Carter & Orchard, 2013; Balini et al., 2015). Faunal turnover at the

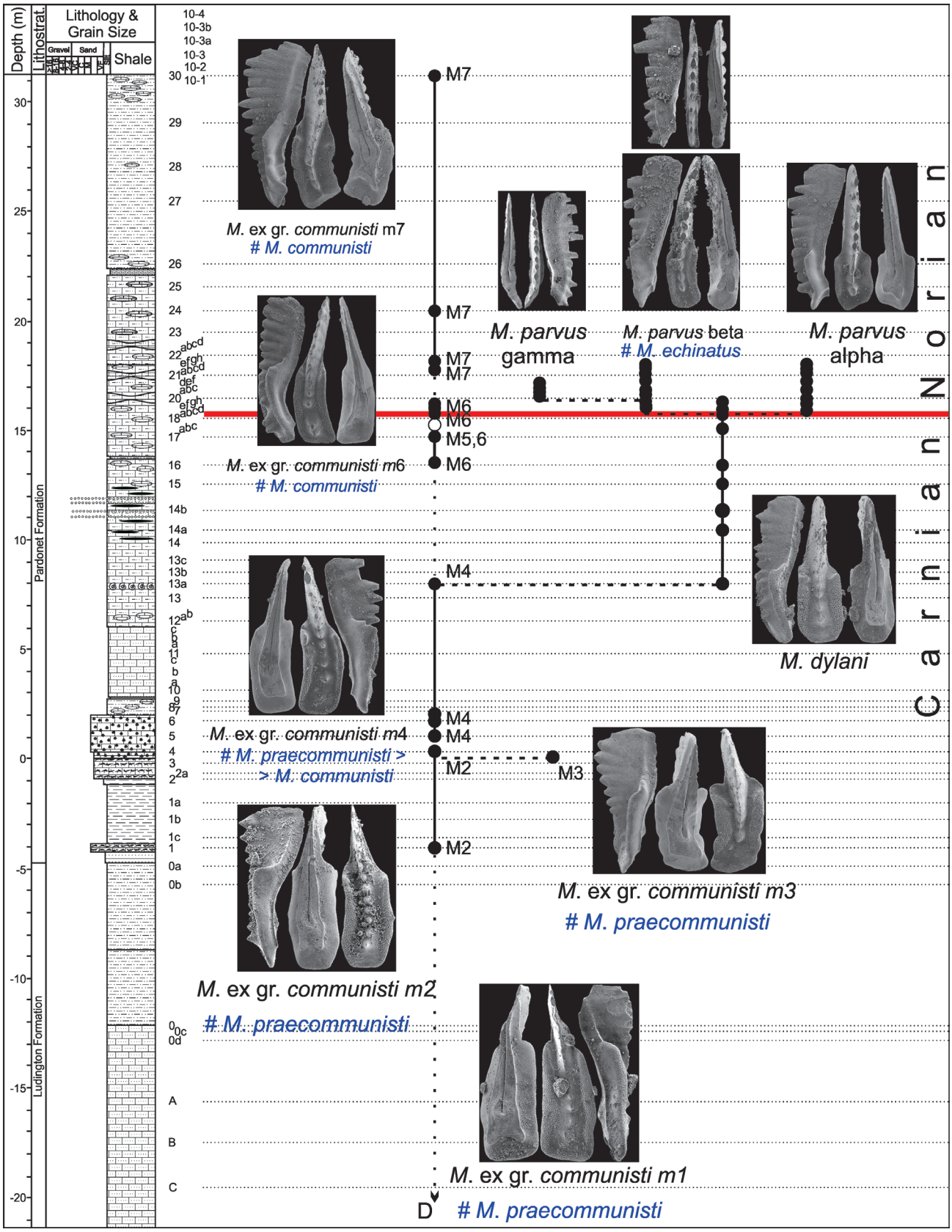

Figure 7a – Evolution and proposed phylogenetic relationships of M. ex. gr. communisti, M. dylani and M. parvus at Black Bear Ridge (modified from fig. 13 of Orchard, 2014). Names after # (and in blue) are those used by Mazza et al. (2018) for these forms

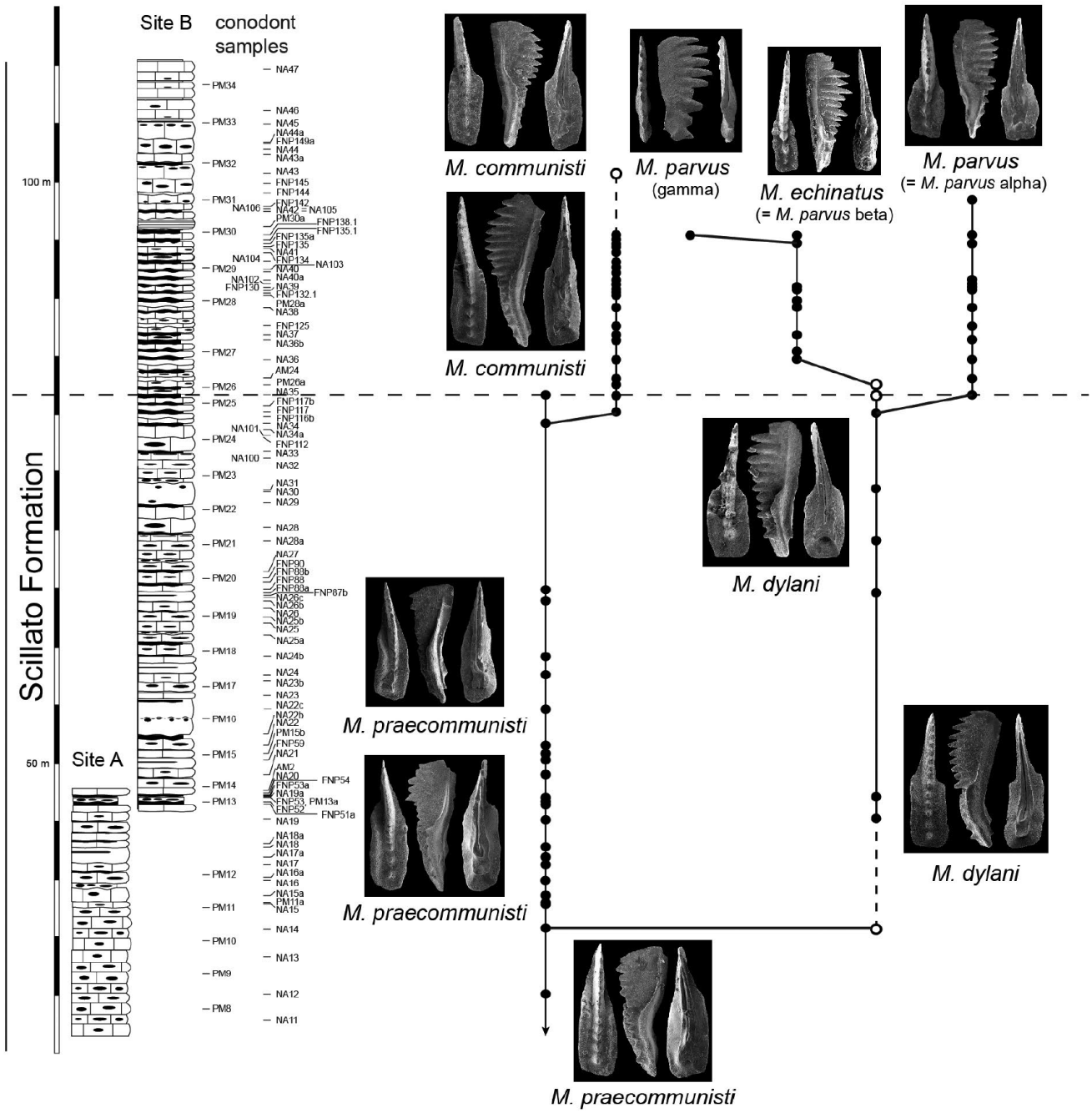

Figure 7b – From Mazza et al. (2018). Evolution and phylogenetic relationships of *Metapolygnathus praecommunisti* Mazza, et al. (2012a), *M. communisti* Hayashi, 1968, *M. dylani* Orchard, 2014, and *M. parvus* Kozur, 1972 at the Pizzo Mondello section. The figure is drawn based on the model of fig. 13 of Orchard (2014) for a better comparison between the conodont ranges and evolution in the two sections. Empty circles in the *M. dylani* range indicate transitional forms, while empty circle in the *M. communisti* range refers to *M.* cf. *communisti*. Conodonts are not to scale.

Carnian-Norian boundary was characterized by a dramatic drop in diversity as several of these conodont stocks disappeared (Figs. 7A, 7B; Mazza et al., 2010; Orchard 2014). Far fewer new taxa appear in the CNB interval; notable amongst these is the short-lived *Metapolygnathus parvus* and similar diminutive elements (Orchard, 2014). Younger Norian faunas at BBR contain only ornate *Acuminatella* and *Primatella* and occasional floods of cool water *Norigondolella* (Trotter et al., 2015; Sun et al., 2020).

At Pizzo Mondello, three conodont faunal turnovers, named T1, T2, and T3, have been identified (Mazza et al., 2010) and correlated between PM and BBR (Mazza et al., 2018; Orchard, 2019; Fig. 8). T2 is characterized by the mass development and expansion of the genus *Metapolygnathus* and the demise of typical Carnian taxa (Mazza et al., 2018). The T2 turnover event is placed at the base of the Metapolygnathus parvus Zone at PM, which corresponds to the base of the *Metapolygnathus parvus*

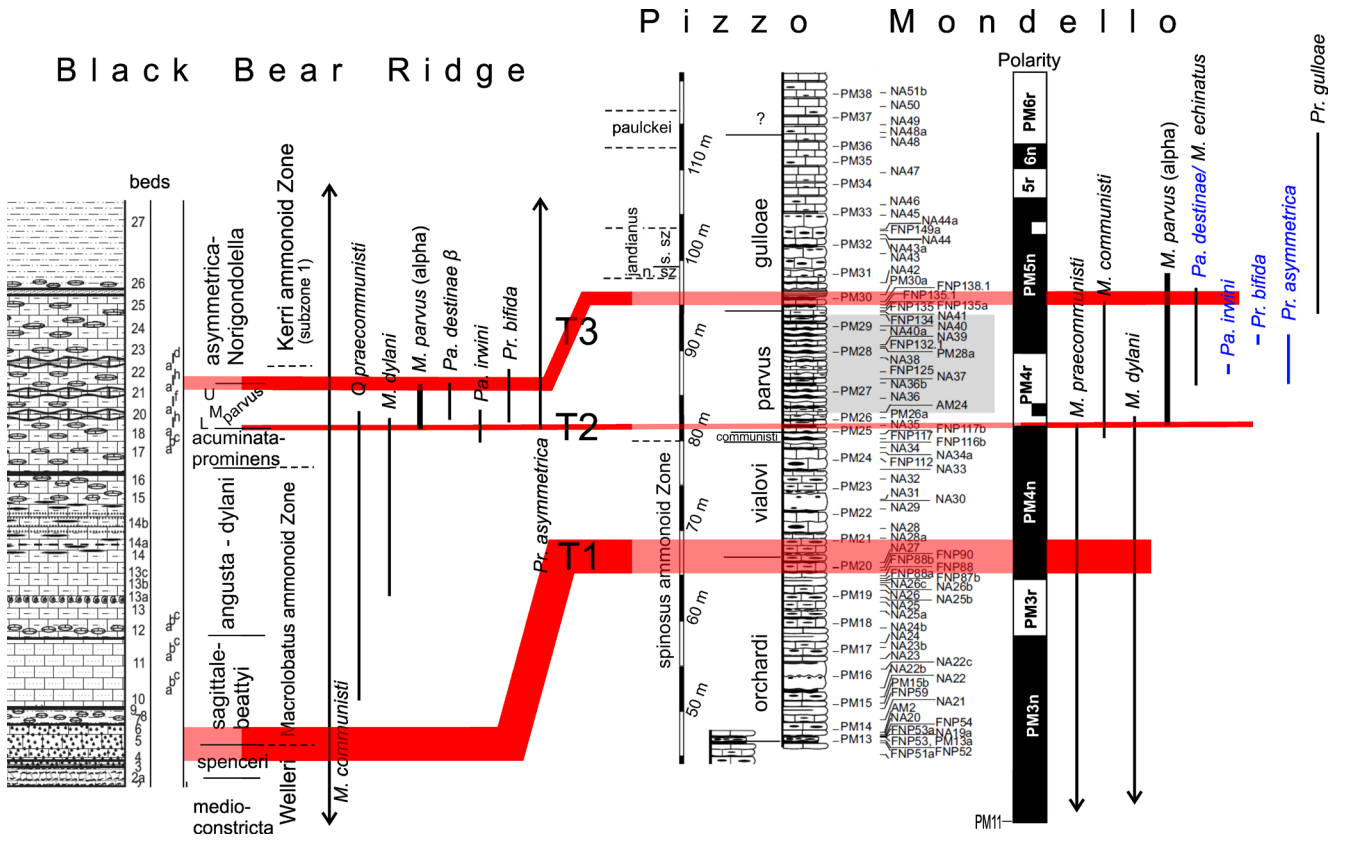

Figure 8 – Correlation between BBR and PM (based on Mazza et al. 2012a; 2018; Orchard, 2019), using the conodont turnovers T1 to T3, and some conodont other taxa (M. = *Metapolygnathus*, Pa. = *Parapetella*, Pr. = *Primatella*, Q.= *Quadralella*), selected to show the similarity in faunas in the *M. parvus* Subzone/Zone in the two sections (those in blue based on Orchard's (2019) evaluation of between-section similarities, based on published illustrations only). Magnetostratigraphic data (magnetozones PM3n to PM6r) from Muttoni et al. (2004), with palaeomagnetic sampling positions (PM13 to PM38) matched to the height scale. Divergent views remain on the β morphotype of *M. parvus* with *Pa. destinae* and *M. echinatus* shown.

Subzone (mid *Primitella primitia* Zone) at BBR. The appearance of the index species *M. parvus* is the key datum common to both sections, together with the appearance of other morphotypes (Figs. 7A, 7B). Their similarity in development refutes the impression of strong provincial differences.

Origin of Metapolygnathus parvus: During the late Tuvalian, several lineages of conodonts exhibited a reduction in platform size (that is the length of the platform relative to that of the blade) and an anterior migration of the pit (e.g. Mazza et al., 2018; Orchard, 2007, 2014, 2019). This is particularly true in *Metapolygnathus* and *Parapatella* (Orchard, 2014). This diminution in *Metapolygnathus* is manifest in the appearance of *M. parvus*, which is an easily recognisable species that descended from *M. dylani* (Orchard, 2014, 2019; Mazza et al., 2018; Figs. 7A, 7B). This phylogenetic lineage is well documented in both candidate GSSP sections.

The conodont *Metapolygnathus parvus* was established by Kozur in 1972 from the section at Silická Brezová (Slovakia), but the illustrated holotype belonged to a juvenile specimen (as noted by Krystyn, 1980) and not to an adult individual of *Me. parvus.* After more than 30 years, the criticisms of *Me. parvus* were addressed by Noyan & Kozur (2007), admitting that the holotype was established from a rich fauna consisting exclusively of juvenile forms of this species, but indicating that adult faunas are also abundant (Noyan & Kozur, 2007, p. 171). Noyan & Kozur (2007) also presented a detailed analysis of the *Metapolygnathus communisti* group, based on new material from the Stefanion section (Argolis, Greece), a pelagic succession belonging to the northern shelf of the Pindos-Huğlu Ocean, in northern Tethys (Fig. 6a). These authors described four species and two subspecies belonging to the communisti group: *Me. communisti communisti* Noyan & Kozur, 2007, *Me. communisti parvus*, *Me. multinodosus* Noyan & Kozur, 2007, *Me. linguiformis*, and *Me. angustus* Kozur, 1972. *Metapolygnathus parvus* was thus defined as a subspecies of *Me. communisti* and re-illustrated and re-described as an *M. communisti* with a shorter platform, with a more forward shifted pit and no nodes on the platform margins (Noyan & Kozur, 2007, fig. 7.1, p. 171). Recently, Orchard (2014, 2019) considered instead *Me. parvus* the descendant of the newly established species *Metapolygnathus dylani* Orchard, 2014: "*Metapolygnathus dylani* sp. nov. is interpreted to have evolved from *Me.* ex gr. *communisti* through reduction of the anterior platform and the relative lengthening of the free blade (Figs. 7A, 7B). A continuation of this trend is thought to have

Table 3. Proposed choices for the Carnian-Norian boundary within the two candidate sections. This also lists the secondary markers which have varying degrees of potential for correlation, some untested.

CHOICES	A	B	C	D
Primary marker	FO of *Me. parvus*	FO of *H. austriaca*	FO of *H. austriaca*	FO of *Me. parvus*
Section	Pizzo Mondello	Black Bear Ridge	Pizzo Mondello	Black Bear Ridge
GSSP 'spike' location	sample NA35	Base of Bed 22	Sample FNP135A	Base of Bed 18c
Biological secondary markers	LO *Me. praecommunisti* (ca. 0 m below NA35) LO *Me. dylani* (ca. 2m below NA35) LO *Gonionotites italicus* subzone, Spinosus Zone (Tuvalian 3, II) (PMAM22bis at 2.5 m below NA35) LO *Halobia lenticularis* (FNP118, ca. 0 m below NA35) LO *Ca. orchardi* (NA33, 6m below) LO. *Ca. psuedodiebeli* (NA32, 7.5 m below).	LO *Me. parvus* (bed 21f. 0.6m below) FO *Guembelites clavatus* (bed 22b, 0.2m above)-Kerri Zone indicator LO of diminutive Pa. destinae β, *Pa. johnpauli*, *Pa. willifordi* and Pr. rhomboidale (bed 21f, 0.6m below). Beginning of stable populations of *Acuminatella* and *Primatella*, +/-*Norigondolella* species (bed 21g, 0.4m below) See below for others	LO *Me. echinatus* (*Pa. destinae* β), FNP138.1, ca. 2 m above FNP135A. FO *Dimorphites noricus* (NA42.1) ca. 3.5 m above FNP135 (first subzone of Jandianus Zone) FO *Ca?. gulloae* (*Primatella* species according to Orchard, 2019), NA43, ca. 0 m below FNP135A. FO *Norigondolella trinacriae*, *Ep. spatula*, *Ep. uniformis* (PM30a, 2m above) FO advanced epigondolellids, assigned to *E. rigoi*), (PM28a, 4m below). FO *Ep. trangularis*, (NA43a, 7.5 m above)	LO of *H. septentrionalis* and FO of *H. selwyni* (in bed 18d, 0.1 m above) FO *Pterosirenites* cf. *auritus* at BBR (in bed 18d, 0.1 m above) FO *Pr. asymmetrica,* Pr. bifida; *Pr. rhomboidale* (bed 18c). LO *Me. dylani* (in 18f, ca. 0.5 m above 18c) FO *Pa. destinae*, *Pa. irwini*, *Pa. permica* (bed 17c, ca. 0.6 m below 18c) LO *Qu. (Me.) praecommunisti* (in 18h, ca. 0.75 m above 18c) See below for others
Chemo-physical secondary markers	Base of PM4r between sites PM25 and PM26, (within 1 metre of NA35) At start of rise to more positive $\delta^{13}C_{carb}$	Ca. 1.8 m below a negative $\delta^{13}C_{carb}$ excursion peak?	Mid part of PM5n (40% into PM5n)	At a small positive peak in $\delta^{13}C_{org}$ Oxygen isotope (in conodonts) drop within Parvus Subzone
Wider regional relationship	Magnetozone PM4r allows correlation to many other sections, (especially Newark Supergroup cyclostratigraphy). Ammonoids allow comparison to Feuerkogel F5 and Jomsom sections	Coincident[1] or near top of the Macrolobatus Zone (Fig. 5 in Orchard, 2019). Near base of radiolarian assemblage 5 (FO of index *Capnodoce fragilis*) Beginning of strata with *Norigondolella navicula* in Boreal Realm.	Magnetozone PM5n allows correlation to many other sections, (especially Newark cyclostratigraphy). Ammonoids allow comparison to Feuerkogel F5 and Jomsom sections.	Within the upper part of the Macrolobatus Zone (Fig. 5 in Orchard, 2019) Near the base of boreal Kinasovi Zone (from *Pterosirenites* cf. *auritus*) in Boreal Realm. Base of radiolarian assemblage 4 (esp. *Capnodoce malaca*, *Dumitricasphaera elegans*, and *Hetalum parvum*)
Estimated duration to closest secondary marker*	Ammonoid LO=120 kyr *Halobia* LO= 0 kyr Conodont LO= 0 kyr PM4n-PM4r boundary= ~50 kyr	Ammonoid FO =50 kyr Conodont LO= 150 kyr Conodont FO=250 kyr	Ammonoid FO= 160 kyr Conodont FO= 0 kyr Conodont LA=106 kyr Base PM5n= 200 kyr	Ammonoid FO= 25 kyr *Halobia* FO/LO= 25kyr Conodont LO= 125 kyr

FO= first occurrence, LO= last occurrence.

*Since, a GSSP point is chronostratigraphic level, a consideration of time is important. As a rough estimate of the duration using height differences, the duration of the range of *Me. parvus* at PM can be estimated using the cyclostratigraphic duration scale (*Me. parvus* range = base PM4r to mid PM5n) in the Newark Supergroup from Kent et al. (2017), which gives an estimated duration from FO to LO of *Me. parvus* of 0.75 Myr at PM. The *Me. parvus* range at BBR and PM in metres is about 3.0 m and 16 m respectively. So, for a 10 kyrs duration this gives a sediment thickness of about 4 cm and 21 cm at BBR and PM respectively. Or for 100 kyrs duration, 0.4m and 2.13 m at BBR and PM respectively. The secondary markers which are greater or equal to an estimated 0.25 myr duration from the primary marker are in green (ca. = 1.0 m distance at BBR, ca. =5.3 m distance at PM).

[1]Macrolobatus Zone is aligned on LO of *Me. parvus*, based on the absence of *Anatropites* in the youngest *Macrolobatus* fauna listed in Fig. 5 in Orchard (2019). Other biological secondary markers at Black Bear Ridge, Option B: LO of *Primatella bifida* and Pr. rotunda (bed 23, ca. 1.0 m above).FO *Acuminatella curvata* (bed 23, ca. 1.0 m above); FO of *Ng. norica* (bed 25, ca. 3.0 m above). Most species of *Kraussodontus*, *Metapolygnathus*, *Parapetella*, and *Quadralella* disappear by end of the Parvus Subzone. Other biological secondary markers at Black Bear Ridge, Option D: FO *Acuminatella acuminata* and *Parapetella posterolata* (bed 17, ca. 1.5 m below 18c); FO *Pa. prominens* and *Primatella triangulare* (bed 17a, ca. 1.3 m below 18c). FO of *Pr. circulare*, and the diminutive *Pa.* n. sp. D of Orchard (2014), *Pa. johnpauli*, *Pa. pumilio*, and *Pa. willifordi* (beds 18e-f, ca. 0.5 m above 18c).

led to *Me. parvus*, which has a substantially reduced platform that is less than half of the total element length and an anterior pit" (Orchard, 2014, p. 10). Orchard (2014) also differentiated three morphotypes that showed different degrees of platform development- similar, but not identical morphotypes can also be found at PM (Figs. 7A, 7B, 8). *Metapolygnathus parvus* Kozur is the α morphotype of Orchard (2014).

The phylogenetic lineage and morphological characteristics of *M. parvus* are well established, and widely accepted amongst conodont workers, making this a suitable 'stable' primary marker for the base of the Norian.

Wider occurrence: *Metapolygnathus parvus* have been collected from different depositional environments, such as periplatform carbonates, distally steepened carbonate ramp/medial to distal slope environments and proximal to deep water pelagic environments, including cherts deposited below the CCD (NE China), and at different paleolatitudes on both sides of Pangea. *Me. parvus* is reported to occur in North America at Black Bear Ridge, Pardonet Hill, and Juvavites Cove in the autochthonous Western Canada Basin (Orchard, 2014, 2019), and at Huxley Island, Sadler Point, and Frederick Island in the allochthonous Panthalassan Wrangel terrane (Carter & Orchard, 2013). Also, it is present in Tethyan successions, such as at Pizzo Mondello and Pizzo Lupo (Sicily, Italy), the Bölücektasi Tepe and Erenkolu Mezarlik sections (Turkey), the Silická Brezová section (Slovakia) (Mazza & Krystyn, 2015), the Csővár borehole (Hungary) (Mazza & Krystyn, 2015), the Gianni Grieco section, Lagonegro Basin (Southern Apennines, Italy) (Rigo et al., 2012a), Slovenia (Kolar-Jurkovsek, 1982), the Argolis section (Greece) (Noyan & Kozur, 2007). In addition, from the Nakijin Formation in the Hedomisaki area (Okinawa, Japan) (Yamashita et al., 2016); and from the mid-Panthalassa Nadandaha Range (Northeast China) (Buryi, 1996), and Mota Hai Luli, Timor-Leste (Orchard and Rigo, unpublished data). Its widespread presence indicates the suitability of *Me. parvus* for defining the base of the Norian.

Lifestyle: Based on its broad distribution, on its occurrence in proximal to distal to open pelagic marine setting, and on $\delta^{18}O_{phosp}$ analysed directly on *Me. parvus* apatite (Trotter et al., 2015), it is concluded that *Me. parvus* was a surface dweller.

2.2 *Metapolygnathus parvus:* reliability and relationship with physical and biotic events

- The species is easily recognisable.
- It is possible to identify the FAD of *Me. parvus* within the hypothesized lineage *Metapolygnathus* ex gr. *communisti* (*praecommunisti*) → *Me. dylani* → *Me. parvus* in both candidate GSSP sections (Pizzo Mondello and Black Bear Ridge).
- *Me. parvus* is documented to occur homotaxially at the base of the evolutionary morphological turnover T2, both at Pizzo Mondello (Tethys) and within the *Me. primitius* Zone at Black Bear Ridge (North America).
- It is coincident with a diminution in some conodont stocks, and the disappearance of many more typically Carnian conodonts

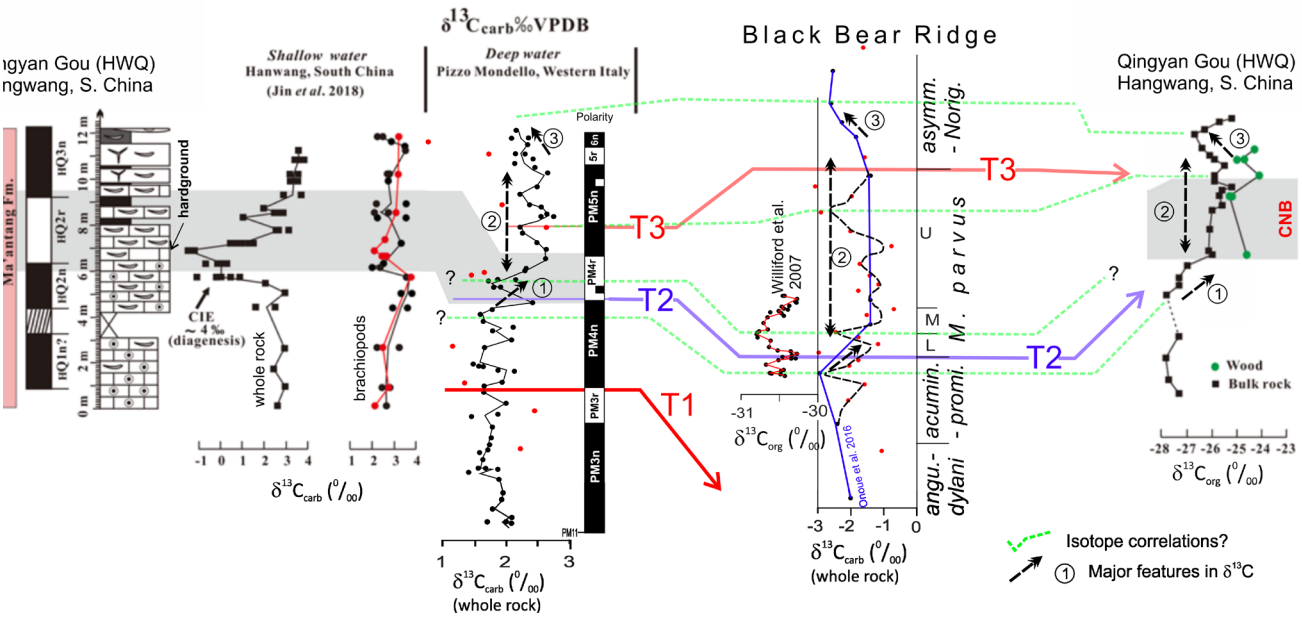

Figure 9 – Carbon isotope data across the Carnian-Norian boundary. Partly based on fig. 11a in Jin et al. (2019), but re-drawn. Carbon isotope data for Pizzo Mondello (PM) and Black Bear Ridge (BBR) based on Muttoni et al. (2004), Williford et al. (2007), Onoue et al. (2016). The BBR data from Onoue et al. (2016) has their original inferred data trend (blue line) and a more 'optimistic', speculative, interpretation of the $^{13}C_{carb}$ data in black dashed line, which seems to show some of the fluctuations in $\delta^{13}C_{carb}$ as also seen at PM. The main features are the rise in ^{13}C, (1) across the T2 turnover, the plateau ((2) in figure) in positive values and the decline (3) above the T3 turnover. The carbonate isotope data from Hangwang shows a quite different response, which is likely diagenesis-impacted. The grey interval is the CNB suggested by Jin et al. (2019), is a proxy for the correlated PM4r/HQ2r magnetozones. (Hounslow)

in both candidate sections. This also coincides with the mass occurrence of evolutionary advanced metapolygnathids at PM, and a flourish of comparable elements assigned to *Parapatella* and *Quadralella* at BBR (and at PM; as assigned by Orchard, 2019; Fig. 8). The range of *Me. parvus* thus marks a turnover between typically Carnian to Norian species, completed by the time of the last occurrence of *Me. parvus*.

- Its first appearance is below the first occurrence of *Halobia austriaca* in both candidate sections, and also at Silická Brezova and Erenkolu Mezarlik (Krystyn & Gallet, 2002).
- It occurs in different marine depositional environments, such as periplatform carbonates, distal ramp/slope, and from bedded cherts deposited below the CCD.

2.3 Potential secondary markers for the base Norian near the FAD of *Me. parvus*

Correlation to other sections without conodonts would be based on associated secondary markers (Table 3):

- At both GSSP candidates, the range of *Me. parvus* is placed between Upper Carnian strata with the ammonoid *Anatropites* and Lower Norian strata with *Guembelites* in North America and *Dimorphites* in the Tethys. The proposed boundary in the candidate sections therefore falls in the 'traditional Carnian-Norian' transition interval. The FO of *Me. parvus* also occurs just prior to *Pterosirenites* cf. *auritus* at BBR (in bed 18D; Fig. 2), an ammonoid species typical of what has been inferred to be earliest Norian (Kinasovi Zone) in the Boreal realm (Konstantinov et al., 2003; Konstantinov, 2019; Balini et al., 2012). The base of the Kinasovi Zone may therefore provide a secondary proxy for the base of the Norian in Boreal sections.
- At Pizzo Mondello, the base of magnetozone PM4r is between sites PM25 and PM26 (Muttoni et al., 2004), and the FO of *Me. parvus* is in sample NA35 (Fig. 8), so these two events are very close, making the base of magnetozone PM4r a closely coincident secondary marker for the base of the Norian.
- Several carbon isotope fluctuations occur in the interval between conodont turnovers T1 and T3, with the most pronounced positive change (indicated as (1) in Fig. 9) near the base of turnover T2, a trend to more positive $\delta^{13}C$ seen in both candidate sections in both carbonate ($\delta^{13}C_{carb}$) and organic matter ($\delta^{13}C_{org}$) (Muttoni et al., 2004, 2014; Mazza et al., 2010; Onoue et al., 2016; WIlliford et al., 2007). This provides a suitable 3rd type of secondary marker for the base of the Norian. The details of any finer resolution, global stratigraphic changes in $\delta^{13}C$, within the T2 to T3 interval, are currently unresolved (see section 4.3).

(Nicora, Orchard, Rigo, Hounslow)

3. KEY ATTRIBUTES OF THE FIRST OCCURRENCE OF *HALOBIA AUSTRIACA* AS A PRIMARY MARKER TO DEFINE THE BASE OF THE NORIAN

Several workers have suggested that the FAD of the bivalve *Halobia austriaca* could act as a good proxy for correlation of the Carnian- Norian boundary (Krystyn & Gallet, 2002; Levera & McRoberts, 2008; McRoberts & Krystyn, 2011; Levera, 2012). Here, the merits of using *H. austriaca* as a primary marker for the base of the Norian are explored, and its potential for high resolution correlation. This section should be read in conjunction with McRoberts (2021) a draft of which was seen by the CNB working group prior to publication, which has more details of the taxonomic issues and particularly discusses North American occurrences of *Halobia austriaca*.

Overview: Halobiids are an extinct family of thin-shelled bivalves, which proliferated during the Late Triassic, which was an interval of rapid evolutionary change in *Halobia*, with a turnover rate that matched or exceeded that of ammonoids (McRoberts, 2010, 2011). Thin-shelled bivalves have also been used elsewhere in the Phanerozoic to define stage bases. The FAD of the inoceramid bivalve *Platyceramus undulatoplicatus* has been used to define the base of the Santonian (Lamolda et al., 2014); and probably an inoceramid bivalve may be used for the forthcoming GSSP of the Coniacian (https://stratigraphy.org/gssps/). A 1970s definition of the base of the Telychian Stage (early Silurian) also used a brachiopod primary marker (https://stratigraphy.org/gssps/).

In these respects, use of *H. austriaca* to define the base of the Norian would be consistent with usage at some other GSSP's. The fact that it is a macrofossil also has additional merit, in that specialists could identify it in the field. *Halobia austriaca* is also a long-standing species (Mojsisovics, 1874), and has a distinctive form (Figs. 10, 11) because of its outline and pattern of ribbing (Levera, 2012; McRoberts, 2021). Synonyms of *H. austriaca* are also quite well understood (Levera, 2012; McRoberts, 2021).

In parallel with the conodont work at Black Bear Ridge and Pizzo Mondello, McRoberts (2011) and Levera (2012) have produced major taxonomic studies of *Halobia* from the candidate sections. Also, Krystyn (1980) and Krystyn & Gallet (2002) summarised the distribution of Halobia near the CNB in Austria and the eastern Mediterranean, with some updates of these data in McRoberts (2021).

3.1 Evolutionary trends, origin and taxonomy of *Halobia austriaca*

Halobia are thought to be several separate lineages derived from ancestors of *Daonella*. This evolutionary transition may be near the base of the Carnian, either directly or through the genus *Aparimella* (McRoberts, 2010). At the moment the species level phylogenetic lineage of *H. austriaca* is uncertain, with a number of possible pathways (McRoberts, 2021).

At the species level, the variety and variability in *Halobia* probably requires further critical taxonomic work to consolidate these. Over the last 100 years, work has led to the proliferation of species, many of which are based on inadequate material (small sample sizes, taphonomically compromised, without regard to population morphological variability; McRoberts, 2010). Of the 300 or so species of *Halobia* assigned, McRoberts (2010) suggested around 30–50 may be valid. The re-evaluation of *H.*

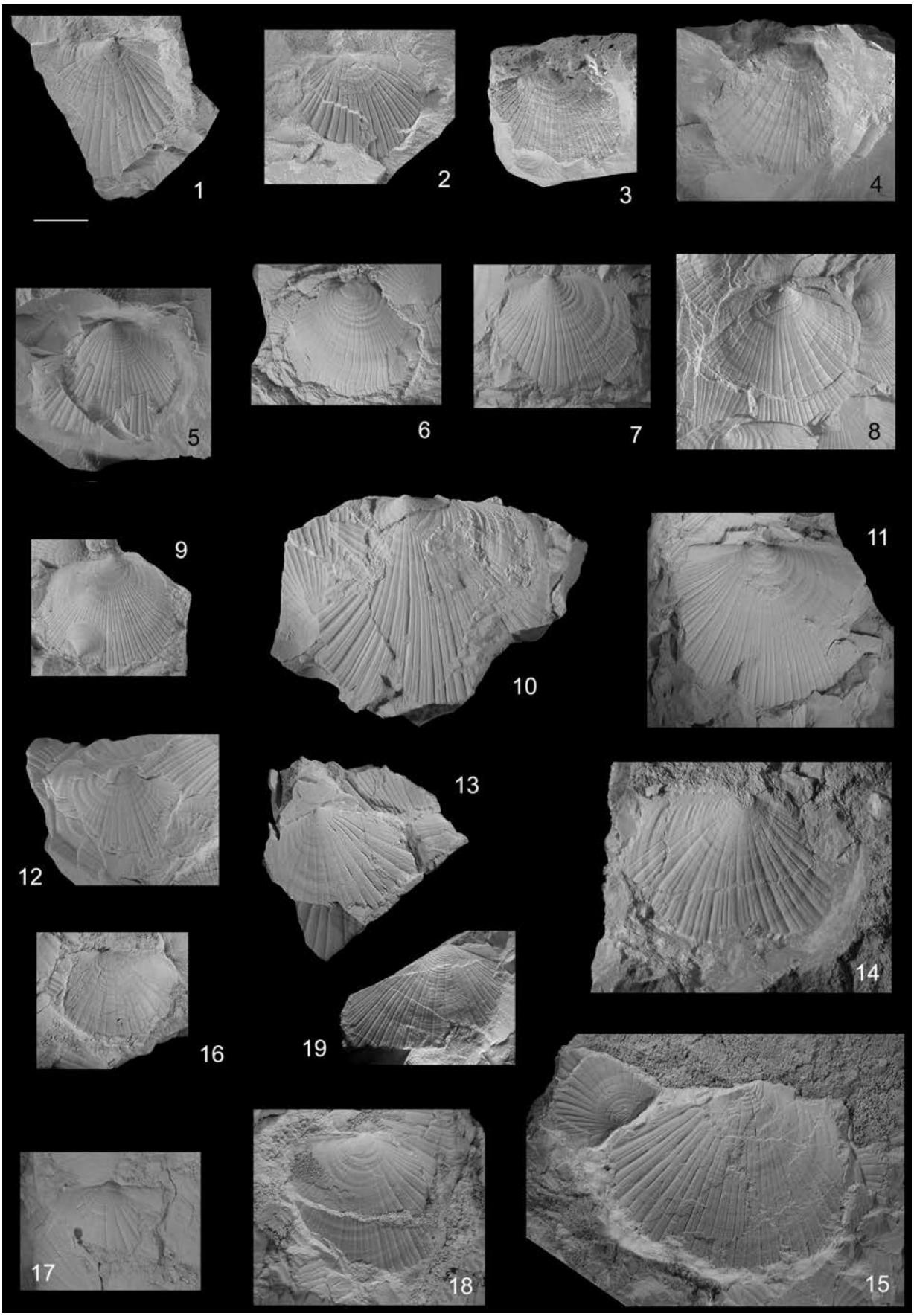

Figure 10 – Specimens of *Halobia austriaca* from Pizzo Mondello (from Levera, 2012).

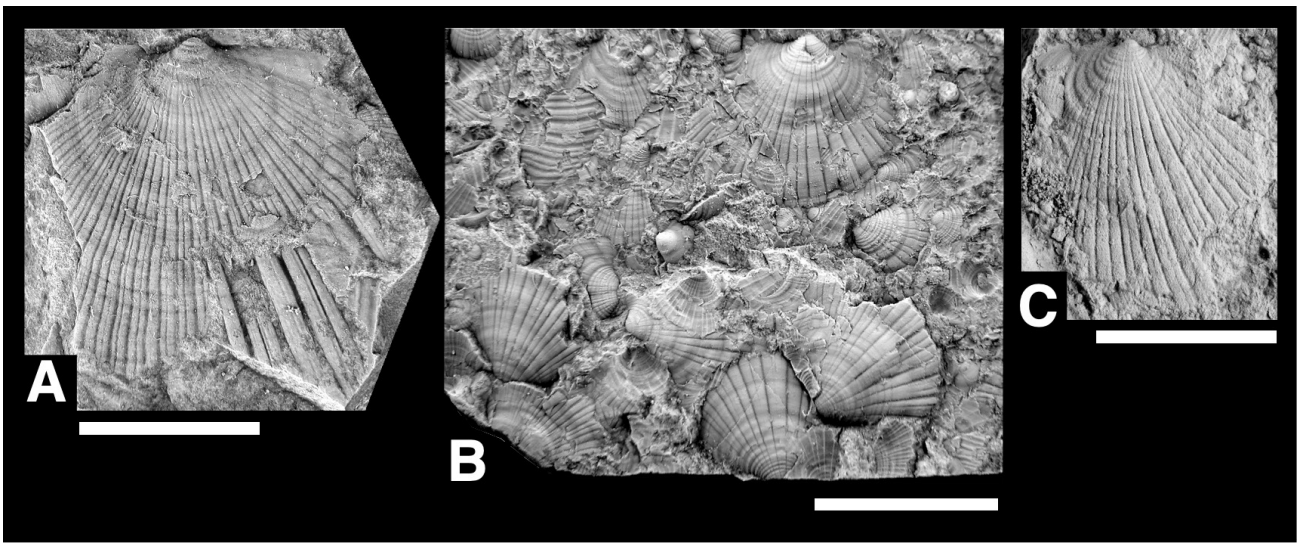

Figure 11 – Specimens of *Halobia austriaca* from Black Bear Ridge (from McRoberts, 2011). Not included are specimens originally identified in McRoberts (2011) as *H. austriaca* that are now assigned to different species (McRoberts, 2021). A, from bed 27; B from bed 22, C, from bed 33.

austriaca by McRoberts (2021) is part of this process.

Morphologic evidence suggests *Halobia* may have either had an epibyssate life mode (weakly attached to floating algal debris?), or a freely resting/reclining mode without byssal attachment. The lack of clearly demonstrated attachment tends to support the later. The thin shells and low profiles suggest a streamlining response. *Halobia* have a strong association with oxygen deficient water masses and sediment, without major evidence of post-mortem transport. Seilacher (1990) proposed that *Halobia* housed symbiotic sulphur-utilising bacteria, which is why they had a preference for oxygen poor environments. It should also be noted that *Halobia* also are found in a variety of fully oxygenated lithofacies, so a preference for dysoxic environments is not obligate. The episodic nature of often monospecific *Halobia* shell beds suggests a low resistance to disturbance and ability for rapid recovery.

***Wider occurrence*:** *Halobia austriaca* is fairly widely spread throughout the southern and northern hemispheres (New Zealand to Alaska) and in low to high palaeolatitudes (eastern Tethys, e.g., Turkey to near the N. paleopole in NE Asia and Siberia) (Table 3, and data in McRoberts, 2021). It occurs in the truly oceanic carbonate and chert realms in Japan, Timor and Oman (Shackleton et al., 1990) to deep water turbiditic systems in the western Quinling in China (Meng et al., 2007). Both carbonate and clastic deeper and open water systems accommodated *Halobia*. Shallow water settings seemed to be less accommodating to *Halobia* (Del Piero et al., 2020). This wide distribution of *H. austriaca* (and other halobiids in general) is thought to be due to halobiid opportunism, and probably having a larval planktonic early life stage, allowing colonisation of widely spread suitable habitats.

This global distribution is a great strength of using *H. austriaca* for correlation and GSSP definition. However, like many macro fossils, episodic occurrence (perhaps less severe than in Late Triassic ammonoids) in sections can limit cm to meter scale resolution studies, which is probably part of the reason there are very few section-focused studies and rather more formation- and site-focused studies (Table 4).

3.2 *Halobia austriaca*: reliability and correlation with physical and biotic events

The relationship between *Halobia austriaca*, conodonts and ammonoids (and geomagnetic and geochemical data) is best defined in section-based data. This can readily be seen Table 4, where *H. austriaca* is apparently associated with a variety of ammonoids and conodonts, which have a typical late Carnian (Tuvalian) (e.g., *Sirenites senticosus*) to early Norian (Lacian) (e.g. *Juvavites* sp.) age range. This apparent wide range in age of *H. austriaca* (in non-section-based datasets), is probably due to lumping together occurrences over a wide stratigraphic range. The most complete and comprehensively integrated datasets around the CNB, with large collections of *Halobia*, are those from Black Bear Ridge and Pizzo Mondello (Fig. 12). Krystyn & Gallet (2002) also describe *H. austriaca* occurrences associated with conodont, ammonoid and geomagnetic data from sections at Silikcá Brezová, Kaavalani, Bolücektasi Tepe and Feuerkogel (Fig. 13; McRoberts, 2021). The exception to this two-fold division in data-quality, are the ranges of *Halobia* species in western North America described by McRoberts (2010, 2011, 2021), from a range of stratigraphically better constrained occurrences, allowing a 'calibration' against North America ammonoid zones (Fig. 14). However, Balini et al. (2012) have argued "…. it is conceptually wrong to use data from scattered localities, ….. to calibrate cm-by-cm sampled sections".

The section-based data from Black Bear Ridge and Pizzo Mondello show the FO of *H. austriaca* at around the T3 conodont turnover near the last occurrence of *Me. parvus* (top of Parvus Zone/Subzone; Fig.12). The re-assessment of the North American faunas over the last 10 years by McRoberts (2021) is substantially different from previous evaluations (McRoberts, 2011), with the lowest assured occurrence in bed 22 at Black Bear Ridge (Fig. 12). Across Williston Lake at Pardonet Hill East (Table 3),

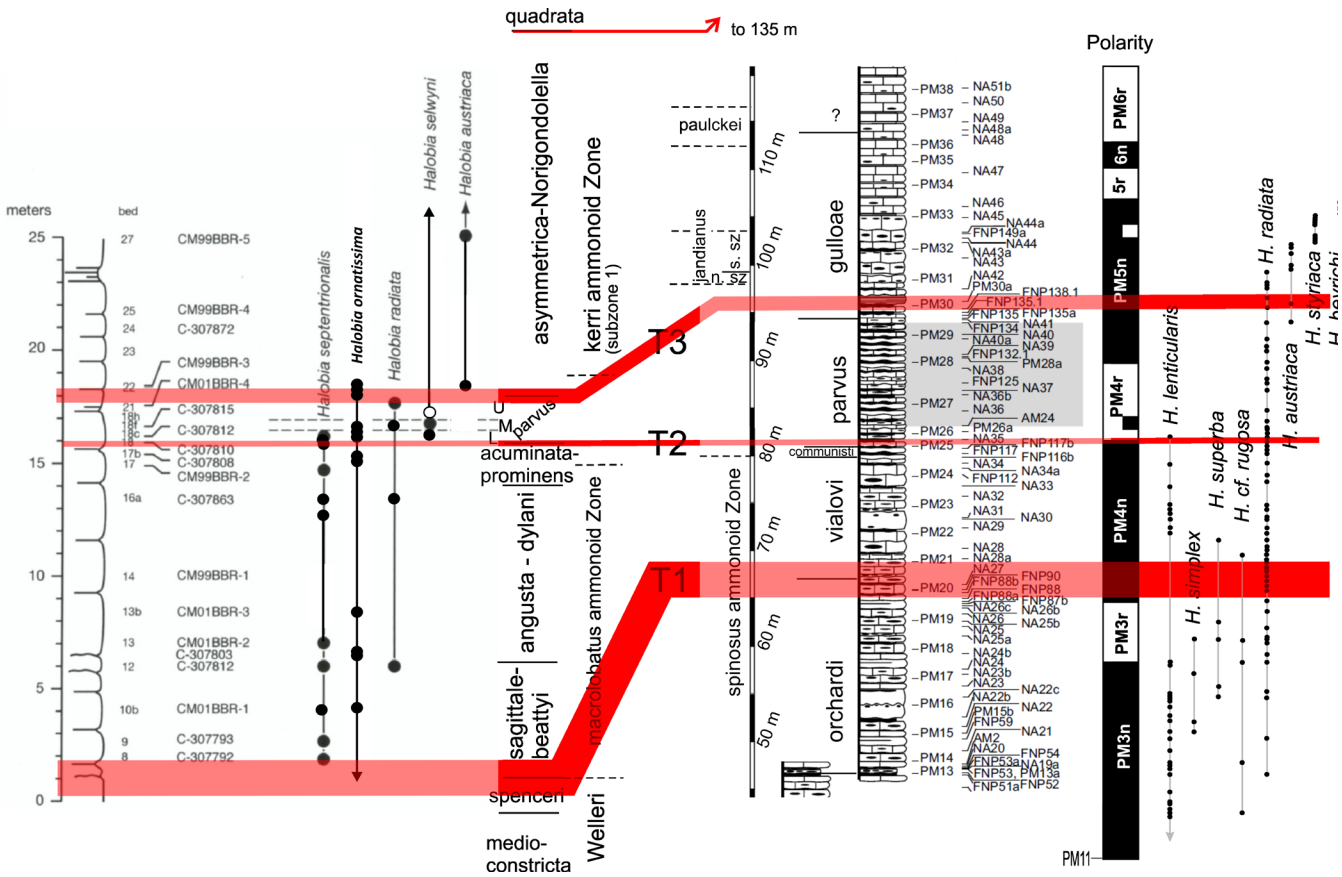

Figure 12 – *Halobia* occurrences at Black Bear Ridge (McRoberts, 2011, 2021) and Pizzo Mondello (Levera, 2012; Balini et al., 2012), with the conodont turnovers, T1, T2, T3 (Mazza et al., 2018; Orchard, 2019) used for correlation between these two sections. Magnetostratigraphy from Muttoni et al. (2004) with boundaries placed according to the PM sample positions in the log from Mazza et al. (2012a).

possible juveniles of ?*H. austriac*a (or more probably *H. selwyni*) occur in the lower part of the Parvus Zone (C-307835. bed 3 and C-307836, bed 4 at Pardonet Hill; McRoberts, 2021). These two levels also contain *Gonionotites*? sp. and *Pterosirenites auritus*. Further details of *H. austriaca* in North America are in McRoberts (2021). Notably, at both Black Bear Ridge and Pizzo Mondello the last occurrence (LO) of *H. radiata* is also near to the T3 conodont turnover (or upper part of Parvus Zone), suggesting that the LO of *H. radiata*–FO *H. austriaca* transition may be a useful approximate proxy for this level, and not far above the base of the *Stikinoceras kerri* ammonoid Zone and *Guembelites jandianus* Zone (Figs. 12, 14; Balini et al., 2012).

In Austrian and Turkish sections (Fig. 13) Krystyn & Gallet (2002) associated the occurrence of *H. austriaca* broadly with the range of '*Me. communisti* morphotype B' (a form species now in part re-assigned to various *Primatella* species by Orchard (2013), *Me. communisti multinodosus* by Noyan & Kozur (2007); Mazza & Martinez-Perez (2015), and in the Turkish sections synonymous with *Neogondolella trinacriae* (Krystyn, person. commun). At Pizzo Mondello *Me. communisti* has a restricted range from within magnetozone PM4n to PM5n (UT12n to UT13n magnetochrons; Fig. 8), largely between the T2 and T3 conodont turnovers (Mazza et al., 2012a), much like that in the Turkish sections (Fig. 13). As at Pizzo Modello, *H. austriaca* is found in the magnetochron UT13n at Bolücektasi Tepe, but lower at Kaavalani within the topmost part of magnetochron UT12r (Figs. 12,13). Therefore, possibly as at Pardonet Hill in British Columbia, the FO of *H. austriaca* in the Kaavalani section is a little lower (around the mid Parvus Zone) within the T2 to T3 interval (compare Figs. 12,13). Consequently, the most detailed data from Pizzo Mondello suggest a polarity zone boundary is not closely coincident with the FO of *H. austriaca*, and hence- perhaps the lower part of magnetochron UT13n is missing in the Kavaalani section?

***Secondary markers*:** If *Halobia austriaca* were chosen as the primary marker for the base of the Norian, then the upper boundary of the Parvus Zone (subzone) and conodont turnover T3, or 'traditional Norian' ammonoids may be suitable secondary markers (Table 3). That is, the base of the *Stikinoceras kerri* Zone (with *Guembelites*) in North America and base of the *G. jandianus* Zone in the western Tethys. In NE Asian sections if the synonymised *Indigirohalobia* (*Popowihalobia*) *brooksi* and *Indigirohalobia* (*Primahalobia*) *kilganaensis* represent forms of *H. austriaca*, then the association in NE Asia (Table 3) is with the ammonoid *Sirenites yakutensis* and the Halobiid Zone *Indigirohalobia asperella* (especially upper part). The details of this relationship to NE Asians sections would need clarification.

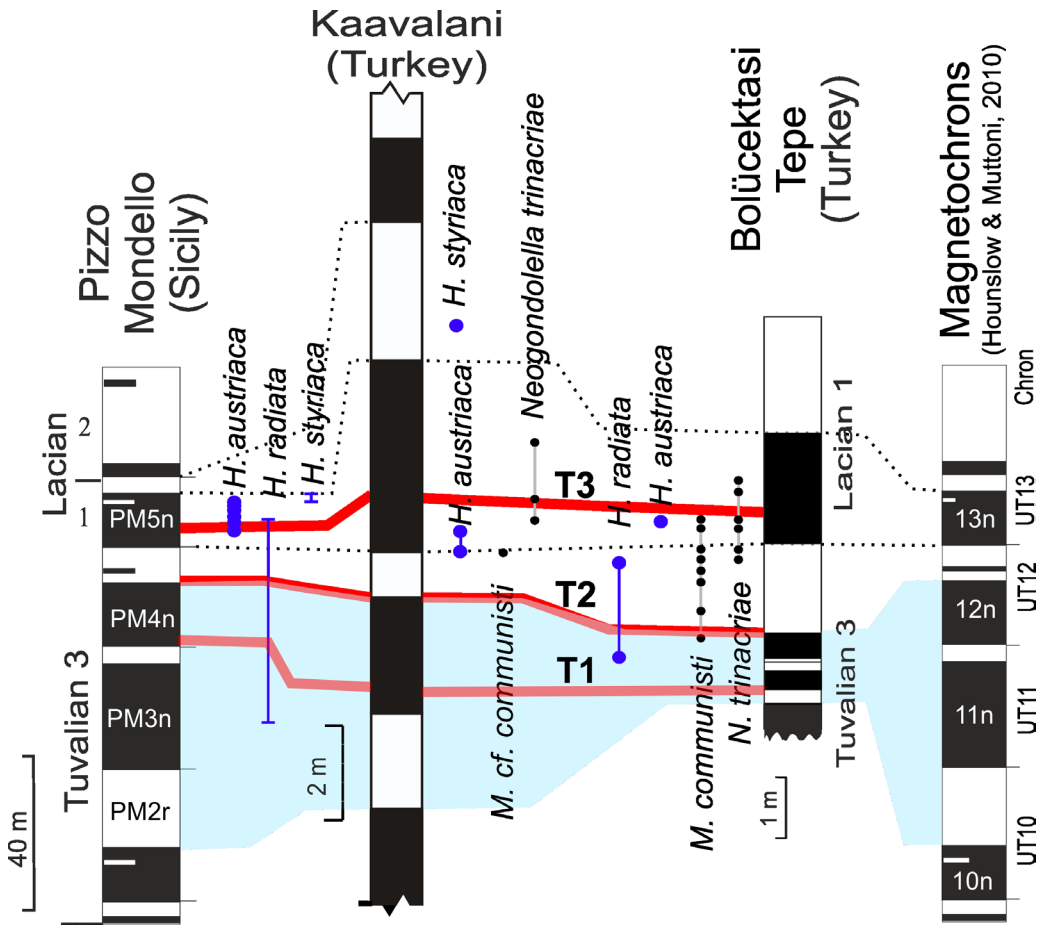

Figure 13 – Relationships between *Halobia* occurrences, selected conodonts and magnetostratigraphy in the Pizzo Mondello, Kaavalani, and Bolücektasi Tepe sections (based on data in Gallet et al., 2000; Krystyn and Gallet, 2002, updated by Krystyn). Blue and dotted lines are magnetostratigraphic correlations, red the correlated conodont turnovers (correlated using position in magnetozones at Pizzo Mondello). Data for Turkish sections updated by L. Krystyn.

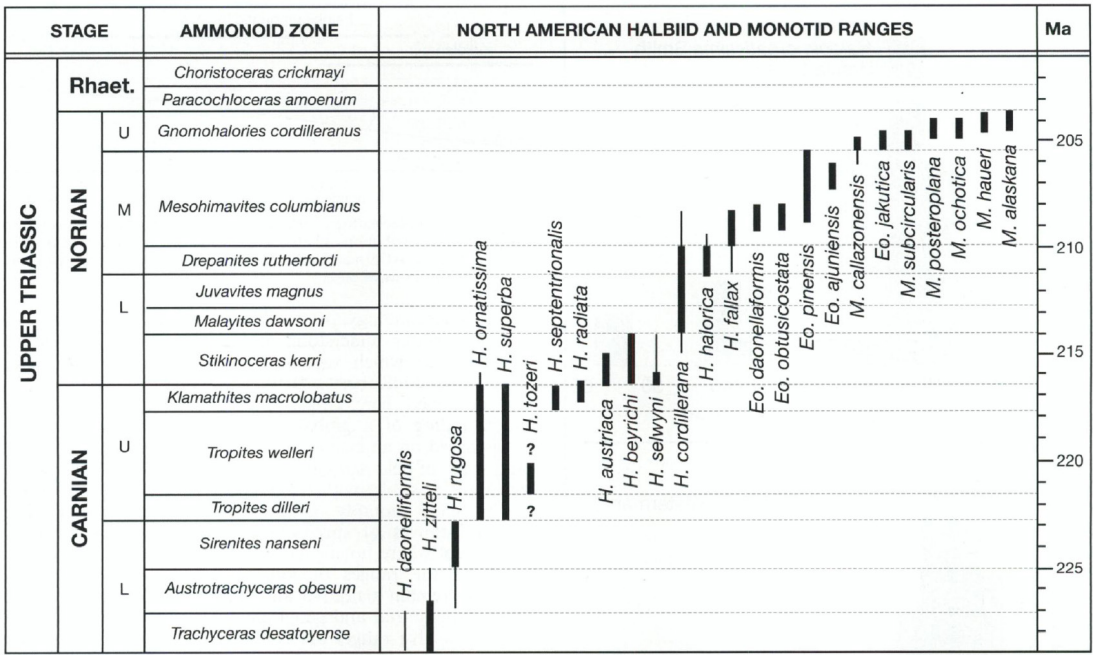

Figure 14 – Ranges of *Halobia* against northern American ammonoid zones (from McRoberts, 2011).

Table 4. List of occurrences of *Halobia austriaca* (and its probable synonyms), and associated fauna (listed at same sampling locality or section) exclusive of candidate Pizzo Mondello and Black Bear Ridge sections.

Location	Fauna associated with *Halobia austriaca* occurrences (and its synonyms)	Section details	Reference
McCarthy C-5 quadrangle, Alaska	*Discophyllites* cf. *D. ebneri* ; *Juvavites* sp. Indet {T/L}	no	MacKevett, 1971, Silberling, 1963
S.W. coast of of Bostwick Inlet, Gravina Island, Alaska	*Arcestes* sp., *Juvavites (Anatomites) externiplicatus* {T} (all in float)	no	Berg & Cruz, 1982
Herring Bay, Admiralty Is., Alaska	*H. ornatissima, H. lineata, Margarites cf. jokelyi, Juvavites externiplicatus, J. knowltoni, J. cf. subinterrutptus , Arcestcs shastensis, Pinacoceras cf. rex, Aulacoceras cf.carlottense* {T}	no	Smith, 1927
Pardonet and Baldonell fms , East Pardonet Hill, Brown Hill, British Columbia, Canada	*Stikinoceras kerri Zone*	yes	McRoberts, 2011
Alaska Canyon, Jackson Mt, Humboldt County, Nevada	*Halobia superba,* (overlying are *Arcestes pacificus; Discotropites ojsvarensis* {T}	yes	Fuller, 1986
Wallowa terrane, Oregon, USA	none	no	Stanley et al., 2008; McRoberts, 1990
Section F1-E, Feuerkogel, Austria	*Metapolygnathus communisti morphotype A, Neogondolella trinacriae, Epigondolella abneptis, Primatella primitia, E. abneptis, Norigondella navicula.*	yes	Krystyn, 1980; Krystyn & Gallet, 2002
Section B, Feuerkogel, Austria	*M. communisti* morphotype A and *Neogondolella trinacriae, E. abneptis, Pr. primitia, N. navicula.*	yes	Krystyn, 1980; Krystyn & Gallet, 2002
F 4 and F 5 N. Feuerkugel, Austria	*M. communisti; E. abneptis,. Pr. primitia, N. navicula; Dimorphites noricus. Griesbachites* sp.,	yes	Krystyn, 1980; Krystyn & Gallet, 2002
Silicka Brezova, Slovakia	*M. communisti* morphotype A and *Neogondolella trinacriae, Carnepigondolella pseudodiebeli, N. navicula.*	Yes	Krystyn & Gallet, 2002
Izvorul Malului klippe, Romania	*H. styriaca, H. falax, H. bukovinensis, Monotis* cf. *haueri*	no	Popescu & Popescu, 2008
Dachstein Limestone, Vaşcău plateau, Romanian	*H. austriaca, H. superba, H. styriaca, Gondolella (Quadralella) polygnathiformis, E. abneptis, Enantiognathus ziegleri, and Prioniodella ctenoides.* Overlying strata have *H. styriaca, H.* cf. *beyrichi, Monotis* ex gr. *haueri ; Juvavites (Anatomites) ducetii* {L}	no	Bucur, 2001
Kaavalani, Turkey	*M. communisti* morphotype A*; C. pseudodiebeli, Placites placodes {L}*	yes	Krystyn & Gallet, 2002; Gallet et al., 2000.
Bolucektasi Tepe, Turkey	*M. communisti* morphotype A and *Neogondolella trinacriae, C. pseudodiebeli,*	yes	Krystyn & Gallet, 2002; Gallet et al., 1992
Turkestan flyscoid belt, Afghanistan	*Sirenites senticosus, {J} Monotis* sp.	no	Montenat, 2009
Sabau river NE of Kapan in West Timor	*Halobia clari*	no	Kristan-Tollmann et al. 1987; Charlton et al., 2009
Kanikeh Formation, Kalimati, Wai Lola Kecil River, Seram Is., Indonesia	*H. styriaca, H. austriaca, Monotis hoernesi, H. superba*	no	Wahyudiono et al., 2018
Oreti River, New Zealand	none	no?	Raine et al., 2012, Campbell, 1994
New Siberian islands, exposure 190, Tikhaya River	(9–13 m) ammonoids *Arctophyllites* cf. *popovi; Zittelihalobia fallax* (17–18 m) bivalves *Halobia* ex gr. *austriaca, Z. indigirensis, Z. fallax; Z.*aff. *obruevi*	yes	Konstantinov et al., 2003
Anyui–Chukotka Fold System, Northeastern Asia	*H. superba*	no	Katkov et al., 2010
Magadan-Kolmya- Omolon, Northeastern Asia	*Sirenites yakutensis* [with *In kilganaensis, H. brooksi]*	yes	Polubotko, 2005
Sirkunovskaya suite, Yana & Indigirka rivers. NE Russia	*Arctophyllites taimyrensis, Ar. popowi, Yanosirenites seimkanensis, Neosirenites armiger,* {T} *N. irregularis, Yakutosirenites pentastichus, Sirenites yakutensis, Striatosirenites kedonensis, St. kinasovi, Proarcestes gaytani, Pr. verchojanicus, Indigirohalobia popowi, In. kudleyi, H. superba, In. asperella, H.* ex gr. *brooksi, Zittelihalobia kiparisovae, In. kilganaensis, H. kegaliensis, H.kinasov*	no	Truschelev & Grinenko, 2016
Xinduqiao Formation, Songpan Terrane, China	*H. gigantea, H. pluriradiata, H. rugosa*	no	Meng et al., 2007
Qugasi Formation, Qinghai-Xizang Plateau, China	*Discophyllites ebneri, Joannites* sp., *Proarcestes* sp., *Lobites* sp. and *Sturia* sp., {D/J}, *H. yunnanensis, H. convexa.*	no	Lin et al., 2007
Bayanhar Group, NW Leixiwudanco and NE Malanshan, Qinghai-Xizang Plateau, Hohxil, China	*H. yunnanensis, H. convexa ,H. banmaensis,H.* cf. *yandongensis*	no	Sha & Grant Mackie, 1996
Pane Chaung Group in Bhopi Vum Area, Myanmar	*H. dalliana, H. styriaca, H. dilatata, H. tozeri, H. comata, H. mediterranea, Daonella* sp., *?Judicarites* sp. and *Posidonia* sp.	no	Tun Min & Maung, 2019
Nam Mu Formation, N. Vietnam	*H. talauana,H. substyriaca, H. superba, Margaritropites fongthoensis,{T} Juvavites sp. and Discotropites sp. {T}*	no	Komatsu et al., 2017; Khuc, 1991
N. Thailand	*Margaritropites phongthoensis {T}, H. talauana, H. styriaca, H. substyriaca, H. austriaca, Z. posterolaevis, Z. rugosa, Indigirohalobia pluriradiata.*	no	Khuc & Huyen, 1998

Table notes: Kristan-Tollmann et al. (1987) also has a map of the distribution of *H. austriaca* globally, and McRoberts (2021) also discusses additional localities in North America. Details on more locations of *H. austriaca* in Greece, Hungary, the Himalayas, Bosnia, Japan and California are discussed in Levera (2012). Ammonoid assemblage ages: {D}= Ladinian ammonoid, {J}= Julian, {T}=Tuvalian, {L}=Lacian (by Krystyn).

4. OTHER CORRELATION ISSUES

4.1 Correlation potential of *Halobia austriaca* into high palaeolatitudes

The species *Halobia austriaca* Mojsisovics, 1874 has been described many times and reviewed in atlases on Triassic faunas for Northeast Asia (Kiparisova, 1947; Vozin & Tikhomirova, 1964; Bychkov et al., 1976). According to Bychkov et al. (1976) and Dagys et al. (1979), this species appears in Northeast Asia in the *Sirenites yakutensis* Zone, there considered Upper Carnian. Subsequently, the *S. yakutensis* Zone was subdivided (Konstantinov & Sobolev, 2000a; 2000b; Konstantinov, 2019) into (from bottom to top) the *Sirenites* (= *Orientosirenites*) *yakutensis* Zone proper, *Orientosirenites bytschkovi* Zone, *Striatosirenites* (= *Kedonosirenites*) *kedonensis* Zone and *Striatosirenites* (= *Omolonosirenites*) *kinasovi* Zone. The Yakutensis, Bytschkovi, and Kedonensis zones, together with the underlying *Yakutosirenites pentastichus* Zone, are now considered by Russian workers to largely relate to the Upper Carnian. In the absence of a GSSP, the lower boundary of the Norian in Northeast Asia has, since 2002, been widely considered as the base of the Kinasovi Zone by Russian workers. The *Omolonosirenites kinasovi* Zone is reliably correlated with the lower subzone of the *Stikinoceras kerri* Zone in British Columbia, since common in both these zones are the species *Pterosirenites auritus* Tozer and *Pinococeras regiforme* Diener. In addition, *P. verchojanicum* Archipov (zonal index of *Pinacoceras verchojanicum* Zone overlying the Kinasovi Zone) has a smooth shell and a less complex suture, and most likely belongs to *Pinacoceras* sp. indet., described by E.T. Tozer in the lower subzone of the *Stikinoceras kerri* Zone (Tozer, 1994; p. 131, table 110, fig. 4).

The zonal scale of halobiids in the Upper Triassic of northeastern Russia (Polubotko, 1986, 2005) places the lower boundary of the Kinasovi Zone within the *Zittelihalobia* (*Obruchevihalobia*) *kiparisovae* beds. However, *H. austriaca* was not assigned by Polubotko to the suite of halobiids from both of these beds, nor in the complexes of the I*ndigirohalobia (Popowihalobia) asperella* Zone and *I. (P.) indigirensis* Zone. In the opinion of I.V. Polubotko (pers. comm to Konstantinov, 2020), *Halobia austriaca* sensu stricto is certainly present in Northeast Asian sections, but it is currently impossible to accurately determine the level of the first appearance of this species in these sections and compare it with the modern ammonoid zonal scale. To use *H. austriaca* in NE Asia sections it would be necessary to revise the most representative sections and taxonomic composition of halobiids in the CNB interval. Despite these circumstances, it is clear that the species *Halobia austriaca* Mojsisovics has a very high potential for correlation due to its almost cosmopolitan distribution at all paleolatitudes (Table 4).

In the Svalbard Archipelago (i.e., Hopen Island) the Flatsalen Formation contains the ammonoids '*Pterosirenites*' (= *Norosirenites*) *nelgehensis* (Archipov) and '*P.*' (=*N.*) *obrucevi* f*orma nabeshi* McLearn (Korchinskaya, 1982), which are correlated with beds in NE Asia containing *Norosirenites nelgehensis* and beds with *Norosirenites obrucevi* – i.e., equivalent to most of the *Pinacoceras verchojanicum* Zone (Konstantinov & Sobolev, 2000b). Since the latter overlies the Kinasovi Zone in the sections of Northeast Asia, the basal Norian (i.e., base the Kinasovi Zone proxy) must be in the underlying unit (the upper part of the De Geerdalen Formation or lower part of the Flatsalen Formation), which are without ammonoids.

Currently, there are problems in tracing stage boundaries in the Boreal Triassic using conodonts (Konstantinov & Klets, 2009). For example, in NE Asia, conodonts are practically unknown in the Induan Stage; and are rarely found in the terrigenous rocks of the Middle and Upper Triassic, where they are limited in distribution to a few individual levels.

(Konstantinov)

At present little is known about biostratigraphic events in the pollen/ spore or in the marine algae (dinoflagellate cysts) records that would correlate closely with the proposed CNB markers. However, in the Barents Sea and Svalbard, the palynofloral succession across the boundary interval inferred by the ammonoids (i.e. the approximate De Geerdalen- Flatsalen boundary) is remarkably consistent and easily recognisable in this area (Paterson & Mangerud, 2020.). This includes the first regional occurrence of several distinctive taxa, including *Cingulizonates rhaeticus*, *Kyrtomisporis gracilis*, *K. laevigatus*, *Limbosporites lundbladiae* and *Retitriletes austroclavatidites*. However, due to provincialism, these occurrences significantly predate the first occurrences of the same taxa in central and southern Europe, so they are unlikely to aid correlation with PM, but could permit correlation to British Columbia, if palynological data could be gathered. Also described from the Flatsalen Formation (on Hopen) in the 1970-1980's are *Halobia aotii*, *H. fallax*, *H.* cf. *maximiliani* and H. cf. *ovbruchi*, but they have no modern re-study or proper evaluation. A search for conodonts in the upper De Geerdalen and Flatsalen formations (by Orchard & Hounslow) failed to yield any useful specimens.

(Paterson, Kürschner, Hounslow)

4.2 Radiolarians at the Carnian-Norian boundary

Radiolarian faunas from the Upper Carnian and Lower Norian are known from several regions of the world, e.g., USA, Baja California Mexico, Western Europe, the Mediterranean, Japan, the Philippines, Timor and the Arctic. However, the best documented successions across the CNB thus far are those from Haida Gwaii (British Columbia) where seven radiolarian assemblages are intercalibrated with the conodont zones established at Black Bear Ridge (Carter et al., 1989, Carter & Orchard, 2000; 2011; 2013).

The radiolarian succession is characterized not by any notable extinction events but rather by the progressive appearance of new species (and over 20 new genera) ranging upward through the boundary interval. Over 35 of these species range from their lowest occurrence in strata age equivalent to the ('late Carnian') Welleri Ammonoid Zone, through the ('early Norian') Kerri Ammonoid Zone.

Based on the study of over 140 species from 44 faunules from 11 localities in Haida Gwaii, seven radiolarian assemblages (Ass.)

were established and calibrated with conodont zones established at Black Bear Ridge, prior to their formal naming (Carter & Orchard, 2013). Orchard (2014, fig. 4) showed the equivalence of the conodont zone names used here. The pertinent ones for the discussion of the boundary interval are Radiolarian Ass. 3 occurring in the Lower Primitia conodont zone (=*Ac. angusta–Me. dylani* and *Ac. acuminata-Pa. prominens* subzones); Ass. 4 in the *Me. parvus* Subzone; and Ass. 5 characteristic of the Upper Primitia Zone (=*Pr. asymmetrica – Norigondolella* Subzone).

Regarding the two possible datums for the CNB, the *Me. parvus* FAD corresponds to the base of Ass. 4, which is characterized by 16 new taxa, notably *Capnodoce malaca* Blome, *Capnuchosphaera crassa* Yeh, *Dumitricasphaera elegans* Tekin, *Hetalum parvum* (Tekin) and *Sepsagon asymmetricus* (Bragin). These are also known from Oregon (Blome 1983, 1984), the Philippines (Yeh 1990) and the Mediterranean regions, where they were formerly regarded as indicating the early Norian. It is notable that nearly all species first appearing in Ass. 4 are rare, becoming more common in Ass. 5 and above.

The *Halobia austriaca* FO approximates the top of the *Me. parvus* Subzone (base of the *Pr. asymmetrica-Norigondolella* Subzone) and is characterized by the appearance of 14 new taxa in Ass. 5, with more abundant occurrence of these appearing earlier in the *Me. parvus* Subzone. Most notable of these is *Capnodoce fragilis* Blome (=*Capnodoce sarisa* De Wever), which is singularly abundant and has been widely recognized in lower Norian samples in North America (Blome 1983, 1984), the Mediterranean (De Wever et al. 1979; Tekin & Yurtsever, 2003 etc.), Japan (Yao et al. 1982, Sugiyama, 1998 and many others), and the Philippines (Yeh and Cheng 1996). This is identified as the key index taxon for recognition of the early Norian (i.e. the Kerri Ammonoid Zone). Also making their first appearance at this level are *Syringocapsa batodes* De Wever, known from European, Mediterranean, and Far East areas (as above); the genus *Fontinella* Carter described previously from the Rhaetian (Carter 1993); and *Corum regium*, *Icrioma praecipua* and *Sarla externa*, all described by Blome (1983, 1984) from central Oregon, USA.

In summary, Ass. 4 fauna is viewed as a prelude to the more definitive changes seen in Ass. 5, which is the most distinctive radiolarian fauna marking the boundary interval. As such, these changes support using the *H. austriaca* FAD for the base of the Norian, and therefore if this were so decided the Ass. 4/5 boundary could be a suitable secondary marker for the base of the Norian using radiolarians. These statements correct some minor textual errors in assignment of samples in Carter & Orchard (2013).

Radiolarians reported from Pizzo Mondello (Nicora et al., 2007, Balini et al., 2008, 2010) come from Upper Carnian strata and contain none of the key species that are known in Haida Gwaii, to first appear in Ass. 4 or Ass. 5 (the 4/5 boundary is at the top of the *Me. parvus* Subzone in British Columbia).

(Carter)

4.3 Isotopic changes for global correlation in the boundary interval?

4.3.1. Carbon isotopes

Muttoni et al. (2014) and Mazza et al. (2010, 2018) have shown a positive peak in $\delta^{13}C_{carb}$ at PM, of ca. 0.7 permil (Figs. 9, 15). This peak is situated around the FAD of *Me. parvus*, at the T2 turnover at the top of normal magnetozone PM4n. Is this peak also present in other sections?

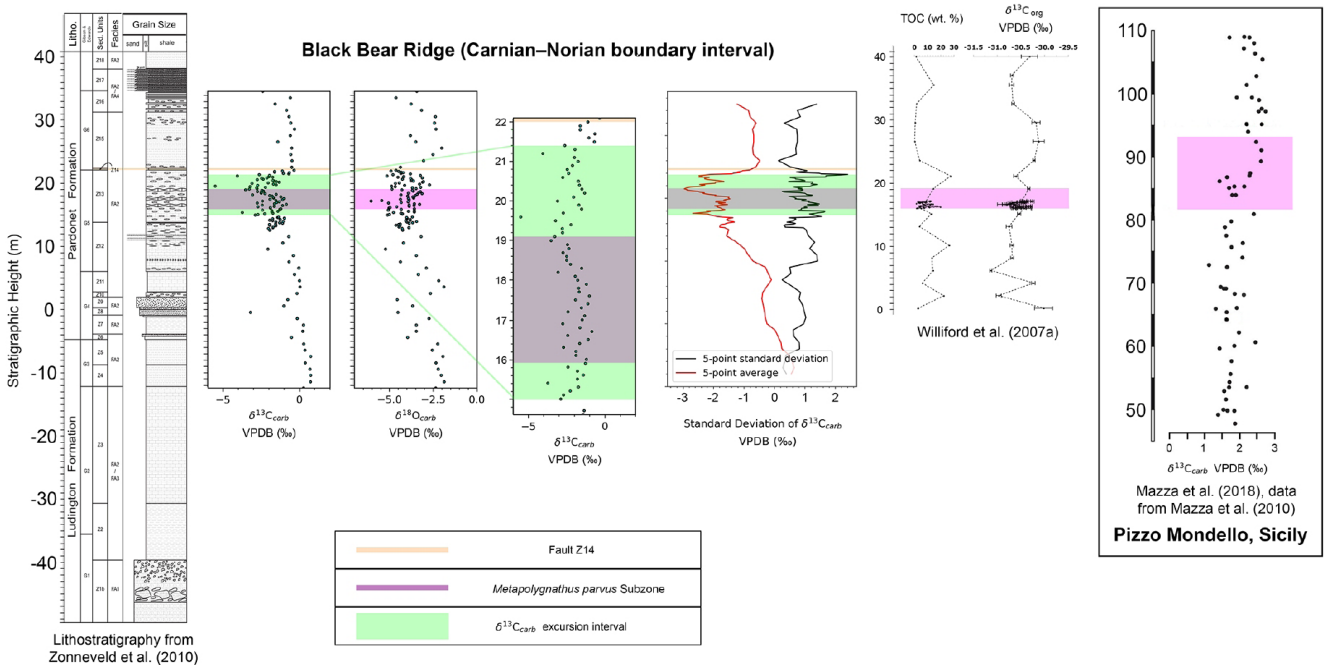

Figure 15 – The carbon isotope data from Black Bear Ridge (from fig. 2 of Lei et al. 2021). All studies are displayed with the same scale for stratigraphic height except for the zoomed (4th column) in $\delta^{13}C_{carb}$ at BBR.

Concerning BBR: The conclusion of Lei et al. (2021) that $\delta^{13}C_{carb}$ values at BBR do not represent diagenetically altered values (Fig. 15) is debatable. Values of -5 to -3‰ in $\delta^{13}C_{carb}$ are unlikely to reflect global oceanic values and may be indicative of significant diagenetic influence. With so many clay-rich samples and with a high TOC, at a conodont alteration index of ca. CAI 3, clay recrystallization could have generated reaction products (which gives values around -5‰ in $\delta^{13}C$, Kaufman & Knoll, 1995), or organic matter remineralization which moves $\delta^{13}C$ of pore fluids toward more negative values, but without necessarily changing the oxygen isotope values (e.g., Marshall, 1992).

Lei et al. (2021) affirm in their conclusion: "This excursion interval displays high point-to-point variability, rapidly oscillating between anomalously low $\delta^{13}C_{carb}$ values and values comparable to the average outside of the excursion. This atypical feature is interpreted as the result of local carbon cycling being disrupted in response to the climatic perturbations at the CNB." An alternative interpretation would be that this high point-to-point variation (green interval in 5th column in Fig. 15) is due to bed-by-bed changes in the diagenetic pathways of $\delta^{13}C_{carb}$. However, the $\delta^{13}C_{carb}$ signal does not appear to show a direct facies dependence, and the anomalously negative values are largely not observed beyond the CNB interval. Therefore, more work is needed to understand if this CNB excursion interval at BBR due to diagenesis or is rather a diagenetic amplification of an existing primary signal or alternatively represents local water column $\delta^{13}C$ values.

The long-lasting trend observed at BBR may be more reliable, as long-lasting trends tend to be conserved in such potentially diagenetically-altered situations. The absence of correlation between the $\delta^{13}C_{carb}$ and $\delta^{13}C_{org}$ curves do not support this idea. The only common features between the two curves is an increase of 2‰ in $\delta^{13}C_{carb}$ and 0.7‰ in $\delta^{13}C_{org}$ at around beds 24 to 26 at BBR, i.e. above the T3 turnover and the FAD of H. austriaca. This could also be due to diagenetic influence, but this could also represent a more global signal, albeit apparently later than at PM. It is also important to note that the sampling frequency for $\delta^{13}C_{carb}$ at BBR is significantly higher than that of $\delta^{13}C_{org}$ at BBR, and either proxy at PM. Hence, the isotope signal in the PM section could perhaps have missed some features seen in the BBR section.

Concerning other sections: Unpublished data (of Richoz) from the Kaavalani and Bolücektasi Tepe sections from Turkey (see Gallet et al., 1992; 2002 for section details) do show a small but consistent increase of 0.4 ‰ in $\delta^{13}C_{carb}$ just below the FO of *H. austriaca,* at the top of equivalent magnetozone PM4r (Figs. 9,13). Korte et al. (2005) also present an increase in $\delta^{13}C_{carb}$ for the Silicka Brezova section of 0.6‰, which should be around the FO of *H. austriaca* at the base of equivalent magnetozone PM5n. It is possible the chemostratigraphy and bio-magnetostratigraphy may be displaced with respect to each other at Silicka Brezova. Gawlick and Böhm (2000) also show a 0.5 ‰ increase in $\delta^{13}C_{carb}$ around the CNB in Austria, but it is not well stratigraphically constrained and corresponds exactly to a lithologic change.

Hence, at the upperpart of this 'potentially correlative increase' the $\delta^{13}C_{carb}$ values are ca. -0.5‰ in BBR, 2.6‰ in PM, 3.5‰ in Bolücektasi Tepe, 3.8‰ in Kaavalani; and around 3.7‰in Silcka Brezeva (Korte et al., 2005). The amplitude of change in $\delta^{13}C_{carb}$ is around 0.4 in Turkey, 0.7‰ at PM and 0.7‰ in $\delta^{13}C_{org}$ in BBR; but around 2 permil in $\delta^{13}C_{carb}$ in BBR. At BBR the far larger amplitude rise in $\delta^{13}C_{carb}$ indicates either the presence of diagenesis, or modification of a global signal by local effects. In terms of timing, it seems this 'potentially correlative increase' appears around the FAD of *Me. parvus* at PM (at the top of magnetozone PM4n); below the FO of *H. austriaca* at the top of equivalent magnetozone PM4r in Turkey, and above the FO of *H. austriaca* at BBR and Silicka Brezeva (here base of equivalent of PM5n). However, all sections with a clear positive trend are in the Western Tethys Ocean. The existence of a truly global, stratigraphically useful $\delta^{13}C_{carb}$ signal at the CNB would need a clearer signal to be gathered from sections in other oceans. Indeed, it has been demonstrated for other time intervals that $\delta^{13}C$ signals for the Tethys Ocean commonly do not reflect those seen in the Panthalassa Ocean.

Hence, the $\delta^{13}C$ signal around the boundary interval varies greatly between sections, with some showing a positive excursion, others a negative shift, and others no signal at all. The $\delta^{13}C$ increase observed in some sections is apparently positioned at different stratigraphic levels between localities and is also of a generally small amplitude, the size of which is typical of diagenetic or lithologic influence on the signal and within the range typical of regional primary influence. Rigo et al. (2012b) showed that PM is situated in an upwelling zone. Variations in upwelling strength in modern oceans can produce the same kind of amplitude in $\delta^{13}C$ we see here. So perhaps we have a global trend toward more positive values, but it is rather weak and influenced by local factors, and with different timing in its onset.

4.3.2. Oxygen and strontium isotopes:

Here the signal of oxygen isotopes analysed from conodont material seems to be resistant to diagenesis at both BBR and PM. As stated in Rigo et al. (2012b) the signal at PM is probably not global but represents the presence of an upwelling zone. The short-term increase in temperature at the boundary at BBR (Sun et al., 2020) has not been reproduced elsewhere, so far, and could also represent a regional event rather than a global one.

The decrease in temperature observed in the early Norian can be recognized at BBR (Sun et al., 2020), and seems to occur globally (except at PM). Its onset is rather close to the FO of *H. austriaca;* however, its position is not well-defined enough at the moment to be a useful stratigraphic marker.

As Onoue et al. (2016) suggested the Sr isotope ratios in BBR are significantly higher than the expected seawater ratios due to thermal alteration. The data from PM probably have oceanic values. Whatever primary GSSP datum is chosen, either section shows a decreasing trend across the boundary (Onoue et al., 2018).

In summary, except perhaps a transient temperature increase (if it could be found outside BBR), there is little evidence for any major synchronous chemostratigraphic event at the CNB that could be recognized across all sections. The $\delta^{13}C$ signal at the CNB is highly variable across localities. A positive shift in $\delta^{13}C$ is observed in several sections and may reflect a global change,

but even when present is typically so small that it could be explained as the result of weak diagenesis, or lithological change. In a broader view, either of the proposed datum are in a trend of decreasing Sr isotopes and around the onset of an increase in oxygen isotopes. Ultimately, chemostratigraphy does not appear to provide much solid help with correlation and deciding which GSSP datum is most suitable.

(Richoz, Golding, Lei et al.)

4.4. Is the stratigraphic record at Black Bear Ridge incomplete?

Using the same meter scale for both PM and BBR shows the approximate 2.4 to 1 expansion in the accumulation rate at PM compared to BBR (Fig. 16) (this is 5.3 to 1 over the range of *Me. parvus*; Table 3). The easiest way to compare the accumulation rate of two sections recording the same bioevents, is by using graphic correlation (Fig. 17). Flat levels in the line of correlation (LOC) imply a missing interval (referred to as a terrace), here marked as possible terraces TA and TB in Fig. 17. Above and below these terraces are two groups of events whose position in the same trend suggests these events are coeval or nearly coeval in both sections:

- The lower coeval group includes turnovers T1 and T2, LO of Anatropites, FO of *Me. communisti*, and FO of *Me. parvus alfa*. The FO of *M. dylani* is out of trend, indicating that this event is diachronous in the two sections.
- The upper coeval group includes LO of *Me. parvus alpha*, LO of *H. radiata*, LO of *H. austriaca* and possibly the LO of *Me. communisti*. The LO of this latter species is recorded for sure in level FNP138.1 at PM, but a single specimen of *Me.* cf. *communisti* has been found in level NA43 (Mazza et al., 2018, tab.1).

Terraces TA and TB can be detected in narrow intervals between the 1st and the 2nd coeval trends (Fig. 17). Terrace TA is located between turnover T2, the FO of *Me. parvus beta* and the FO of *H. austriaca*. Terrace TB is identified by turnover T3, the LAD of *M. parvus alpha* and the LAD of *H. radiata*. Terraces TA and TB suggest possible condensation at BBR, in beds 18 and 21. Considering that the setting of BBR is in the deepest portion of the Williston Basin, and that the transgression in the surrounding areas took place around the CNB interval (e.g., Zonneveld et al., 2010; Fig. 18), these terraces could be interpreted as non-depositional surfaces.

The position of the two non-depositional surfaces appears to be confirmed by the extraordinarily accurate numerical analysis of the conodont faunas provided by Orchard (2014, fig. 6). Figure 19 shows that the two non-depositional surfaces are in the two narrow intervals with the highest concentration of conodont last occurrences.

(Balini)

4.4.1 Is there sedimentological evidence of hiatus?

The inference of hiatus (hence possible erosion) at BBR using graphic correlation techniques (Fig. 17), is at odds with the sedimentology and palaeoenvironmental setting. The BBR section has been studied intensely, and no evidence of erosion or scour or contour currents or other current events in the boundary interval have been found. This is also the case for many metres above and below. This succession was deposited in a quiescent offshore depositional setting. Also, the boundary interval occurs within the Pardonet Formation, some 17 m above its contact with the underlying Ludington Formation (L.F. in Fig. 18). Sedimentation rates were quite low through the CNB interval (i.e. demonstrated in Fig. 16), and, as a result, conodont collections are well-preserved, abundant and diverse.

The Baldonnel Formation occurs primarily in the eastern part of the outcrop belt of the W. Canada Sedimentary Basin and does represent shallower water deposition (a shallow mixed siliciclastic-carbonate ramp succession). This formation is not present at BBR, but occurs on Williston Lake at the Pardonet Hill East, Brown Hill, McLay Spur, East Carbon Creek and West Schooler Creek sites, which are very different from each other. The Pardonet Hill East section occurs a few Km's from BBR, and the sections are rather different (Fig. 18) since they occur on different thrust sheets and were moved closer together during post-Triassic tectonism. Everywhere the Pardonet Formation represents distal offshore, deep-water deposition (even in eastern, more proximal settings). Also, the palaeogeography indicates that during the time of the CNB interval the location of the Black Bear Ridge section was ca. 150 to 200 km offshore from the nearest shoreline. Therefore, the likelihood of a sedimentation hiatus in the section is very low.

(Zonneveld)

4.4.2 The veracity of the conodont datums used in the graphic correlation

There is no doubt that the three turnover events (T1, T2, T) are recognized at both BBR and PM (Figs. 8,12, 16), but the basis for the exact positioning of the turnover T1 and T3 differs in the two sections, probably leading to some 'apparent diachroneity' in their exact placement. The turnover events T1, T2, and T3 were originally based on the PM conodont succession, and the FO and LO of the cohort of conodonts.

The T1 event at PM was based on the replacement of *Carnepigondolella* by '*Epigondolella*', which is manifest as the *'C'. orchardi* – '*E'. vialovi* zonal boundary at PM (Mazza et al., 2010). Orchard (2014) noted a significant turnover at the top of the Samueli Zone at BBR (the 'BBR event datum'), where *Carnepigondolella* is replaced by *Primatella*. Consideration of the taxonomy of the '*Epigondolella*' species at PM led Orchard (2019, fig. 3) to revise the correlation of the BBR event datum to a position within the Vialovi Zone. Hence, the precise placement of the BBR datum at PM is unclear (for details, see Orchard, 2019, p. 53), so any correlation at this turnover may be diachronous.

The T2 event at PM was originally placed at the level at which *Metapolygnathus* became dominant over '*Epigondolella*' (Mazza et al., 2010), which was placed within the Communisti Zone at PM. New definitions (Mazza et al., 2018) reduced the latter zone to a single bed and placed turnover T2 at the FO of *Me. parvus*. Hence, in agreement, the revised T2 now correlates with the base of the Parvus Subzone at BBR, so chronostratigraphic correlation at this level may be near-synchronous.

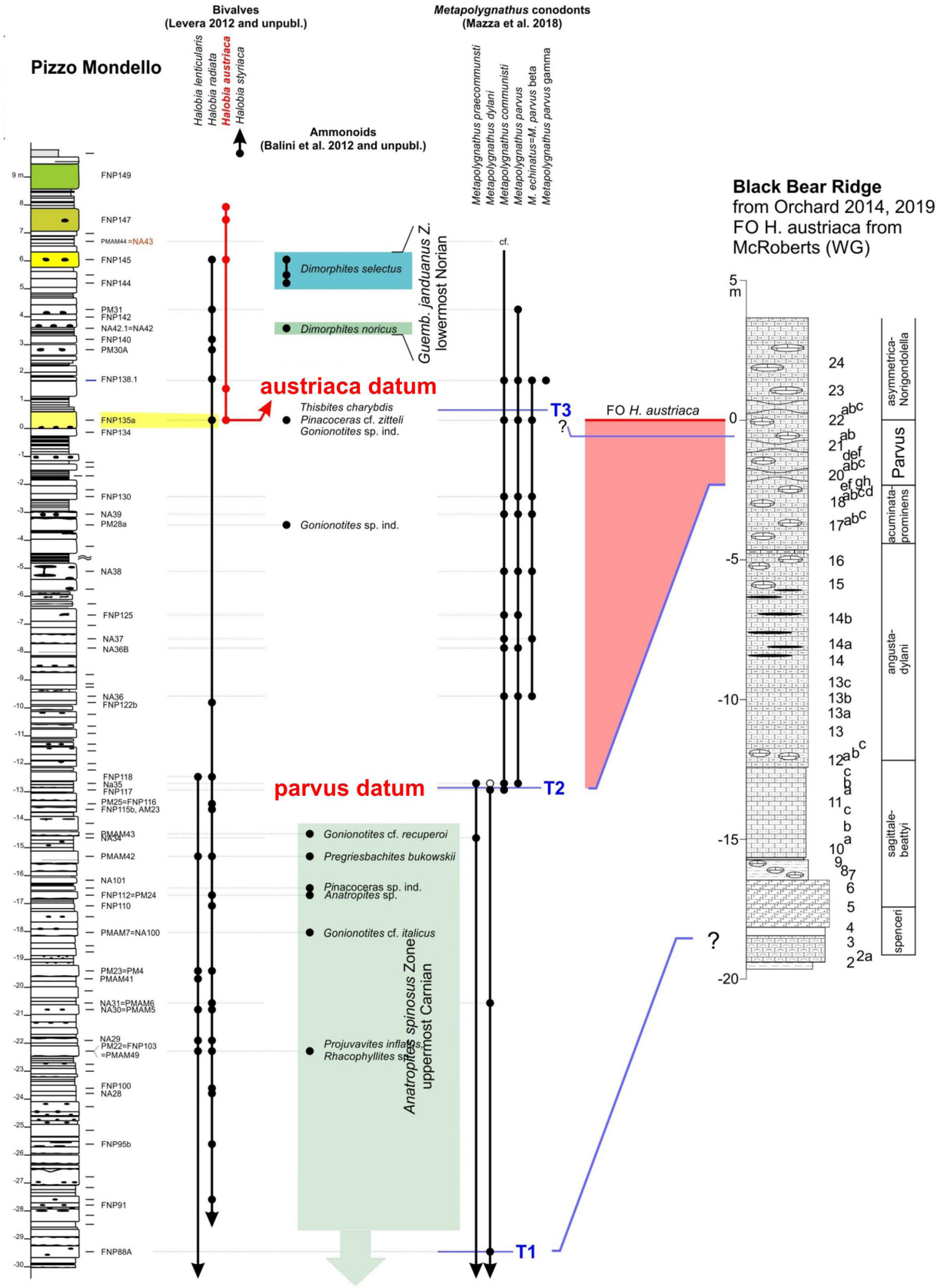

Figure 16 – Tentative correlation of Pizzo Mondello and Black Bear Ridge sections, using the same meter scale for both logs. BBR log is from Orchard (2014), zonation and tentative position of conodont turnover events T1, T2 and T3 are from Orchard (2019). (Balini)

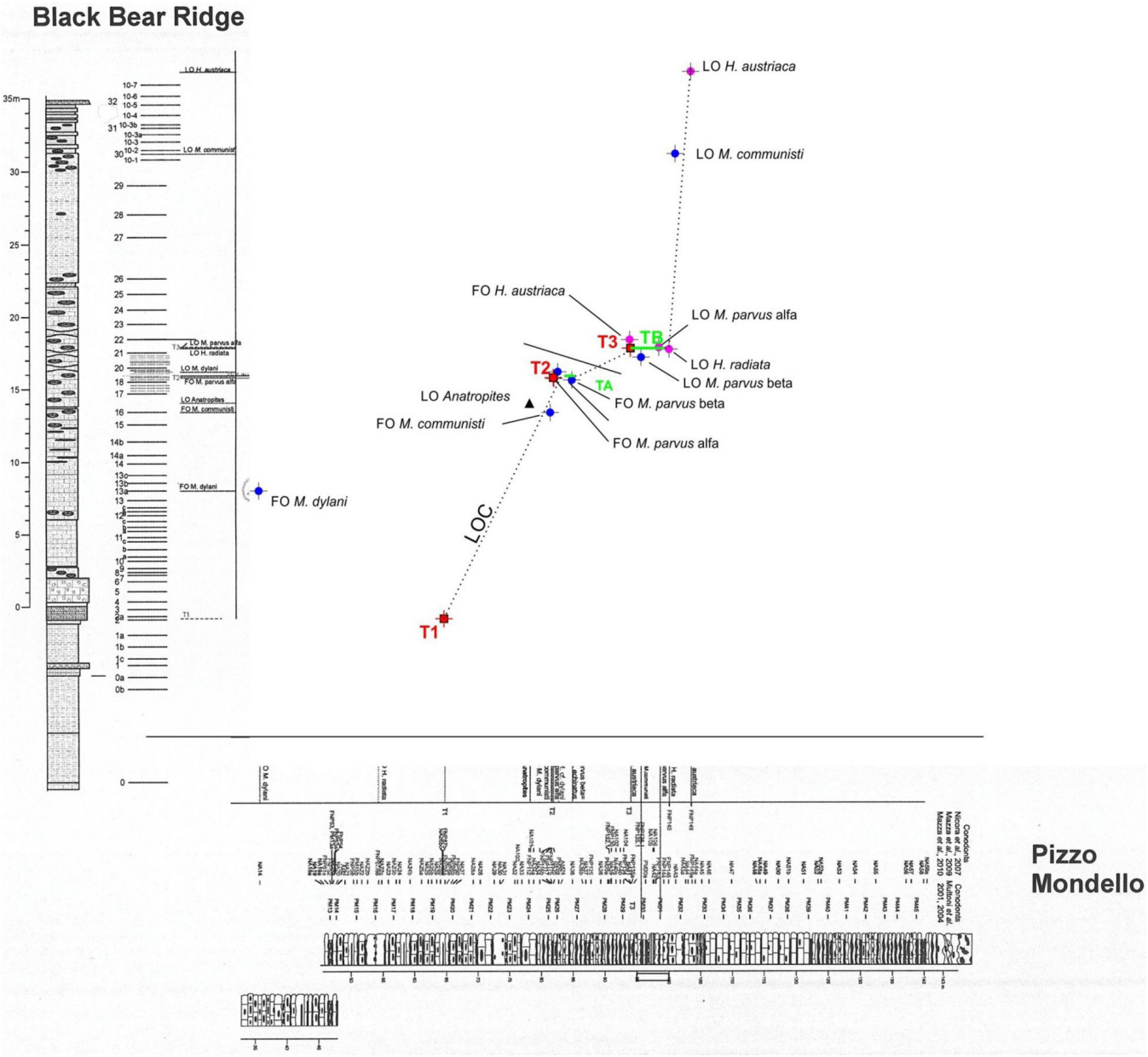

Figure 17 – Graphic correlation of first and last occurrence (FO and LO) events between BBR and PM. LOC=line of correlation (Balini).

The T3 event at PM was originally identified by *Metapolygnathus* largely disappearing and being replaced with advanced '*Epigondolella*' (probably *Primatella*) plus *Norigondolella*. These characteristics also identify the base of the *P. asymmetrica-Norigondolella* Subzone of Orchard (2014) at BBR. However, the re-definition of T3 as the base of the *Carnepigondolella*? *gulloae* Zone of Rigo et al. (2018) confuses the picture because this position is lower than the top of the Parvus Zone at PM and therefore not directly correlated with BBR, because the species *C. gulloae* has been interpreted to lie within a spectrum of *Primatella* species (Orchard, 2019, p. 61), so correlation using this turnover may be diachronous.

Other taxa used in Fig. 17: *Metapolygnathus communisti* are rare at BBR, where Orchard (2014, fig. 46) differentiated five uncommon but different morphotypes that occurred in isolated beds through much of the Upper Carnian section. They were grouped as *Me*. ex gr. *communisti* and characterized by an anteriorly shifted pit and either a lack of, or poorly developed, anterior nodes, as per the definition of Mazza et al. (2012a). Later, Mazza et al. (2018) assigned most of the morphotypes to an extraordinarily broad species *M. praecommunisti*, but Orchard believes older representatives of *Me*. ex gr. *communisti* gave rise to *Me. dylani*, whereas a parallel development saw *Quadralella praecommunisti* developed from *Q. noah* and similar forms (Orchard, 2014, figs. 8, 13). Hence, the occurrence (and FO, LO) of *Me. communisti* sensu stricto at BBR is poorly constrained, so correlation at this level is almost certainty diachronous.

Metapolygnathus dylani: Representatives, including the types of this species from BBR, are mostly inornate like those of its forbearer, *Me*. ex gr. *communisti*, whereas many of those illustrated

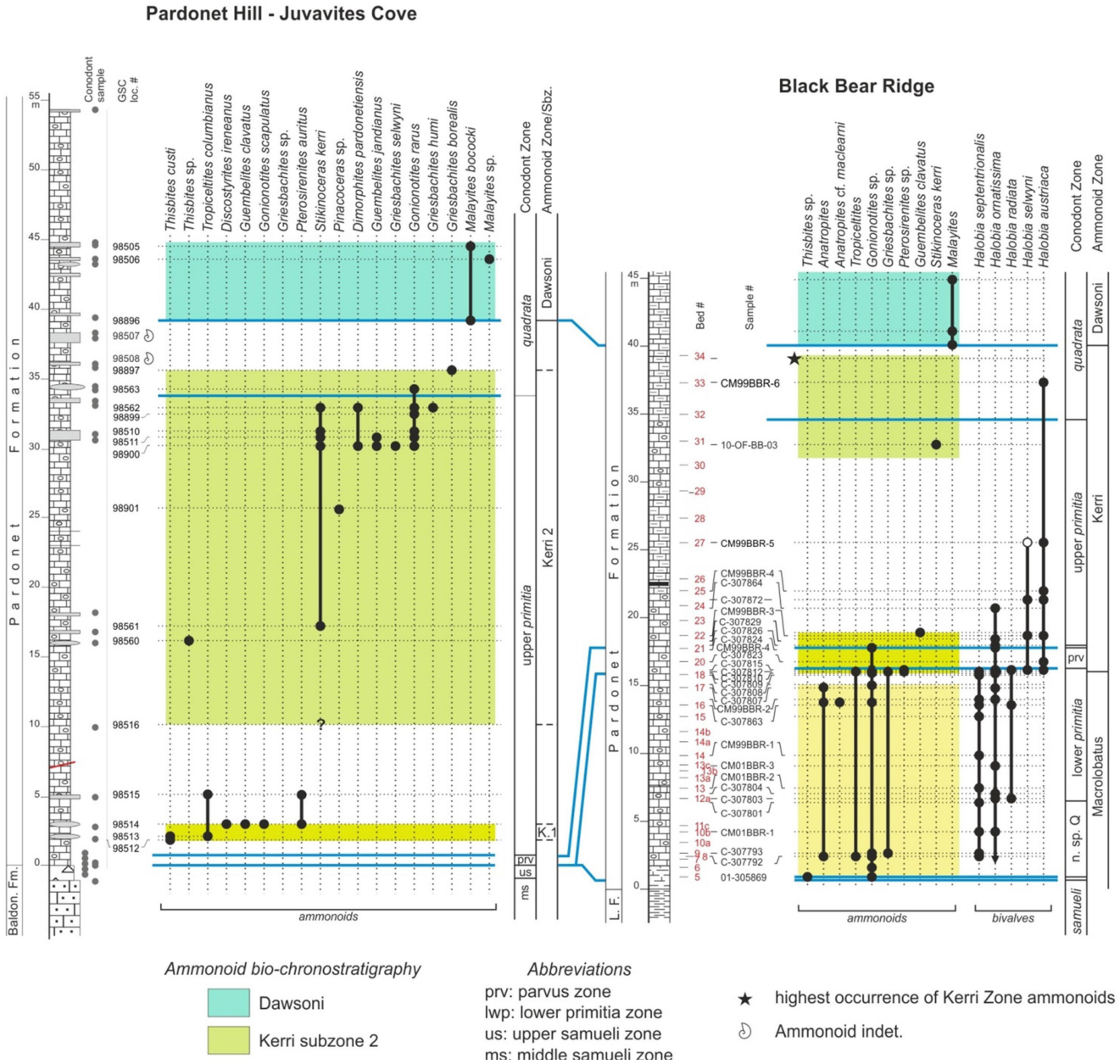

Figure 18 – Correlation of the Juvavites Cove (Pardonet Hill East) and Black Bear Ridge sections (from Balini et al. 2015, fig. 13). The Parvus Zone is documented at the very base of Pardonet Formation, thus documenting that the transgression of the Pardonet Formation on the Baldonnel Formation (at Pardonet Hill) took place at the beginning of the Kerri Zone, and slightly later in the formation at BBR. L.F= Luddington Fm. In this figure the lower boundary of the Kerri Subzone-1 is placed at the FO of *Pterosirenites*, although the chronostratigraphic significance of this event is not calibrated (Balini et al., 2012). The distribution of *Halobia* in this figure is also not that recently suggested by McRoberts (2021)- see Fig. 12.

from PM have nodes (Mazza et al., 2018). Interpreted in this broad way, this species may have a different range in the two sections (See Orchard 2019, p. 60, for details), readily accounting for its apparent diachroneity in the graphic correlation (Fig. 17).

Metapolygnathus parvus, morphotypes: Both Orchard (2014) and Mazza et al. (2018) recognized three morphotypes of this species, but two of the three do not correspond (Orchard 2019, p. 55). The elongate beta morphotype, which lacks strong nodes or denticles, was erroneously called *Me. echinatus* by Orchard (2007), a determination that was followed by Mazza et al. (2012b, 2018) who included in the morphotype additional elements with a distinctive pair of anterior nodes or denticles. These latter elements were assigned to *Pa. destinae* by Orchard (2014), so the occurrence of *Me. parvus beta* morphotype at PM is unverified. Similarly, the gamma morphotype of *Me. parvus* described by Orchard (2014) has a much longer posterior process than that illustrated by Mazza et al. (2018) and is not clearly the same taxon. The subrectangular-oval alpha morphotype, close to the holotype of the species, is the more stable concept and occurs in both sections, hence the proposal in Section 2 as the

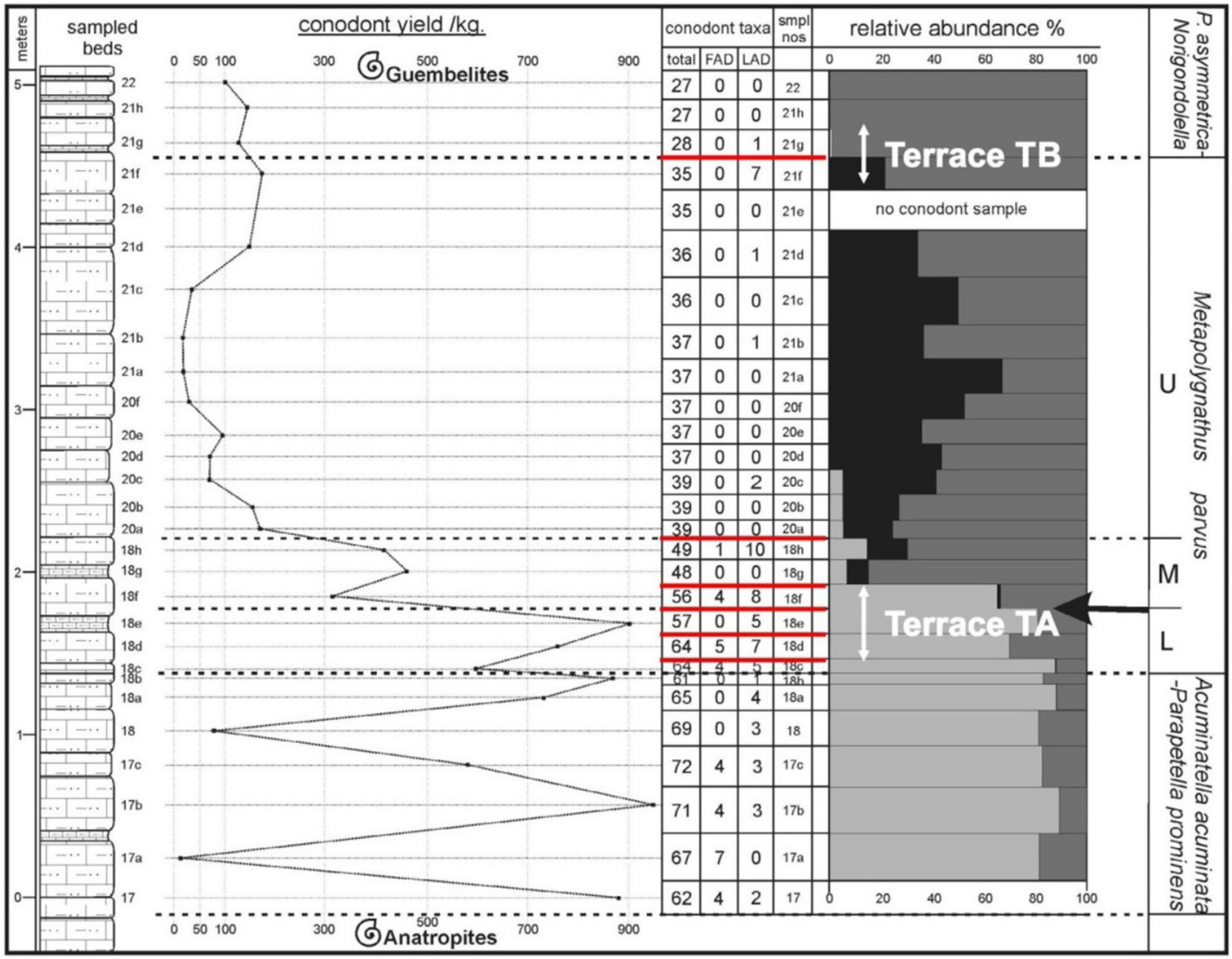

Figure 19 – Conodont faunas at BBR (from Orchard, 2014; fig. 6). The position of the inferred terraces TA and TB coincides with two intervals with highest number of LADs. In red, the bed surfaces with number of LADs greater than 4.

potential CNB datum.

Hence, any graphic correlation (i.e., Fig. 17) needs to consider the probable diachroneity and uncertainty of some of these taxa 'datums'. A more realistic and holistic approach would place three best-fit straight lines to the data in Fig. 17, in so doing remove the very small terraces TA and TB from the likely line of correlation. Although sharing many taxa with BBR, the conodont-based correlation with Pizzo Mondello both within and above the parvus interval are rather more problematic (Orchard, 2019).

The entire Pardonet Formation at BBR is relatively condensed, but the completeness of the fossil succession is globally unrivalled. The cm scale sampling of the boundary beds at BBR has enabled the development of a refined temporal framework supported by detailed conodont morphogenesis (Orchard, 2014). The inference of hiatus at BBR from the graphic correlation shown in Fig. 17 therefore seems unfounded.

The number of conodont LAD and FAD in Fig. 19 reflect the relative 'taxonomic splitting', something that is concealed in the taxonomic 'lumping' at PM. The turnovers may not be very different if the taxonomies were fully aligned in both sections? An alternate explanation for the faunal turnovers (based on oxygen isotopes from BBR conodont elements), is a marked increase in temperature in the lower part of the Parvus Subzone, and a return to 'normal' temperatures in the *P. asymmetrica-Norigondolella* Subzone (Sun et al., 2020). i.e., a climatic control of the turnovers rather than any hiatus.

(Orchard)

4.5. Using the *Halobia austriaca* datum promotes biochronological stability

In North America, the 'standard' ammonoid chronology around the CNB are the zones of the 'latest Carnian' *Klamathites macrolobatus* and 'earliest Norian' *Stikinoceras kerri* (Tozer, 1994). From studies dating back 50 years the Kerri Zone is consistently characterized by species of *Primatella* and *Norigondolella* conodonts. It has been shown that the Macrolobatus Zone is more diverse and includes several evolving conodont lineages divided into subzones at BBR (e.g., Fig. 14), with the youngest

being the Parvus Subzone and its Lower, Middle and Upper sub-divisions (Orchard, 2014).

At BBR, ca. 5 m of Pardonet Formation strata separates Macrolobatus and Kerri Zone ammonoid indicators (Fig. 18), which includes all of the Parvus Subzone. Therefore, the ammonoid zonal position of the Parvus Subzone at BBR is unfixed (using the FO of *Pterosirenites* for the base of the Kerri Zone as in Fig. 18 is highly speculative). However, from elsewhere in British Columbia, Parvus Subzone conodonts are only known in association with Macrolobatus Zone ammonoids, which suggests the FAD of *Metapolygnathus parvus* lies within the Macrolobatus Zone (i.e., not as in Fig. 18). Therefore, if using the FAD of *Me. parvus* for the base of the Norian, part of this traditionally Carnian age ammonoid zone would be earliest Norian.

All strata overlying the Parvus Subzone in North America contain the conodont associates *Primatella* and *Norigondolella*, which widely occur in the Kerri Zone. At BBR, the top of the Parvus Subzone/ base of the succeeding *Pr. symmetrica-Norigondolella* Subzone, the FO of the Kerri Zone ammonoid Guembelites, and the FO of *Halobia austriaca* (revised by McRoberts, 2021) are all within about half a meter (Fig. 12). This revision of the halobiids brings into close alignment traditional Norian indicators and provides several proxies for a CNB that could be defined at around this level. Unfortunately, because only conodont last occurrences are known, no index conodont FAD can be proposed.

In summary, the *H. austriaca* datum for the base Norian definition, better preserves the N. American biochronostratigraphic tradition. This level would also consolidate the expected Carnian range of several conodont genera, with this boundary post-dating or very near their final demise. Also, at BBR this level broadly corresponds to a cooling event after marine temperature fluctuations in the Parvus Subzone (Sun et al., 2020). It is also towards the end of an excursion interval in the carbonate $\delta^{13}C$ record that suggests ecosystem instability around the parvus Subzone (Lei et al., 2021). The succession at BBR also enables conodont-based correlation of the CNB with NE Asian Boreal regions where *Norigondolella navicula* occurs alone in the lower Norian of northern Siberia (Konstantinov et al., 2003). Similar sirenitid ammonoids present in the BBR section but unknown in Tethys provide further correlation potential (Section 4.2). Therefore, BBR provides an essential link between Boreal and Tethyan faunas (Konstantinov & Klets, 2009, Section 4.2).

(Orchard)

5. THE OUTCOME OF FORMAL VOTING WITHIN THE WORKING GROUP

The Norian boundary working group was asked to rank the four options (as below, Table 3) for the boundary position. This unusual ICS voting procedure (due to the four options available) was cleared by the ICS executive.

Option A: The first occurrence of *Metapolygnathus parvus* at Pizzo Mondello

Option B: The first occurrence of **Halobia austria***ca* at Black Bear Ridge

Option C: The first occurrence of *Halobia austriaca* at Pizzo Mondello

Option D: The first occurrence of *Metapolygnathus parvus* at Black Bear Ridge

By the deadline of midnight (GMT) on 6th May 2021, 24 of the 25 members of the CNB working group had voted (96% of members). The rankings were converted to scores by assigning rankings of 1 to 4 with the scores of 4 to 1, respectively (i.e. rank 1=score of 4; rank 4= score of 1, etc.). The cumulative scores for the four options were:

Option A	58
Option B	57
Option C	68
Option D	51

This made Option A and C move to the second round of voting. Although it made no difference for the outcome of this vote, if the scores of only ranks 1 and 2 are counted (i.e. first and second choices), the following scores would be obtained for the options, A=46, B=42, C=53, D=24, which also indicates the same preference for Options A and C.

Following the first round of voting, one of the two options listed below were voted-on for the base-Norian GSSP position. Therefore, Options A and C (as below, Table 3) formed the second round of voting, and the results of this second ballot are indicated below. By the voting deadline of midnight (GMT) on 26th July 2021, 20 of the 25 members of the CNB working group had voted (80% of members). The ballot results were:

Option A: 8 ballots cast (40% of those who voted)
Option C: 12 ballots cast (60% of those who voted)

Those voting for Option A were, Bachmann, Benton, Nicora, Onoue, Rigo, Tekin, Zhang and Zonneveld, and those voting for Option-C were: Balini, Carter, Golding, Hounslow, Konstantinov, Krystyn, Lucas, McRoberts, Muttoni, Orchard, Richoz, Sun.

Both the number of ballots cast and majority of votes (both set at 60% by ICS voting rules), makes Option C the choice selected by the working group to define the base of the Norian. That is the first occurrence of *Halobia austriaca* in the Pizzo Mondello section is the suggested GSSP 'golden spike' for the Norian (Table 3).

CONCLUSIONS

The first occurrence of *Halobia austriaca* at Pizzo Mondello has been chosen by the Carnian-Norian boundary working group as the primary datum for the base of the Norian. This will be put forward to the STS as the formal proposal for the base Norian GSSP. This level corresponds to the base of bed FNP135A at Pizzo

Modello. The placement at this level in many ways embodies the historical precedence of the ammonoid zonations widely used in the Late Triassic, since this level, whilst not exactly equivalent, is close to the base of the traditional Norian in North America, Europe and probably in the Boreal realm in NE Asia. Closely associated potential secondary markers for the boundary in the section include: 1) the lower part of magnetozone PM5n, allowing correlation into terrestrial systems and those not bearing suitable fossils; and 2) the major turnover of conodonts (event T3) near the top of the Parvus Zone.

REFERENCES

Balini, M., Bertinelli, A., Di Stefano, P., Dumitrica, P., Furin, S., Gullo, M., Guaiumi, C., Hungerbuehler, A., Levera, M., Mazza, M., McRoberts, C.A., Muttoni, G., Nicora, A., Preto, N. & Rigo, M. 2008, Integrated stratigraphy of the Norian GSSP candidate Pizzo Mondello section (Sicani Mountains, Sicily): Berichte der Geologischen Bundesanstalt, 76: 23-25.

Balini, M., Bertinelli A., Di Stefano P., Guaiumi C., Levera M., Mazza M., Muttoni G., Nicora A., Preto N. & Rigo M. 2010. The Late Carnian-Rhaetian succession at Pizzo Mondello (Sicani Mountains). Albertiana, 39: 36-58.

Balini, M., Krystyn L., Levera M. & Tripodo A. 2012. Late Carnian-early Norian ammonoids from the GSSP candidate section Pizzo Mondello (Sicani Mountains, Sicily). Rivista Italiana di Paleontologia e Stratigrafia, 118: 47-84.

Balini, M., Jenks J.F., Martin R., McRoberts C.A., Orchard M.J. & Silberling N.J. 2015. The Carnian/Norian boundary succession at Berlin-Ichthyosaur State Park (Upper Triassic, central Nevada, USA). Paläontologische Zeitschrift, 89: 399-433.

Bellanca, A., Di Stefano, P. & Neri, R. 1995. Sedimentology and isotope geochemistry of Carnian deep-water marl/limestone deposits from the Sicani Mountains, Sicily: Environmental implications and evidence for a planktonic source of lime mud. Palaeogeography, Palaeoclimatology, Palaeoecology, 114(1): 111-129.

Berg, H.C. & Cruz, E.L. 1982. Map and table describing fossil collections and related samples in the Ketchikan and Prince Rupert quadrangles, southeastern Alaska. US Geog Survey openfile report 82-1088, Ancorage, Alaska.

Blome, C.D. 1983. Upper Triassic Capnuchosphaeridae and Capnodocinae (Radiolaria) from east-central Oregon: Micropaleontology 2, 9: 11-49.

Blome, C.D. 1984. Upper Triassic Radiolaria and radiolarian zonation from western North America: Bulletins of American Paleontology, 85: 1-88.

Bucur, I.I. 2001. Upper Triassic deposits of the Vascau plateau. In, Bucur II, Filipescu S. & Sasaran E.(Eds). Algae and carbonate platforms in the western part of Romania. 4th Regional Meeting of IFAA, Cluj-Napoca, Romania, August 29-September 5, 2001. Field Trip Guidebook.

Buryi, G.I. 1996. Triassic conodonts from the cherts of Nadandaha Range, Northeast China. Acta Micropaleontologica Sinica, 13: 207-214.

Bychkov, Yu.M., Dagys, A.S., Efimova, A.F. & Polubotko, I.V. 1976. Atlas of Triassic Fauna and Flora of the Northeastern USSR, Moscow: Nedra [in Russian].

Campbell, H.J. 1994. The Triassic bivalves *Daonella* and *Halobia* in New Zealand, New Caledonia, and Svalbard (No. 66). Institute of Geological & Nuclear Sciences Ltd.

Carter, E.S. 1993. Biochronology and paleontology of uppermost Triassic (Rhaetian) radiolarians, Queen Charlotte Islands, British Columbia, Canada. Mémoires de Géologie (Lausanne), 11, 75pp.

Carter, E.S. & Orchard, M.J. 2000, Intercalibrated conodont-radiolarian biostratigraphy and potential datums for the Carnian-Norian boundary within the Upper Triassic Peril Formation, Queen Charlotte Islands, British Columbia. Geological Survey of Canada, Current Research 2000- A7, 11p.

Carter, E.S. & Orchard, M.J. 2011, Radiolarians and conodonts across the Carnian-Norian Boundary in Haida Gwaii, British Columbia: Canadian Paleontology Conference, Proceedings No. 9, Vancouver, BC, August 19-22, 2011, p. 15.

Carter, E.S. & Orchard, M.J. 2013. Intercalibration of conodont and radiolarian faunas from the Carnian-Norian boundary interval in Haida Gwaii, British Columbia, Canada. In, Tanner, L. H., Spielmann, J. A. & Lucas, S. G. (Eds.). The Triassic System: New Developments in Stratigraphy and Paleontology: Bulletin 61: 67-92, New Mexico Museum of Natural History and Science.

Carter, E.S., Orchard, M.J. & Tozer, E.T. 1989, Integrated ammonoid conodont- radiolarian biostratigraphy, Late Triassic Kunga Group, Queen Charlotte Islands, British Columbia: Geological Survey of Canada, Paper 89-1H, p. 23-30.

Charlton, T.R., Barber, A.J., McGowan, A.J., Nicoll, R.S., Roniewicz, E., Cook, S.E., Barkham, S.T. & Bird, P.R. 2009. The Triassic of Timor: Lithostratigraphy, chronostratigraphy and palaeogeography. Journal of Asian Earth Sciences, 36: 341-363.

Dagys, A.S., Arkhipov,Yu.V. & Bychkov,Yu.M. 1979. Stratigraphy of the Triassic System of the North-Eastern Asia, Moscow: Nauka [in Russian].

De Wever, P., Sanfilippo, A., Riedel, W.R. & Gruber, B. 1979. Triassic Radiolaria from Greece, Sicily and Turkey: Micropaleontology, 25: 193-209.

Del Piero, N., Rigaud, S., Takahashi, S., Poulton, S.W. & Martini, R. 2020. Unravelling the paleoecology of flat clams: new insights from an Upper Triassic halobiid bivalve. Global and Planetary Change, 190: 103195, doi.org/10.1016/j.gloplacha.2020.103195.

Fuller, L.R. 1986. General Geology of Triassic Rocks at Alaska Canyon in the Jackson Mountains, Humboldt County, Nevada (MSc dissertation, University of Nevada, Reno).

Gawlick, H.J. & Böhm, F. 2000. Sequence and isotope stratigraphy of Late Triassic distal periplatform limestones from the northern Calcareous Alps (Kälberstein Quarry, Berchtesgaden Hallstatt Zone). International Journal of Earth Sciences, 89: 108-129.

Gallet, Y., Besse, J., Krystyn, L., Marcoux, J. & Théveniaut, H.

1992. Magnetostratigraphy of the Late Triassic Bolücektası Tepe section (southwestern Turkey): implications for changes in magnetic reversal frequency. Physics of the Earth and Planetary Interiors, 73: 85-108.

Gallet, Y., Besse, J., Krystyn, L., Marcoux, J., Guex, J. & Théveniaut, H. 2000. Magnetostratigraphy of the Kaavalani section (southwestern Turkey): Consequence for the origin of the Antalya Calcareous Nappes (Turkey) and for the Norian (Late Triassic) magnetic polarity timescale. Geophysical Research Letters: 27, 2033-2036.

Guaiumi, C. 2008. Sedimentology of Upper Triassic hemipelagic micrites (Lagonegro and Sicani basins). PhD Thesis, Padua Univ.

Hounslow, M.W. & Muttoni, G. 2010. The geomagnetic polarity timescale for the Triassic: linkage to stage boundary definitions. In, Lucas, S.G (ed). The Triassic timescale. Geological Society, London, Special Publications, 334: 61-102.

Hüsing, S.K., Deenen, M.H., Koopmans, J.G. & Krijgsman, W. 2011. Magnetostratigraphic dating of the proposed Rhaetian GSSP at Steinbergkogel (Upper Triassic, Austria): Implications for the Late Triassic time scale. Earth and Planetary Science Letters, 302: 203-216.

Jin, X., McRoberts, C.A, Shi, Z., Mietto, P., Rigo, M. Roghi, G., Manfrin, S., Franceschi, M. & Preto, N. 2019. The aftermath of the CPE and the Carnian–Norian transition in northwestern Sichuan Basin, South China Journal of the Geological Society, 176: 179–196

Katkov, S.M., Miller, E.L. & Toro, J. 2010. Structural assemblies and age of deformation in the western sector of the Anyui-Chukotka Fold System, Northeastern Asia. Geotectonics, 44: 424-442.

Kaufman, A.J. & Knoll, A.H. 1995. Neoproterozoic variations in the C-isotopic composition of seawater: stratigraphic and biogeochemical implications. Precambrian Research, 73: 27-49.

Kent, D. V., Olsen, P. E. & Muttoni, G. 2017. Astrochronostratigraphic polarity time scale (APTS) for the Late Triassic and Early Jurassic from continental sediments and correlation with standard marine stages. Earth-Science Reviews, 166: 153-180.

Khuc, V. & Huyen, D.T. 1998. Triassic correlation of the Southeast Asian mainland. Palaeogeography, Palaeoclimatology, Palaeoecology, 143: 285-291.

Khuc, V. 1991.Paleontological Atlas of Vietnam, vol. 3, Mollusca. 207 pp. Science and Technics Publishing.

Kiparisova, L.D. 1947. Atlas of the Index Forms of the Fossil Faunas of the USSR. Vol. 7: Triassic System, Moscow: Gosgeolizdat [in Russian].

Kolar-Jurkovsek T. 1982. Konodonti iz amfiklìnskìh skladov in baškega dolomita - Conodonts from Amphiclina beds and Baca dolomite. Geologija, 25: 167-188.

Komatsu, T., Shigeta, Y., Doan, H.D., Trinh, H.T., Nguyen, H.B., Nguyen, M.T., Kusuhashi, N., Tsuihiji, T., Maekawa, T., Legrand, J. & Manabe, M. 2017. Upper Triassic (Carnian) mollusks from the Suoi Bang Formation in Me area, Ninh Binh Province, northern Vietnam. Bulleton National Musuem Natural Science, Series. C, 43: 1–10.

Konstantinov, A. G. 2019. A New Ammonoid Zone of the Upper Carnian Substage in Northeastern Russia. Russian Journal of Pacific Geology, 13: 522–534.

Konstantinov, A. G. & Klets, E. S. 2009. Stage Boundaries of the Triassic in Northeast Asia. Stratigraphy and Geological Correlation, 17: 173-191.

Konstantinov, A. G. & Sobolev 2000a. Biostratigraphy of the Carnian and Lower Norian in Northeastern Russia. Paper 1. Description of Sections, and Stratigraphic Distribution of Cephalopods. Geology of the Pacific Ocean, 16: 1-30.

Konstantinov, A. G. & Sobolev 2000b. Biostratigraphic Scheme of the Carnian and Lower Norian in NE Russia. Paper 2. New Zonal Scales and Correlation. Geology of Pacific Ocean, 16: 643-666.

Konstantinov, A. G. Sobolev, E. S. & Klets, T. V. 2003. New Data on Fauna and Biostratigraphy of Norian Deposits in the Kotel'nyi Island (New Siberian Islands). Stratigraphy and Geological Correlation, 11: 231–243.

Korchinskaya, M.V. 1082. Explanatory Note to the Stratigraphic Scheme of Mesozoic (Triassic) of Svalbard, Leningrad: PGO 'Sevmorgeologiya' [in Russian].

Korte, C., Kozur, H.W. & Veizer, J. 2005. $\delta^{13}C$ and $\delta^{18}O$ values of Triassic brachiopods and carbonate rocks as proxies for coeval seawater and palaeotemperature. Palaeogeography, Palaeoclimatology, Palaeoecology, 226: 287-306.

Kristan-Tollmann, E., Barkham, S. & Gruber, B. 1987. Pötschenschichten, zlambachmergel (Hallstätter Obertrias) und liasfleckenmergel in zentraltimor, Nebst ihren faunenelementen. Mitteilungen der österreichischen geologischen Gesellschaft, 80: 229-285.

Krystyn, L. 1980. Stratigraphy of the Hallstatt region. Guidebook, Abstracts, Second European Conodont Symposium-ECOS II. Abhandlungen der Geologischen Bundesanstalt, 35: 69-98.

Krystyn, L. & Gallet, Y. 2002. Towards a Tethyan Carnian-Norian boundary GSSP. Albertiana, 27: 12-19.

Lamolda, M.A., Paul, C.R.C., Peryt, D. & Pons, J.M. 2014. The global boundary stratotype and section point (GSSP) for the base of the Santonian Stage,' Cantera de Margas', Olazagutia, northern Spain. Episodes, 37: 2-13.

Lei, J.Z.X., Husson, J.M., Golding, M.L., Orchard, M.J. & Zonneveld, J.-P. 2021. Stable carbon isotope record of carbonate across the Carnian–Norian boundary at the prospective GSSP section at Black Bear Ridge, British Columbia, Canada. Albertiana, 46: 1–10.

Levera, M. & McRoberts, C.A. 2008. Carnian/Norian halobiids from Pizzo Mondello succession (Sicani Mountains, Sicily). Berichte Geol. B.-A., 76 – Upper Triassic …Bad Goisern.

Levera, M. 2012. The halobiids from the Norian GSSP candidate section of Pizzo Mondello (Western Sicily, Italy): systematics and correlations. Rivista Italiana di Paleontologia e Stratigrafia, 118: 3-45.

Lin, L., Zhu, L., Pang, Y. & Sha, J. 2007. A new genus of Pergamidiidae (Bivalvia) from the Late Triassic of the Changtai-Gacun area, eastern Qinghai-Xizang Plateau, China. Journal of Asian Earth Sciences, 30: 108-112.

Lucas, S. G. 2010. The Triassic chronostratigraphic scale: history and status. In, Lucas, S.G (ed). The Triassic timescale.

Geological Society, London, Special Publications, 334: 17-39.

MacKevett, E.M. 1971. Stratigraphy and General Geology of the McCarthy C-5 Quadrangle; Alaska. US. Geological Survey Bulletin 1323, US printing Office Washington.

Marshall, J.D. 1992. Climatic and oceanographic isotopic signals from the carbonate rock record and their preservation: Geological Magazine, 129: 143-160.

Mazza, M. & Krystyn L. 2015. The revised Upper Triassic conodont record of the Tethys: a new step towards a better definition of the conodont bioevents around the base of the Norian stage. Ber Inst Erdwiss K-F-Univ Graz, 21: 243

Mazza, M. & Martinez-Perez, C. 2015. Unravelling conodont (Conodonta) ontogenetic processes in the Late Triassic through growth series reconstructions and X-ray microtomography. Bollettino della Società Paleontologica Italiana, 54: 161-186.

Mazza, M. & Martínez-Pérez, C. 2016. Evolutionary convergence in conodonts revealed by Synchrotron-based tomographic microscopy. Palaeontologia Electronica 19.3.52A: 1–11 palaeo-electronica.org/content/2016/1710- conodont-x-ray-tomographies

Mazza, M., Furin, S., Spötl, C. & Rigo, M. 2010. Generic turnovers of Carnian/Norian conodonts: Climatic control or competition? Palaeogeography, Palaeoclimatology, Palaeoecology, 290: 120-137.

Mazza, M., Rigo, M. & Nicora, A. 2011. A new *Metapolygnathus* platform conodont species and its implications for Upper Carnian global correlations. Acta Palaeontologica Polonica, 56: 121-131.

Mazza, M., Rigo, M. & Gullo, M. 2012a. Taxonomy and biostratigraphic record of the Upper Triassic conodonts of the Pizzo Mondello section (western Sicily, Italy), GSSP candidate for the base of the Norian. Rivista Italiana di Paleontologia e Stratigrafia, 118: 85-130.

Mazza, M., Cau, A. & Rigo, M. 2012a. Application of numerical cladistic analyses to the Carnian–Norian conodonts: a new approach for phylogenetic interpretations. Journal of Systematic Palaeontology, 10: 401-422.

Mazza, M., Nicora, A. & Rigo, M. 2018. *Metapolygnathus parvus* Kozur, 1972 (Conodonta): a potential primary marker for the Norian GSSP (Upper Triassic). Bollettino della Società Paleontologica Italiana, 57: 81-101.

McRoberts, C.A. 1990. Systematic paleontology stratigraphic occurrence and paleoecology of halobiid bivalves from the Martin Bridge Formation (Upper Triassic) Wallowa Terrane Oregon. MSc Theisis, Univeristy of Montana, Missoua, 156 p.

McRoberts C.A. 2007. The halobid bivalve succession across a potential Carnian/Norian GSSP at Black Bear Ridge, Williston Lake, northeast British Columbia, Canada. Albertiana, 36: 142-145.

McRoberts, C. A. 2010. Biochronology of Triassic bivalves. In: Lucas, S.G (Ed.) The Triassic timescale. Geological Society, London, Special Publications, 334: 201–219.

McRoberts, C.A. 2011. Late Triassic Bivalvia (Chiefly Halobiidae and Monotidae) from the Pardonet Formation, Williston Lake Area, Northeastern British Columbia, Canada. Journal of Paleontology, 85: 613-664.

McRoberts, C.A. 2021. *Halobia austriaca* in North America with a reappraisal of its distribution across the Carnian-Norian boundary interval at Black Bear Ridge (northeastern British Columbia, Canada). Albertiana, vol. 46, 13–46.

McRoberts, C.A. & Krystyn, L. 2011. The FOD of *Halobia austriaca* at Black Bear Ridge (northeastern British Columbia) as the base-Norian GSSP. 21st Canadian Paleontology Conference, UBC, August 19–21, Proceedings 9: 38–9.

Meng, Q., Qu, H. & Hu, J. 2007. Triassic deep-marine sedimentation in the western Qinling and Songpan terrane. Science in China Series D: Earth Sciences, 50: 246-263.

Mietto, P., Jin, X., Manfrin, S., Lu, G., Shi, Z., Gianolla, P., Huang, X. & Preto, N. 2021. Onset of sedimentation near the Carnian/Norian boundary in the northwestern Sichuan Basin: New evidence from ammonoid biostratigraphy and zircon UPb geochronology. Palaeogeography, Palaeoclimatology, Palaeoecology, 567: doi.org/10.1016/j.palaeo.2021.110246.

Mojsisovics, E. von. 1869. Über die Gliederung der oberen Triasbildungen der östlichen Alpen. Geologische Reichsanstalt. Jahrbuch, 24:91-150.

Mojsisovics, E. von. 1874. Über Die Triadischen Pelecypoden–Gattungen *Daonella* und *Halobia*. Abhandlungen der k. k. Geologischen Reichsanstalt, 7: 1–35

Montenat, C. 2009. The Mesozoic of Afghanistan. GeoArabia, 14: 147-210.

Muttoni G., Kent D.V., Di Stefano P., Gullo M., Nicora A., Tait J. & Lowrie W. 2001a. Magnetostratigraphy and biostratigraphy of the Carnian/Norian boundry interval from the Pizzo Mondello section (Sicani Mountains, Sicily). Palaeogeography, Palaeoclimatology, Palaeoecology, 166: 383-399.

Muttoni, G., Kent, D. V. & Orchard, M. J. 2001b. Paleomagnetic reconnaissance of early Mesozoic carbonates from Williston Lake, northeastern British Columbia, Canada: evidence for late Mesozoic remagnetization. Canadian Journal of Earth Sciences, 38:1157-1168.

Muttoni G., Kent D.V., Olsen P.E., Di Stefano P., Lowrie W., Bernasconi S.M. & Hernández F.M. 2004 Tethyan magnetostratigraphy from Pizzo Mondello (Sicily) and correlation to the Late Triassic Newark astrochronological polarity time scale. Geological Society America Bulletin, 116: 1043–1058.

Muttoni G., Mazza M., Mosher D., Katz M.E., Kent D.V. & Balini M. 2014. A Middle–Late Triassic (Ladinian–Rhaetian) carbon and oxygen isotope record from the Tethyan Ocean. Palaeogeography, Palaeoclimatology, Palaeoecology, 399: 246–259.

Nicora A., Balini M., Bellanca A., Bertinelli A., Bowring S.A., Di Stefano P., Dumitrica P., Guaiumi C., Gullo M., Hungerbuehler A., Levera M., Mazza M., McRoberts C.A., Muttoni G., Preto N. & Rigo M. 2007. The Carnian/Norian boundary interval at Pizzo Mondello (Sicani Mountains, Sicily) and its bearing for the definition of the GSSP of the Norian Stage. Albertiana, 36: 115-129.

Noyan O. & Kozur H. 2007. Revision of the late Carnian-early Norian conodonts from the Stefanion section (Argolis, Greece) and their paleobiogeographic implications. Neues Jahrbuch für Geologie und Paleontologie Abhandlungen, 245: 159-178.

Onoue, T., Zonneveld, J. P., Orchard, M. J., Yamashita, M.,

Yamashita, K., Sato, H. & Kusaka, S. 2016. Paleoenvironmental changes across the Carnian/Norian boundary in the Black Bear Ridge section, British Columbia, Canada. Palaeogeography, Palaeoclimatology, Palaeoecology, 441: 721-733.

Onoue, T., Yamashita, K., Fukuda, C., Soda, K., Tomimatsu, Y., Abate, B. & Rigo, M. 2018. Sr isotope variations in the Upper Triassic succession at Pizzo Mondello, Sicily: Constraints on the timing of the Cimmerian Orogeny. Palaeogeography, Palaeoclimatology, Palaeoecology, 499: 131-137.

Orchard, M.J. 2007. A proposed Carnian-Norian Boundary GSSP at Black Bear Ridge, northeast British Columbia, and a new conodont framework for the boundary interval. Albertiana, 36: 130-141.

Orchard, M.J. 2010. Triassic conodonts and their role in stage boundary definitions. In Lucas S.G. (ed.), The Triassic Timescale. Geological Society, Special Publication, 334: 139-161.

Orchard, M.J. 2013. Five new genera of conodonts from the Carnian-Norian boundary beds of Black Bear Ridge, northeast British Columbia, Canada. In: Tanner, L.H., Spielmann, J.A. and Lucas, S.G. (eds.), The Triassic system. New Mexico Museum of Natural History and Science Bulletin, 61, 445-457.

Orchard, M.J. 2014. Conodonts from the Carnian-Norian Boundary (Upper Triassic) of Black Bear Ridge, Northeastern British Columbia, Canada. New Mexico Museum of Natural History and Science Bullettin, 64, 139 pp.

Orchard, M.J. 2019. The Carnian-Norian boundary GSSP candidate at Black Bear Ridge, British Columbia, Canada: update, correlation, and conodont taxonomy. Albertiana, 45: 50-68.

Orchard, M.J., McRoberts, C.A., Tozer, E.T., Johns, M.J., Sandy, M.R. & Shaner, J.S. 2001. An intercalibrated biostratigraphy of the Upper Triassic of Black Bear Ridge, Williston Lake, northeast British Columbia. Natural Resources Canada, Geological Survey of Canada.

Orchard, M.J., Zonneveld, J.P., Johns, M.J., McRoberts, C.A., Sandy, M.R., Tozer, E.T. & Carrelli, G.G. 2001. Fossil succession and sequence stratigraphy of the Upper Triassic of Black Bear Ridge, Northeast British Columbia, a GSSP prospect for the Carnian–Norian boundary. Albertiana, 25: 10–22.

Paterson, N.W. & Mangerud, G. 2020. A revised palynozonation for the Middle–Upper Triassic (Anisian–Rhaetian) series of the Norwegian Arctic. Geological Magazine, 157: 1568-1592.

Polubotko, I.V. 2005. Halobiide based biozonation of the Upper Triassic in the Northeast Russia. In Mater. Vseross. nauchn. konf., posvyashch. pamyati akad. KV Simakova iv chest'ego 70-letiya 'Nauka Severo-Vostoka Rossii–nachalo veka' (Magadan, 26–28 april, 2005.), pp. 26-28.

Polubotko, I.V. 1986. Zonal complexes of Late Triassic halobiids in the northeastern USSR. In: Yanshin, A.L. (ed). Mesozoic Biostratigraphy of Siberia and the Far East. Transactions of the Institute of Geology and Geophysics, Novosibirsk, 648: 63-72 [in Russian].

Popescu, D.A. & Popescu, L.G. 2008. Microfacies of the Triassic limestones in the Izvorul Malului klippe (Rarău Syncline, Transylvanian Nappes, Eastern Carpathians, Romania). Georeview: Scientific Annals of Stefan cel Mare University of Suceava. Geography Series, 17: 113-131.

Preto, N., Agnini, C., Rigo, M., Sprovieri, M. & Westphal, H. 2013. The calcareous nannofossil *Prinsiosphaera* achieved rock-forming abundances in the latest Triassic of western Tethys: consequences for the $\delta^{13}C$ of bulk carbonate. Rivista Italiana di Paleontologia e Stratigrafia, 118: 131-141.

Raine, J.I., Beu, A.G., Boyes, A.F., Campbell, H.J., Cooper, R.A., Crampton, J.S., Crundwell, M.P., Hollis, C.J. & Morgans, H.E.G. 2012. Revised calibration of the New Zealand geological timescale. NZGT2015/1. GNS Science report, 39: 1-53.

Riediger, C., Carrelli, G.G. & Zonneveld, J.P. 2004. Hydrocarbon source rock characterization and thermal maturity of the Upper Triassic Baldonnel and Pardonet formations, northeastern British Columbia, Canada. Bulletin of Canadian Petroleum Geology, 52: 277-301.

Rigo M., Preto N., Franceschi M. & Guaiumi C. 2012a. Stratigraphy of the Carnian-Norian Calcari con Selce Formation in the Lagonegro Basin, Southern Apennines. Rivista Italia Paleontologica Stratigraphy, 118: 143–154.

Rigo, M., Trotter, J.A., Preto, N. & Williams, I.S. 2012b. Oxygen isotopic evidence for Late Triassic monsoonal upwelling in the northwestern Tethys. Geology, 40: 515–518.

Rigo M., Mazza M., Karádi V. & Nicora A. 2018. New Upper Triassic conodont biozonation on of the Tethyan Realm. In: Tanner L.H. (ed.), The Late Triassic World: Earth in a Time of Transition, Topics in Geobiology 46: 189-235, Springer.

Seilacher, A. 1990. Aberrations in bivalve evolution related to photo-and chemosymbiosis. Historical Biology, 3: 289-311.

Sha, J. & Grant-Mackie, J.A. 1996. Late Permian to Miocene bivalve assemblages from Hohxil, Qinghai-Xizang Plateau, China. Journal of the Royal Society of New Zealand, 26: 429-455.

Shackleton, R.M., Ries, A.C., Bird, P.R., Filbrandt, J.B., Lee, C.W. & Cunningham, G.C. 1990. The Batain Melange of NE Oman. In, Robertson, A. H. F., Searle, M. P. & Raes, A. C. (eds), The Geology and Tectonics of the Oman Region. Geological Society Special Publication, 49: 673-696.

Silberling, N.J. 1963. Field guide to halobiid and monotid pelecypods of the Alaskan Triassic. US Geological Survey Open File Report, pp.1-9.

Smith, J.P. 1927. Upper Triassic marine invertebrate faunas of North America. US Geol. Survey, Professional paper 141. US Gov't. Printing Office.

Stanley, G.D., McRoberts, C.A. & Whalen, M.T. 2008. Stratigraphy of the Triassic Martin Bridge Formation, Wallowa terrane: stratigraphy and depositional setting. Geological Society of America Special Papers, 442: 227-250.

Sun, Y. D., Orchard, M. J., Kocsis, Á. T. & Joachimski, M. M. 2020. Carnian–Norian (Late Triassic) climate change: Evidence from conodont oxygen isotope thermometry with implications for reef development and Wrangellian tectonics. Earth and Planetary Science Letters, 534: doi.org/10.1016/j.epsl.2020.116082.

Tekin, U.K. & Yurtsever, T.S.,2003. Late Triassic (early to middle

Norian) radiolarians from the Antalya nappes, Antalya, SW Turkey. Journal of Micropalaeontology, 22: 147-162.

Tozer, E.T. 1994. Canadian Triassic ammonoid faunas, Bulletin Geological Survey Canada, 467: 1–663.

Trotter J.A., Williams I.S., Nicora A., Mazza M. & Rigo M. 2015 Long-term cycles of Triassic climate change: a new $\delta^{18}O$ record from conodont apatite. Earth and Planetary Science Letters, 415: 165–174.

Truschelev, A.M. & Grinenko, V.S. 2016. Boreal Trias in the Yana and Indigirka rivers- new sheet Q-53 stratigraphy-Verkhoyansk. Bulletin of Goskomgeologii, 15: 33-75.

Tun Min, T. & Maung, M. 2019. Stratigraphy of Pane Chaung Group in Bhopi Vum Area, Tiddim Township, Chin State. The Third Myanmar National Conference on Earth Sciences (MNCES, 2019) November 7-8, Yadanabon University, Mandalay, Myanmar, pp. 186-194.

Visscher, H. & Krystyn, L. 1978. Aspects of Late Triassic palynology. 4. A palynological assemblage from ammonoid-controlled Late Karnian (Tuvalian) sediments of Sicily. Review of Palaeobotany and Palynology, 26: 93-112.

Vozin, V.F. & Tikhomirova,V.V. 1964. Field Atlas of Bivalves and Cephalopods from the Triassic Deposits of the Northeastern USSR, Moscow: Nauka [in Russian].

Wahyudiono, J., Susilo, A., Adlan, R., Salimudin, B., Gibran, A.K. & Wiratmoko, E.S. 2018. Integrated Field Mapping, Organic Chemistry and Subsurface Geological Interpretation of Kanikeh Formation as Potential Source Rock in Seram Island. Proceedings, Indonesian Petroleum Association, Forty-Second Annual Convention & Exhibition, May 2018, House, Hanoi.

Williford K.A., Orchard, M.J., Zonneveld, J.P. McRoberts, C.A. & Beatty, T.W. 2007. A record of stable organic carbon isotopes from the Carnian Norian boundary section at Black Bear Ridge, Williston Lake, British Columbia, Canada. Albertiana, 36: 146-148.

Yamashita D, Yasuda C, Ishibashi T., Martini R. & Onoue T. 2016. Stratigraphy and conodont and ammonoid ages of Upper Triassic Nakijin Formation in Hedomisaki area, Okinawa-jima, Japan. Journal Geological Society Japan, 122: 477–493.

Zonneveld, J. P., Beatty, T. W., Williford, K. H., Orchard, M. J. & McRoberts, C. A. 2010. Stratigraphy and sedimentology of the lower Black Bear Ridge section, British Columbia: candidate for the base-Norian GSSP. Stratigraphy, 7: 61-82.